Roles of Central Amygdala and Hypothalamic Paraventricular Nucleus Neuronal Activities in Regulating Sympathetic Nerve Activity in Conscious Rats

Roles of Central Amygdala and Hypothalamic Paraventricular Nucleus Neuronal Activities in Regulating Sympathetic Nerve Activity in Conscious Rats

Shizuka Ikegame

The Graduate School of Human and Sciences,

Nara Women's University

June, 2022

Contents

Chapter 1

Simultaneous Measurement of Central Amygdala Neuronal Activity and Sympathetic Nerve Activity during Daily Activities in Rats

ABSTRACT

The central amygdala (CeA) mediates diverse changes in sympathetic nerve activity (SNA) in response to changes in daily behavioural states. However, the functional relationships between CeA neuronal activity (CeANA) and SNA in daily activities are still unclear. In the present study, we developed a method for simultaneous and continuous measurement of amygdala neuronal activity and SNA in freely moving rats. Wistar rats were chronically instrumented with multiple electrodes (100-μm stainless-steel wire) for the measurement of CeANA, of renal SNA (RSNA) and of lumbar SNA (LSNA), and electroencephalogram, electromyogram (EMG), and electrocardiogram electrodes as well as catheters for measurement of arterial pressure (AP). During the transition from non-rapid-eye movement (NREM) sleep to quiet wakefulness, moving, and grooming states, a significant linear relationship was observed between CeANA and RSNA ($P < 0.0001$), between CeANA and LSNA (P=0.0309), between CeANA and heart rate (HR) ($P = 0.0123$), and between CeANA and EMG (P=0.0089), but no significant correlation was observed between CeANA and AP (P=0.5139). During rapid eye movement sleep, the relationships between CeANA and RSNA, LSNA, HR, AP, and EMG deviated from the previously observed linear relationships, but the time course of RSNA and HR changes was the mirror image of that of CeANA, while the time course of changes in LSNA and AP was not related to that of CeANA. In conclusion, CeANA influences RSNA, LSNA, and HR in a behavioural state-dependent and regionally different manner, while CeANA was tightly associated with RSNA and HR across all behavioural states

INTRODUCTION

The central nucleus of the amygdala (CeA) orchestrates a diverse set of adaptive behaviours, including anxiety, fear, sleep, arousal and feeding states (Davis & Whalen, 2001; Duvarci et al., 2011; Fadok et al., 2018); each of these behavioural states is associated with a distinct pattern of changes in autonomic functions, thus resulting in diverse adaptive cardiovascular responses during different behavioural states (Hagenaars et al., 2014; Kleshchova et al., 2019; Kondo et al., 2021; Kozlowska et al., 2015; Miki et al., 2022; Stock et al., 1981). The CeA has widespread projections to the cortical, hypothalamic and brainstem regions (Johnson, 2019; van der Kooy et al., 1984). Extensive anatomical tract tracing studies among those nuclei have shown that the central nucleus of the amygdala (CeA) projects to several nuclei, including the paraventricular nucleus (LeDoux et al., 1988), the rostral ventrolateral medulla (RVLM) (Saha, 2005; Salome et al., 2001) and the nucleus tractus solitarii (Higgins & Schwaber, 1983), which form the primary network for regulation of sympathetic and parasympathetic nerve activity, thus causing changes in cardiovascular function. Although the anatomical connections between the CeA and the nuclei responsible for regulating autonomic function are clear, the functional interrelationships between the CeA and autonomic function remain elusive.

Only a small number of studies have examined CeA neuronal activity (CeANA) during daily behavioural states. Most studies on the functional role of the amygdala in regulation of autonomic neuronal activity have been carried out under general anaesthesia (Cox et al., 1987; Roder et al., 1999). The neuronal activity in brain areas including the limbic system and medulla is known to be significantly affected by general anaesthesia, which has been consistently reported to be a crucial factor when investigating the amygdaloid complex in relationship to autonomic and cardiovascular regulation (Gelsema et al., 1987; Iwata et al., 1987; Stock et al., 1981). A few attempts have been

made to measure amygdaloid nerve activity in conscious cats (Sawa & Delgado, 1963; Stock et al., 1981) and rabbits (Pascoe & Kapp, 1985), but autonomic nerve activity was not measured in these studies. To our knowledge, no previous study has simultaneously measured the changes in CeANA and autonomic activity in addition to cardiovascular function in the same set-up in conscious animals. Thus, simultaneous and continuous measurement of CeA and sympathetic nerve activity (SNA) in the same rats during daily activity might provide useful insights into the functional significance of the role of the CeA in regulating SNA and cardiovascular function.

To this end, in the present study, microelectrodes were implanted chronically in the CeA area and on renal and lumbar sympathetic nerves, and CeANA, renal sympathetic nerve activity (RSNA), lumbar sympathetic nerve activity (LSNA), arterial pressure (AP) and heart rate (HR) were measured continuously and simultaneously in the same rats after they had completely recovered from the surgery. This approach could illustrate the quantitative relationships between CeANA and RSNA and LSNA during daily activities, including rapid eye movement (REM) sleep, non-REM (NREM) sleep and quiet awake, moving and grooming states.

METHODS

Ethical approval

All procedures were conducted in accordance with the Guiding Principles in the Care and Use of Animals in the Fields of Physiological Sciences, published by The Physiological Society of Japan (Physiological Society Japan, 2015), with the prior approval of the Animal Care Committee of Nara Women's University (#17-11). The experiments were performed on 20 male Wistar rats weighing 280.3 ± 2.53 g (mean ± SD) purchased from SLC (Hamamatsu, Shizuoka, Japan). The animals were

housed individually and kept in a chamber (Espec, Osaka, Japan) with controlled temperature (24°C) and humidity (60%) and a 12 h–12 h light–dark cycle (light on at 07.00 h). Food and water were available ad libitum.

Fabrication of the electrode for measurement of CeANA

Figure 1 shows an overview of the electrode used for measurement of CeANA. Coated stainless-steel wires (length, 2 cm; diameter, 100 μm; Unique Medical, Tokyo) were connected to four conductor-shielded cables (length, 75 cm; diameter, 2.2 mm). A 1 cm length of the coat was removed from the conductor-shielded cables and the epoxy-coated stainless-steel wires, and each of the conductor-shielded cables was soldered to one of the stainless-steel wires; these served as the electrodes for CeANA neuronal recording. The three epoxy-coated stainless-steel wires were passed through a stainless-steel needle (24 gauge; length, 7 mm) to maintain a proper distance among the wires. The shielding of the cable was soldered to the multiple stranded wires (length, 70 mm; AS6733; Cooner, Chatsworth, CA, USA) and served as the earth electrode.

Animal instrumentation

The animals were operated on in two stages. All procedures were performed aseptically in an operating theatre. During the first surgery, the electrodes for measurement for RSNA, LSNA and ECG were implanted. The rats were premedicated with pentobarbital sodium (65 mg/kg, i.p.), anaesthetized with isoflurane (1.5–2.0% in air at a rate of 1–1.5 L/min) and administered antibiotics (gentamicin sulphate, 10 mg/kg s.c., Schering-Plough, Whitehouse Station, NJ, USA). The electrodes for measurement of RSNA and LSNA were implanted as described in our previous reports (Miki et al., 2002, 2004). Briefly, the left kidney was exposed retroperitoneally through a

flank incision. Approximately 2 mm of the renal sympathetic nerve was carefully isolated, and a bipolar stainless-steel wire electrode (AS633) was hooked onto the renal nerve. Both electrode and nerve were embedded in a two-component silicone rubber shield (932; Wacker, Munich, Germany). A mid-line abdominal incision was made to implant the LSNA electrode. After retraction of the intestines, the abdominal aorta and vena cava were gently pulled aside to expose a lumbar nerve. Approximately 3 mm of the left lumbar sympathetic trunk was carefully isolated from the connective tissue. A bipolar stainless-steel wire electrode (AS633) was hooked onto the sympathetic trunk between L3 and L4, and both were embedded in a two-component silicone rubber shield. The bipolar ECG electrode was implanted under the skin at the manubrium of the sternum and xiphoid process. The electrodes were exteriorized at the back of the neck and passed through the centre of a circular Ducron sheet, which was fixed into lace by suturing to the skin and protected by plastic tubes, after which 4 days were allowed for the recovery.

During the second surgery, rats were anaesthetized with the same as for the first surgery and the electrodes for measurement of CeANA and the cervical EMG electrode and arterial catheter were implanted. The head of the rat was secured in a stereotaxic apparatus (Stoelting, Wood Dale, IL, USA), and EEG electrodes were implanted over the frontal cortex (anteroposterior, 1.5 mm and mediolateral, –2.0 mm from bregma), the parietal cortex (anteroposterior, –3 mm and mediolateral, –2.0 mm from bregma) and the cerebellum (1.5 mm posterior to lambda). Three stainless-steel miniature screws (1.0 mm in diameter), which served as electrodes, were screwed into the skull. Subsequently, implantation of the electrode for measurement of CeANA was carried out. An area ~1.5 mm in diameter was thinned in the parietal cortex bone (anteroposterior, –4.5 mm and mediolateral, –2.3 from bregma) using a drill. The remaining thin cranial plate and dura were removed by hooking them under the microscope using a syringe needle (27 gauge) with a bent tip

<1 mm in length. The electrode was then lowered stereotaxically into the right central nucleus of the amygdala through the cranial hole at a speed of 0.1 mm/min (DMA-1510; Narishige, Tokyo, Japan) until action potentials with pyramidal cell firing characteristics were recorded. The electrode signals were amplified by a differential amplifier (Biotex, Kyoto, Japan), displayed on an oscilloscope and made audible with an audio amplifier. After confirming CeANA, the CeANA and EEG electrodes were fixed on the skull with dental cement, and the four stainless-steel screws were anchored to the skull. Next, the arterial catheter was implanted into the abdominal aorta via the tail artery (Miki, Yoshimoto, et al., 2003).

Upon completion of each surgery, antibiotics were administered (fradiomycin 200 μg/kg i.p.; Mochida-Seiyaku, Tokyo, Japan), and jelly (sugar gelatin jelly, Jelly Ace, House Foods Corporation, Tokyo, Japan) and a blanket were provided. To control postoperative pain, a non-steroidal anti-inflammatory drug (diclofenac sodium, 0.5–3.0 mg/kg; Novartis Japan, Tokyo, Japan) mixed with jelly was given orally when necessary. The daily examinations included assessments of posture, activity, breathing, coat, eyes, body weight, food intake, urine volume and faecal volume. The arterial catheter was filled with heparin sodium solution (250 IU/ml) and flushed every day. The animals were housed individually in transparent plastic cages and allowed standard laboratory rat chow and water ad libitum thereafter.

Measurements

Signals from the implanted electrodes for CeANA were amplified by a differential amplifier (MK-1; Biotex: the gain and bandwidth were ×20,000 and 250–8,000 Hz, respectively) fed into the recording system (Recorder; Plexon, Dallas, TX, USA) and displayed on the computer monitor. Spike activity was isolated using a voltage threshold, and waveforms that crossed the threshold

were sampled, time stamped, and stored at 40 kHz throughout the experimental period. At the end of the experiment, waveforms were processed offline (Offline Sorter; Plexon) to remove artefacts using principal components analysis, and spike counts every 1 s were calculated and stored on the disc.

The EEG, EMG, ECG, RSNA and LSNA signals were amplified by a differential amplifier (MK-2; Biotex; the gain and bandwidth, respectively, were as follows: ×10,000 and 0.16–50 Hz for EEG; ×100 and 100–2,000 Hz for EMG; ×1,000 and 0.16–150 Hz for ECG; and ×50,000 and 150–2,000 Hz for RSNA and LSNA). The AP was measured by connecting the arterial catheters to pressure transducers (DX-100; Nihon Kohden, Tokyo, Japan). The HR was determined with a cardiotachometer (AT-601G; Nihon Kohden) triggered by the ECG. The amplified RSNA was integrated using a voltage integrator with a time constant of 50 ms (AD-600G; Nihon Kohden). The signals for EEG, EMG, ECG, RSNA, integrated RSNA, LSNA, integrated LSNA, AP and HR were displayed continuously on an oscilloscope and recorded simultaneously on thermal head recording paper (ORP1200; Yokogawa, Tokyo, Japan). The EEG, EMG, AP, HR, integrated RSNA and integrated LSNA signals were sampled for analog-to-digital conversion at 2 kHz intervals. The digitized EEG signal underwent Fourier analysis in 1 s epochs using a computerized data-acquisition program (LabVIEW; National Instruments, Austin, TX, USA). The power spectrum was averaged simultaneously in two frequency bands: delta (0.5–4 Hz) and theta (6–9 Hz). The digitized EMG signal was simultaneously converted to the mean square root value. With the aid of a data-acquisition programme (LabVIEW), data for the power spectrums of EEG and the root mean square values of EMG, AP, HR, integrated RSNA and integrated LSNA were averaged simultaneously and continuously every 1 s, displayed on the computer monitor, and stored on a hard disk.

Experimental protocol

After the second surgery, the rats were allowed a minimum of 3 days to recover. Experiments were performed with the animals in their home cage, and they were given free access to food and water. Each experiment was performed over a period of 2–3 h, beginning at ~11.00 h, following a stabilization period of 1 h of recording data after connecting all electrodes and catheters to the measuring instruments.

Behavioural states were scored by standard criteria on the basis of EEG and EMG and behavioural observations noted at the time of data collection. The behaviour of the animal was classified into REM sleep, NREM sleep, dozing (Doz), quiet awake (Quiet), moving (Mov) or grooming (Groom) states.

The REM sleep was characterized by body relaxation, irregular breathing, and muscle twitches in different parts of the body. The EEG was desynchronized and displayed low-voltage and high-frequency waves; the predominant EEG power density occurred within the date frequency band, with a high theta/delta ratio and dramatic suppression of EMG. The onset of REM sleep was defined as the point at which both a high value of the theta/delta ratio and suppression of EMG occurred. During NREM sleep, the animal lay immobile with eyes closed; the EEG was synchronized and displayed high-voltage and low-frequency waves, high-power density values in the delta-frequency band and a low EMG. Dozing was identified by low-amplitude EEG, with the animal maintaining a lying position with its eyes closed. Quiet awake state was identified by low-amplitude EEG, and the animal maintaining a lying position with its eyes open. Moving, grooming, drinking and eating states were identified by visual observations taken during data acquisition. The moving state included any body movement except grooming, drinking and eating, such as stretching, exploring

and rearing.

At the end of the entire procedure, rats were anaesthetized with the same as for the first surgery, and the locations of the electrodes were marked by passing a DC current of 40 μA through the anode during 2 s. The rats were then killed with an overdose of pentobarbital sodium (>200 mg/kg i.v.), and the brain was removed and fixed by immersion in a 1% potassium ferrocyanide solution in formalin for 7 days. The iron deposits could then be observed as Prussian Blue spots after they reacted with the ferrocyanide.

Histology

For the prevention of ice crystal formation for the preparation of of frozen sections, the brains were transferred to 15% sucrose in 0.1 mol/L phosphate buffer solution for 24 h and were stored in a 25% sucrose in 0.1 mol/L phosphate buffer solution after 48 h. Brains were sliced into 50-μm-thick sections with a freezing micro- tome (CM3050 Leica, Germany). Every other section was collected on a slide and stained with Cresyl Violet. The positions of the tips of the electrodes were identified (Figure 2). Electrode tips located outside the area of the CeA were excluded from the data analysis. Simultaneous measurements of CeANA, RSNA and LSNA were obtained successfully in freely moving states in six rats.

Statistical analyses

Statistical analysis was performed with SPSS (IBM, Chicago, IL) for analysis of variance (ANOVA) and multiple comparisons for repeated measures. When the F-values were significant ($P < 0.05$), individual comparisons were made using the Dunnett's multiple comparison test. Values are reported as means ± SD. $P < 0.05$ was considered to indicate a significant difference.

Correlations between CeANA and RSNA, LSNA, HR, AP, and EMG were quantified using a least-squares linear regression analysis (Pearson's r) using SPSS.

RESULTS

Out of the 20 rats included in the experiment, we succeeded in measuring CeANA, RSNA, LSNA, AP, HR, EEG, EMG, and ECG in the same individual simultaneously and continuously in six rats. Data corresponding to each behavioural state were averaged for each rat and used for the analyses displayed in Figures 4, 5, and 6

Figure 3 shows typical recordings of CeANA, RSNA, and LSNA in a fast chart speed. CeANA appears as a series of successive spikes, and the intervals between the spikes are not constant but show dispersed activity. On the other hand, RSNA and LSNA show repeated burst activity.

Figure 4 shows changes in the averaged values of CeANA, RSNA, LSNA, HR, and AP across the behavioural states. Since NREM sleep is the most stable and long-lasting daily activity in rats, the values observed during NREM sleep period were used as the reference (100%). The mean durations of REM and NREM sleep, and dozing, quiet awake, moving, and grooming states were (mean ± SD, n=6 rats) 98.5 ± 13.9, 254.8 ± 68.0, 22.3 ± 8.8, 18.4 ± 3.8, 22.0 ± 5.9, 45.2 ± 32.3 sec, respectively.

CeANA was the lowest during NREM sleep among all categories of activity shown in this figure, and it increased as the level of activity increased over the dozing, quiet awake, moving, and grooming states. Similarly, RSNA, LSNA, HR, AP, and EMG increased with an increase in physical activity from NREM sleep to the dozing, quiet awake, moving, and grooming states. However, CeANA, RSNA, LSNA, HR, AP, and EMG did not change in the same direction during REM sleep.

CeANA increased by 41.8% relative to NREM sleep ($P < 0.0003$) during REM sleep, which was the most active among the behavioural states. Meanwhile, RSNA and HR decreased by 41.8% ($P < 0.0001$) and 26.8 beats/min ($P = 0.0156$) relative to NREM sleep, respectively, during REM sleep. In contrast, LSNA and MAP increased slightly by 11.8% ($P = 0.8652$) and 5.89 mmHg ($P = 0.4874$) relative to NREM sleep, respectively, during REM sleep.

In Figure 5, the relationships between CeANA and RSNA, HR, EMG, LSNA, and AP were examined by linear correlations in the data for NREM sleep, and dozing, quiet awake, moving, and grooming states. A significant linear relationship was observed between CeANA and RSNA ($r = 0.7823$, $P < 0.0001$), CeANA and EMG ($r = 0.4693$, $P = 0.0089$), CeANA and HR ($r = 0.4515$, $P = 0.0123$), and CeANA and LSNA ($r = 0.3948$, $P = 0.0309$) . In contrast CeANA and MAP ($r = 0.1240$, $P = 0.5139$) showed no significant linear relationship.

Figure 6 shows the time course of changes in CeANA, RSNA, LSNA, HR, and AP during the transition from NREM to REM sleep. CeANA started to increase approximately 12 s before the onset of REM sleep, and RSNA and HR simultaneously started to decrease. Meanwhile, LSNA and MAP remained unchanged during the period prior to the onset of REM sleep. During the REM sleep period, CeANA maintained an increased level, while RSNA and HR maintained a reduced level. The changes in RSNA and HR during REM showed a mirror-image change in CeANA, although in the opposite direction. The LSNA and MAP did not show changes linked to CeANA during the transition from the NREM to REM sleep period.

DISCUSSION

The novel challenge in this study was simultaneous measurements of CeANA, RSNA, and LSNA

in the same conscious rats. This methodological advantage could allow analyses of the quantitative state-related relationships between CeANA vs. RSNA, LSNA, HR, and MAP. This study demonstrated that CeANA showed significantly close linear links to RSNA, LSNA, and HR during NREM, dozing, quiet awake, moving, and grooming states. During the transition from NREM to REM sleep, changes in CeANA were tightly associated with RSNA and HR but weakly associated with LSNA and MAP. This tight association of CeANA with RSNA and HR across all behavioural states explains how the amygdala is involved in mediating the regionally different responses of SNA and the specific patterns of cardiovascular function induced by fear and anxiety.

CeANA influences RSNA, LSNA, and HR in a behavioural state-dependent manner

To our knowledge, no previous reports have described simultaneous CeANA and SNA measurements in the same setup for conscious freely moving animals. However, some studies have measured CeANA and SNA separately (Mgaloblishvili & Mandzhavidze, 1985; Frysinger *et al*., 1988; Miki *et al*., 2003a; Jha *et al*., 2005; Yoshimoto *et al*., 2011), and their results are in good agreement with the findings of this study. As shown in Figure 5, the relationship between CeANA and RSNA, LSNA, HR, AP, and EMG can be divided into two groups; 1) responses observed during NREM, dozing, quiet awake, moving, and grooming states and 2) responses observed during REM sleep, which are dissociated from the other behavioural states. Therefore, the possible role of CeANA in regulating RSNA, LSNA, HR, and MAP has been discussed separately for these two phases.

Responses observed during NREM, dozing, quiet awake, moving, and grooming states

The CeANA is the lowest during the NREM sleep and increases progressively over the dozing,

quiet awake, moving, and grooming states, as shown in Figure 4. Consistent with the present observations, CeANA in cats and rats has been reported to be lower in the NREM state than in the awake state (Mgaloblishvili & Mandzhavidze, 1985; Frysinger *et al*., 1988; Jha *et al*., 2005). Although, to our knowledge, previous reports on CeANA during moving and grooming in animals were not available, the fact that significant linear relationship exists between CeANA and EMG (Figure 4) suggests that CeANA increases across NREM sleep, dozing, quiet awake, moving, and grooming states in proportion with the increase in EMG activity. Since the amygdala receives somatosensory information (Sah *et al*., 2003), CeANA possibly increase in proportion to the magnitude of increase in EMG, namely physical activity. Another possibility is that since CeA is positioned to modulate behaviour (Fadok *et al*., 2018), changes in CeANA may be linked to motor-neuron activity, resulting in an increase in EMG. Although cause and effect relationships between CeANA and EMG are unknown, it is clear that a simple increase in physical activity increases CeANA in a behaviour-dependent manner. Moreover, RSNA and LSNA increased associated with increase in physical activity from NREM, dozing, quiet awake, moving, to grooming states (Figure 4), which is consistent with previous reports (Miki *et al*., 2003a; Yoshimoto *et al*., 2011). Taken together, the changes in CeANA, RSNA, and LSNA across the NREM, dozing, quiet awake, moving, and grooming states are in good agreement with previously measured results for each of these parameters separately. It should be emphasized that these neural activities were measured continuously and simultaneously in the same freely moving individual, thereby ensuring that the quantitative analysis of the interrelationships between these variables was reliable.

The novel finding of this study is that there was a significant linear relationship between CeANA and RSNA, while the relationship between CeANA and LSNA was weak but did reach statistical significance. These results are supported by the anatomical evidence that CeANA projects to

sympathetic premotor neurons, including RVLM, directly (Saha *et al*., 2005) and indirectly through the hypothalamus and periaqueductal gray (Price, 2003). These results suggest that CeANA, RSNA, LSNA, and EMG change in a linear relationship when physical activity increases, such as in the sequence of transitions from NREM, dozing, quiet awake, moving, and grooming.

Responses observed during REM sleep

CeANA was significantly increased during REM sleep relative to NREM sleep, consistent with previous reports from cats (Frysinger *et al*., 1988) and rats (Mgaloblishvili & Mandzhavidze, 1985; Jha *et al*., 2005), and this was associated with decreases in RSNA and EMG as well as with a slight increase in LSNA. Therefore, the relationship between CeANA and RSNA during REM sleep deviated from the linear relationship observed during NREM, dozing, quiet awake, moving, and grooming states. NREM and REM sleep are controlled by specific neuronal circuits (Chen *et al*., 2018). CeA possibly communicates with these networks and could mediate the generation of regionally different changes in RSNA and LSNA aimed to adapt cardiovascular function to the REM sleep state (Yoshimoto *et al*., 2011). Thus, the influence of CeA on SNA is likely to be dependent on the behavioural state.

One might speculate that the coupling between CeANA and RSNA may become weaker and more independent during REM sleep in comparison with the other states. However, the time course of changes in RSNA was a mirror image of that of CeANA during the transition from NREM to REM sleep, suggesting that CeANA and RSNA continue to maintain a tight relationship during the transition from NREM to REM sleep. In contrast, LSNA does not appear to change in concert with changes in CeANA during the transition from NREM to REM sleep. Thus, CeANA and RSNA likely maintain tight connections even though the direction of change is opposite, while CeANA

and LSNA have a weak connection with CeANA during the transition from NREM to REM sleep. The anatomical observations from RVLM support this view. The anatomical subdivisions within the RVLM have been reported to correspond to the regional output of sympathetic activity (McAllen & May, 1994; Mueller *et al*., 2011). Thus, there may be anatomical or functional differences in the projection of CeANA neurons to the RSNA and LSNA of their respective premotor neurons. Indeed, the present study provides direct evidence showing that CeA may be positioned to mediate the regional difference in RSNA and LSNA.

To summarise the above discussion, CeANA influences RSNA, LSNA, HR in a behavioural state-dependent and regionally different manner. Meanwhile, CeANA shows a tight neural activity connection with RSNA across the all-behavioural states including REM sleep, while CeANA and LSNA show a less connection during REM sleep. Thus, the CeA is positioned for mediating a regional difference in RSNA and LSNA and may exert as stronger influence on the sympathetic output to the kidney than to the hindlimb.

CeANA exerts a significant influence on HR and does not directly influence AP

The relationship between CeANA and HR is similar to the relationship between CeANA and RSNA. We observed a significant linear relationship between CeANA and HR across changes in behavioural states from NREM, dozing, quiet awake, moving, and grooming (Figure 5). Moreover, HR decreased during the transition from NREM to REM sleep in a mirror image of the changes in CeANA (Figure 6), as observed in RSNA. One possible explanation for this tight association between CeANA and HR may be that cardiac SNA changes in a similar manner as the changes in RSNA. Another possible explanation is that CeANA projects to the NTS (Saha, 2005), and the changes in CeANA may modulate the cardiac vagal nerve activity via projections from the NTS to

motoneurons of the cardiac vagus nerve in the dorsal vagal motor nucleus and some neurons in the nucleus ambiguus (Wehrwein *et al*., 2016). Since the amygdala is known to be the centre for emotional responses, the tight linkage between HR and CeANA observed in this study can explain the fact that fear and anxiety is associated with robust changes in HR.

The relationship between CeANA and AP and LSNA did not reach statistical significance, which is similar to that between CeANA and LSNA. AP is determined as the product of cardiac output and total peripheral vascular resistance. Although RSNA is linearly related to renal vascular resistance, changes in RSNA can change renal vascular resistance in a minimum range (Yoshimoto *et al*., 2004). LSNA is involved in the regulation of vascular resistance in the organs of the lower extremities, including muscle and skin. Changes in muscle SNA can significantly alter muscle vascular resistance over a wide range (Rowell *et al*., 1996). Thus, the changes in cardiac output by HR and renal vascular resistance by RSNA may be buffered by changes in muscle vascular resistance, resulting in less correlation between CeANA and AP. This view is consistent with the findings of previous reports in animals and humans, which stated that emotional stress causes robust changes in HR, but AP is not directly related to changes in HR (Kozlowska *et al*., 2015a; Proverbio *et al*., 2015; Kondo *et al*., 2021).

Perspective

A sustained increase in RSNA has been observed during freezing behaviours induced by loud noise exposure in rats (Yoshimoto *et al*., 2010; Kondo *et al*., 2021). Freezing behaviour is an index of fear. Repeated exposure to anxiety, fear, or recall of fear memories is linked to cardiovascular dysfunction such as hypertension (Lim *et al*., 2021; Nagai *et al*., 2022). The increased RSNA leads

to increased Na^+ reabsorption, decreased renal blood flow, and activation of the renin-angiotensin system, all of which contribute to the development of hypertension (DiBona, 2003; Hall *et al*., 2020). This study demonstrates a tight neuronal association between CeANA and RSNA, which is a key factor for elucidating the mechanism underlying kidney-induced cardiovascular dysfunction induced by anxiety, fear, and recall of fearful memories.

REFERENCES

Chen KS, Xu M, Zhang Z, Chang WC, Gaj T, Schaffer DV & Dan Y (2018). A Hypothalamic Switch for REM and Non-REM Sleep. *Neuron* **97,** 1168-1176 e1164.

Cox GE, Jordan D, Paton JF, Spyer KM & Wood LM (1987). Cardiovascular and phrenic nerve responses to stimulation of the amygdala central nucleus in the anaesthetized rabbit. *J Physiol* **389,** 541-556.

Davis M & Whalen PJ (2001). The amygdala: vigilance and emotion. *Mol Psychiatry* **6,** 13-34.

DiBona GF (2003). Neural control of the kidney: past, present, and future. *Hypertension* **41,** 621-624.

Duvarci S, Popa D & Pare D (2011). Central amygdala activity during fear conditioning. *J Neurosci* **31,** 289-294.

Fadok JP, Markovic M, Tovote P & Luthi A (2018). New perspectives on central amygdala function. *Curr Opin Neurobiol* **49,** 141-147.

Frysinger RC, Zhang JX & Harper RM (1988). Cardiovascular and respiratory relationships with neuronal discharge in the central nucleus of the amygdala during sleep-waking states. *Sleep* **11,** 317-332.

Gelsema AJ, McKitrick DJ & Calaresu FR (1987). Cardiovascular responses to chemical and electrical stimulation of amygdala in rats. *Am J Physiol* **253,** R712-718.

Hagenaars MA, Roelofs K & Stins JF (2014). Human freezing in response to affective films. *Anxiety Stress Coping* **27,** 27-37.

Hall JE, Mouton AJ, da Silva AA, Omoto ACM, Wang Z, Li X & do Carmo JM (2020). Obesity, kidney dysfunction, and inflammation: interactions in hypertension. *Cardiovascular Research* **117,** 1859-1876.

Higgins GA & Schwaber JS (1983). Somatostatinergic projections from the central nucleus of the amygdala to the vagal nuclei. *Peptides* **4,** 657-662.

Iwata J, Chida K & LeDoux JE (1987). Cardiovascular responses elicited by stimulation of neurons in the central amygdaloid nucleus in awake but not anesthetized rats resemble conditioned emotional responses. *Brain Res* **418,** 183-188.

Jha SK, Ross RJ & Morrison AR (2005). Sleep-related neurons in the central nucleus of the amygdala of rats and their modulation by the dorsal raphe nucleus. *Physiol Behav* **86,** 415-426.

Johnson HM (2019). Anxiety and Hypertension: Is There a Link? A Literature Review of the Comorbidity Relationship Between Anxiety and Hypertension. *Current Hypertension*

Reports **21,** 66.

Kleshchova O, Rieder JK, Grinband J & Weierich MR (2019). Resting amygdala connectivity and basal sympathetic tone as markers of chronic hypervigilance. *Psychoneuroendocrinology* **102,** 68-78.

Kondo N, Yoshimoto M, Ikegame S & Miki K (2021). Differential shifts in baroreflex control of renal and lumbar sympathetic nerve activity induced by freezing behaviour in rats. *Exp Physiol* **106,** 2060-2069.

Kozlowska K, Walker P, McLean L & Carrive P (2015a). Fear and the Defense Cascade: Clinical Implications and Management. *Harv Rev Psychiatry* **23,** 263-287.

Kozlowska K, Walker P, McLean L & Carrive P (2015b). Fear and the defense cascade: Clinical implications and management. *Harvard Review of Psychiatry* **23,** 263-287.

LeDoux JE, Iwata J, Cicchetti P & Reis DJ (1988). Different projections of the central amygdaloid nucleus mediate autonomic and behavioral correlates of conditioned fear. *J Neurosci* **8,** 2517-2529.

Lim LF, Solmi M & Cortese S (2021). Association between anxiety and hypertension in adults: A systematic review and meta-analysis. *Neurosci Biobehav Rev* **131,** 96-119.

McAllen RM & May CN (1994). Differential drives from rostral ventrolateral medullary neurons to three identified sympathetic outflows. *Am J Physiol* **267,** R935-944.

Mgaloblishvili MM & Mandzhavidze SD (1985). Neuronal activity in the amygdaloid structure during the sleep-wake cycle of the rat. *Neurophysiology* **17,** 533-540.

Miki K, Ikegame S & Yoshimoto M (2022). Regional Differences in Sympathetic Nerve Activity Are Generated by Multiple Arterial Baroreflex Loops Arranged in Parallel. *Frontiers in Physiology* **13,** 1-8.

Miki K, Kato M & Kajii S (2003a). Relationship between renal sympathetic nerve activity and arterial pressure during REM sleep in rats. *Am J Physiol Regul Integr Comp Physiol* **284,** R467-473.

Miki K, Kosho A & Hayashida Y (2002). Method for continuous measurements of renal sympathetic nerve activity and cardiovascular function during exercise in rats. *Exp Physiol* **87,** 33-39.

Miki K, Oda M, Kamijyo N, Kawahara K & Yoshimoto M (2004). Lumbar sympathetic nerve activity and hindquarter blood flow during REM sleep in rats. *J Physiol* **557,** 261-271.

Miki K, Yoshimoto M & Tanimizu M (2003b). Acute shifts of baroreflex control of renal sympathetic nerve activity induced by treadmill exercise in rats. *J Physiol* **548,** 313-322.

Mueller PJ, Mischel NA & Scislo TJ (2011). Differential activation of adrenal, renal, and lumbar sympathetic nerves following stimulation of the rostral ventrolateral medulla of the rat. *Am J Physiol Regul Integr Comp Physiol* **300,** R1230-1240.

Nagai M, Kato M & Keigo D (2022). Anxiety and hypertension in the COVID-19 era: how is the central autonomic network linked? *Hypertens Res*.

Pascoe JP & Kapp BS (1985). Electrophysiological characteristics of amygdaloid central nucleus neurons during Pavlovian fear conditioning in the rabbit. *Behav Brain Res* **16,** 117-133.

Physiological Society Japan (2015). Guiding Principles in the Care and Use of Animals in the Fields of Physiological Sciences. *http://physiology.jp/wp-content/uploads/2015/07/animal-guideline-20150302.pdf*.

Price JL (2003). Comparative aspects of amygdala connectivity. *Ann N Y Acad Sci* **985,** 50-58.

Proverbio AM, Manfrin L, Arcari LA, De Benedetto F, Gazzola M, Guardamagna M, Lozano Nasi V & Zani A (2015). Non-expert listeners show decreased heart rate and increased blood pressure (fear bradycardia) in response to atonal music. *Frontiers in Psychology* **6**.

Roder S, Rosas-Arellano MP & Ciriello J (1999). Effect of noradrenergic inputs on the cardiovascular depressor responses to stimulation of central nucleus of the amygdala. *Brain*

Res **818,** 531-535.

Rowell LB, O'Leary DS & Kellogg DL (1996). Integration of Cardiovascular Control Systems in Dynamic Exercise. In *Comprehensive Physiology*, pp. 770-838.

Sah P, Faber ES, Lopez De Armentia M & Power J (2003). The amygdaloid complex: anatomy and physiology. *Physiol Rev* **83,** 803-834.

Saha S (2005). Role of the central nucleus of the amygdala in the control of blood pressure : desending pathways to medullary cardiovascular nulei. *Clinical and Experimental Pharmacology and Physiology* **32,** 450-456.

Saha S, Drinkhill MJ, Moore JP & Batten TF (2005). Central nucleus of amygdala projections to rostral ventrolateral medulla neurones activated by decreased blood pressure. *Eur J Neurosci* **21,** 1921-1930.

Salome N, Viltart O, Leman S & Sequeira H (2001). Activation of ventrolateral medullary neurons projecting to spinal autonomic areas after chemical stimulation of the central nucleus of amygdala: a neuroanatomical study in the rat. *Brain Res* **890,** 287-295.

Sawa M & Delgado JM (1963). Amygdala Unitary Activity in the Unrestrained Cat. *Electroencephalogr Clin Neurophysiol* **15,** 637-650.

Stock G, Rupprecht U, Stumpf H & Schlor KH (1981). Cardiovascular changes during arousal elicited by stimulation of amygdala, hypothalamus and locus coeruleus. *J Auton Nerv Syst* **3,** 503-510.

van der Kooy D, Koda LY, McGinty JF, Gerfen CR & Bloom FE (1984). The organization of projections from the cortex, amygdala, and hypothalamus to the nucleus of the solitary tract in rat. *J Comp Neurol* **224,** 1-24.

Wehrwein EA, Orer HS & Barman SM (2016). Overview of the Anatomy, Physiology, and Pharmacology of the Autonomic Nervous System. *Compr Physiol* **6,** 1239-1278.

Yoshimoto M, Nagata K & Miki K (2010). Differential control of renal and lumbar sympathetic nerve activity during freezing behavior in conscious rats. *Am J Physiol Regul Integr Comp Physiol* **299,** R1114-1120.

Yoshimoto M, Sakagami T, Nagura S & Miki K (2004). Relationship between renal sympathetic nerve activity and renal blood flow during natural behavior in rats. *Am J Physiol Regul Integr Comp Physiol* **286,** R881-887.

Yoshimoto M, Yoshida I & Miki K (2011). Functional role of diverse changes in sympathetic nerve activity in regulating arterial pressure during REM sleep. *Sleep* **34,** 1093-1101.

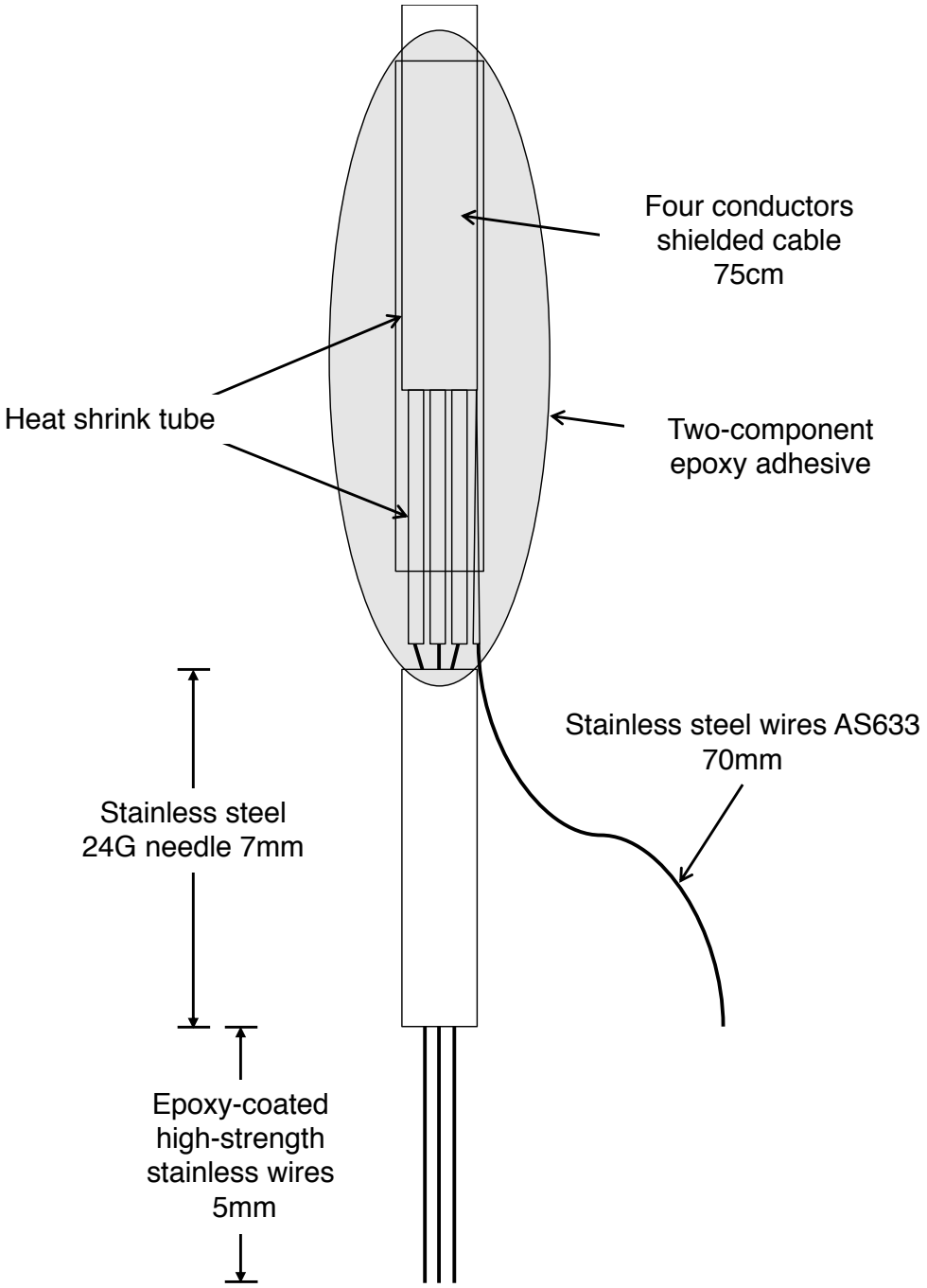

Figure 1. Schematic representation of the electrode used for central amygdala neuronal activity (CeANA) measurement.

The electrode consists of three straight epoxy-coated stainless-steel wires (100 μm) and a ground wire, all soldered to four conductor-shielded wires. The three wires were inserted slowly and precisely at the position of the central amygdala. See text for details.

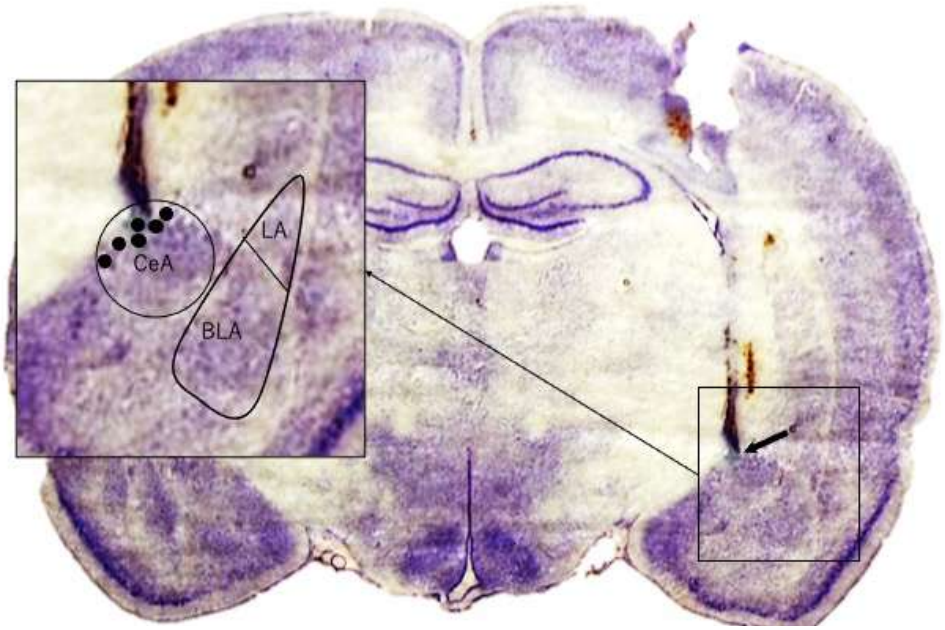

Figure 2. Site of the tip of the electrode where CeANA was recorded

In cresyl violet staining of a coronal rat brain section, the blue spot indicated by the arrow marks the tip of the electrode in an individual rat. The central amygdala (CeA) region is enlarged and shown in the upper left corner of the figure. The six black dots in the CeA region represent the results obtained from six rats in which CeA nerve activity (CeANA) was measured simultaneously with renal and lumbar sympathetic nerve activity, arterial pressure heart rate, electromyogram, and electrocardiogram in the same individual. LA, Lateral nucleus; BLA, basolateral nucleus.

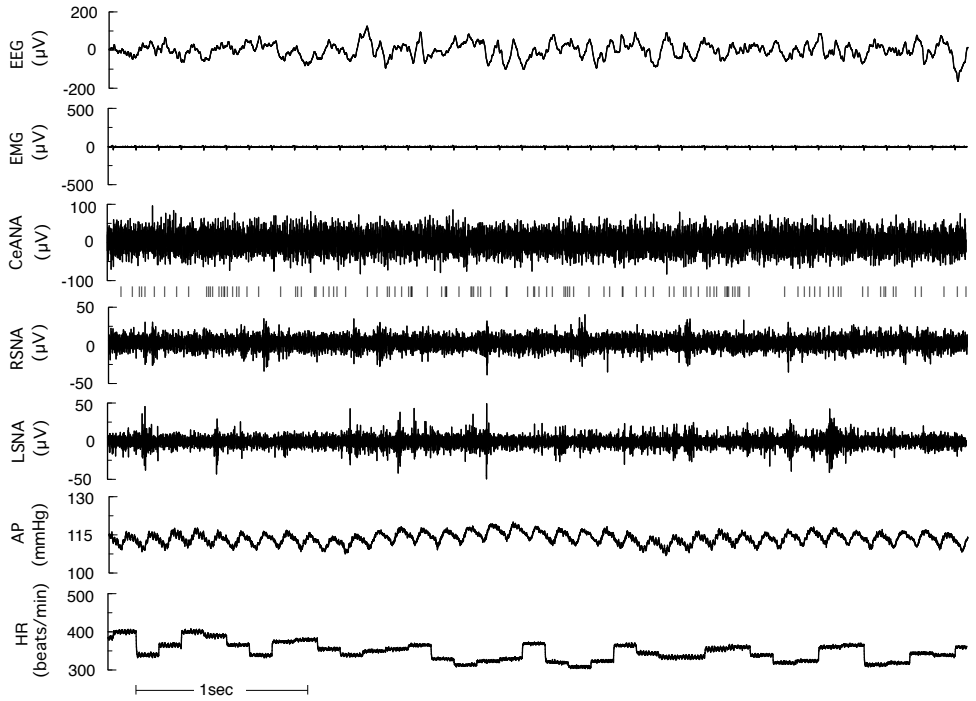

Figure 3. Typical recordings during NREM sleep in an individual rat.

From the top, electrocardiogram (ECG), electromyogram (EMG), central amygdala neuronal activity (CeANA), CeANA raster plot, renal sympathetic nerve activity (RSNA), RSNA raster plot, lumbar sympathetic nerve activity (LSNA), LSNA raster plot, arterial pressure (AP), and heart rate (HR) are shown.

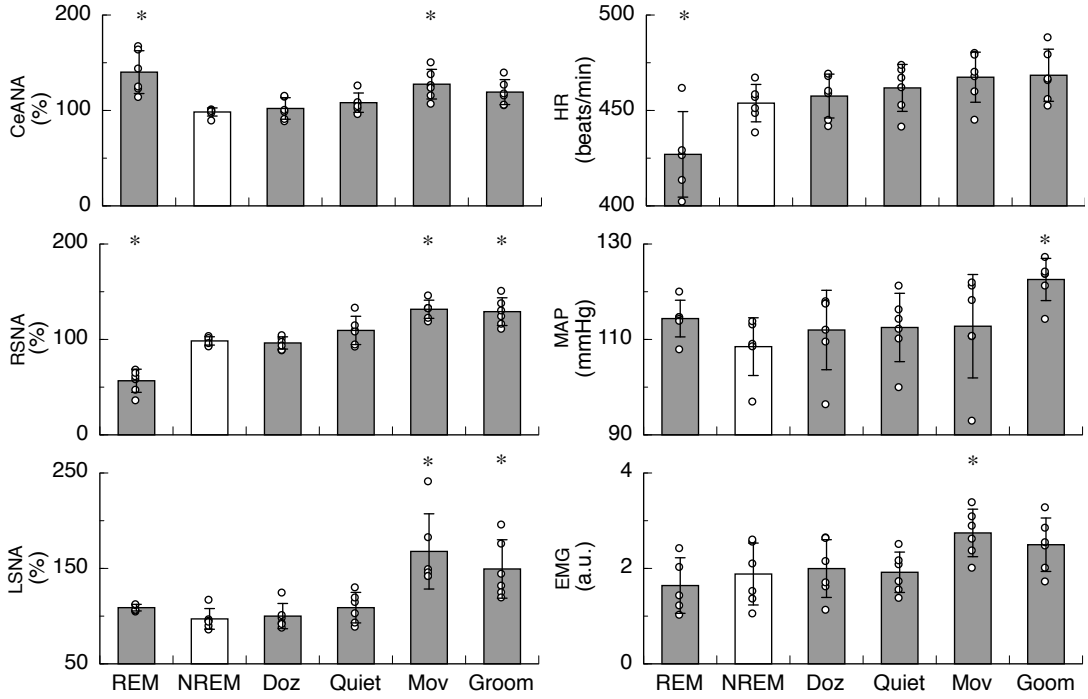

Figure 4. Changes in CeANA, RSNA, LSNA, HR, mean AP (MAP), and EMG during daily activities.

Data were recorded during rapid-eye movement sleep (REM), non-REM sleep (NREM), dozing (Doz), quiet awake (Quiet), moving (Mov), and grooming (Groom) states. Each column and error bar represents the mean ± SD (n=6 rats). $^{*}P < 0.05$ vs. NREM sleep.

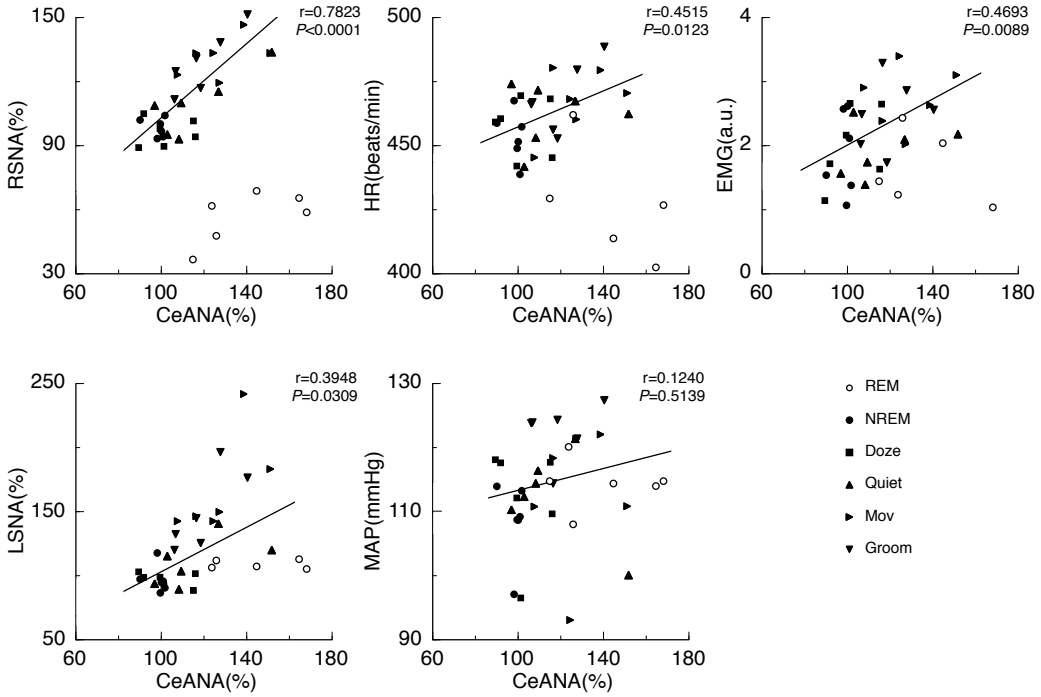

Figure 5. Relationship between CeANA and RSNA, HR, EMG, LSNA, and MAP across the changes in behaviour from rapid-eye movement sleep (REM) to the non-REM sleep (NREM,), dozing (Doz), quiet awake (Quiet), moving (Mov), and grooming (Groom) states.

A significant linear relationship was observed between CeANA and RSNA, CeANA and LSNA, CeANA and HR, and CeANA and EMG while the linear relationship between CeANA and MAP did not reach statistical significance. The relationships between CeANA and RSNA, LSNA, HR, AP, and EMG during REM sleep, which are shown in open circles, deviated from linearity.

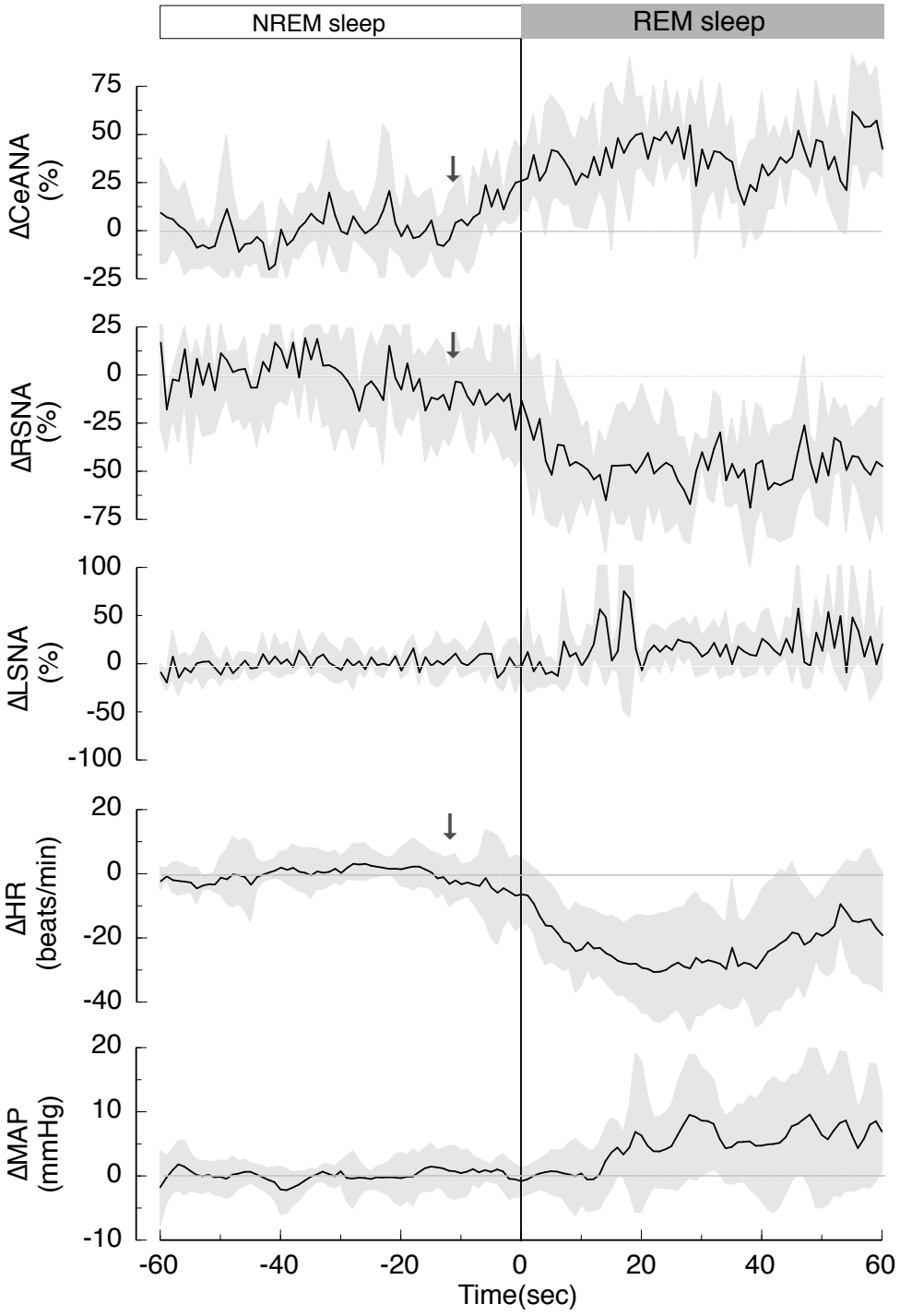

Figure 6. Time course of the changes in CeANA, RSNA, LSNA, HR, and MAP during the transition from NREM to REM sleep.

Each line shows the changes in mean values (n = 6 rats) relative to basal levels from 0 to 30 seconds during NREM sleep. Arrows indicate the point at which the changes were initiated. The shaded area represents ± SD.

Chapter 2

Roles of Central Amygdala Neuronal Activity in Regulating Sympathetic Nerve Activity and Cardiovascular Function in Fear Conditioning

INTRODUCTION

Olfaction is one of the major sensory inputs that caused changes in behavior, autonomic nerve system, and cardiovascular function. Odor input evoked emotional sensation and is play a critical role in inducing fear and anxiety responses. Amygdala receives to olfactory information directly and relays information causing behavior and autonomic and cardiovascular responses. Pavlovian fear conditioning is a paradigm in which organizations learn to predict aversive event. Predator odor causes a patterned response of freezing, autonomic and cardiovascular responses. Odor has been used as a conditioned stimulus (CS) paired with aversive (unconditioned) stimulus (US), an electrical foot shock. The specific odor becomes a stimulus causing fear response by learned fear conditioning. The olfactory system has unique connections to the amygdala. Unlike other sensory systems, olfactory information does not reach the amygdala through a thalamic input. The cortical nucleus of the amygdala (CoA) receives odor information from the olfactory bulb (Price, 1973; McDonald, 1998), and in turn, sends projections to the basolateral nucleus group and central nucleus of amygdala (CeA). CeA sends projection the periaqueductal gray (PAG) (Rizvi *et al*., 1991; Behbehani, 1995) and rostral ventrolateral medulla (RVLM) (Salome *et al*., 2001; Saha *et al*., 2005). The information of conditioned odor reaches directly corticomedial amygdala and then relay to CeANA, PAG, and RVLM coursing behavioral and autonomic responses.

The olfactory fear conditioning has been widely studied though a various approach including anatomical. Majority of these study employ electric lesion of CeA or pharmacological inactivation of CeA function(Goosens & Maren, 2001; Nader *et al*., 2001; Wilensky *et al*., 2006; Zimmerman *et al*., 2007). These studies clearly showed that CeA needed to cause odor cue responses. However quantitatively inter relationship of CeANA, SNA, and freeing has not been showed.

We have not aware of any studies where central amygdala neuronal activity (CeA), sympathetic

nerve activity (SNA), cardiovascular function, and freezing behavior were recorded simultaneously and continuously. Therefor how and when CeA coursed fear responses of freezing, SNA, and cardiovascular function triggered by the olfactory fear conditioning remains unclear.

METHODS

Experiments were performed on 25 Wistar male rats, weighting 254.6 ± 1.8 g. Rats were housed individually in a temperature-controlled (24°C) and light- controlled (12 h: 12 h light-dark cycle, light 0700-1900) room. The animals were allowed standard laboratory rat chow and water ad libitum and were handled every day. All procedures were undertaken in accordance with the Guiding Principles in the Care and Use of Animals in the Field of Physiological Sciences published by the Physiological Society of Japan (Physiological Society of Japan, 2002), and with the prior approval of the Animal Care committee of Nara Women's University.

Surgical procedures

The animals were operated on in two stages. All procedures were performed aseptically in operating theater. First surgery: Implantation of the electrodes for measurement for RSNA and LSNA, and electrocardiogram (ECG), cervical electromyogram (EMG) electrodes was performed. Rats were anesthetized with pentobarbital sodium (75mg/ kg ip) and isoflurane. Briefly, the electrodes for measurement for RSNA and LSNA were implanted as described in our previous reports. Briefly, the left kidney was exposed retroperitoneally through a flank incision. Approximately 2mm of the renal sympathetic nerve was carefully isolated, and a bipolar stainless steel wire electrode (AS633 Cooner, Chatsworth, CA) was hooked onto the renal nerve. Both were

embedded in a two-component silicone rubber. To implant the LSNA electrode, a midline abdominal incision was made. After retraction of the intestines, the abdominal aorta and vena cava were gently pulled aside to expose a lumbar nerve. Approximately 3mm of the left lumbar sympathetic trunk was carefully isolated from the connective tissue. A bipolar stainless steel wire electrode (AS633) was hooked onto the sympathetic trunk between L3 and L4 both were embedded in a two-component silicone rubber. The bipolar EMG electrodes were implanted bilaterally in both trapezium muscles. The bipolar ECG electrode was implanted under the skin at the manubrium of the sternum and xiphoid process. The electrodes were exteriorized at the back of the neck and passed through the center of circular Ducron sheet, which was fixed into lace by suturing to the skin and protected by plastic tubes. The electrodes were exteriorized as described above. Second surgery; A period of at least 4 days was allowed before second surgery, at which time the electrodes for measurement of central amygdala neuronal activity, and cervical electromyogram electrode, and arterial catheter were implanted. The head of the rat was then secured in a stereotaxic apparatus (David Kopf, Tujunga, CA), EEG electrodes were implanted over frontal cortex (AP: 1.5 mm, ML: -2.0 mm from the bregama), parietal cortex (AP: -3 mm, ML: -2.0 mm from the bregama), and over the cerebellum (1.5mm posterior to lambda). Three stainless steel miniature screws (1.0 mm diamerer), which served as electrodes, were screwed in the skull. Then, the implantation of the electrode for measurement of central amygdala neuronal activity was carried out. An area approximately 1.5mm in diameter was thinned in parietal cortex (anteroposterior -4.5 mm, mediolateral -2.3 from bregma) bone using a dril. Drilling (1.5mm diameter) was performed until episual and pial vessels were visible. The thin cranial plate and the dura in a hole were carefully removed by distorted needle under the microscope (POM-50II, Konan Medical Inc. Hyogo, Japan). The electrode then were lowered stereotaxically into the right central nucleus of amygdala through

the cranial hole at the speed of 0.1 mm per min until action potentials with pyramidal cell firing characteristics were recorded. The signal of electrodes was amplified by a differential amplifier (Biotex, Kyoto, Japan) and displayed on an oscilloscope and made audible with an audio amplifier. After confirming the CeANA, CeANA and EEG electrodes were fixed on the skull with dental cement and four stainless steel screws were anchored to the skull. Thereafter, the arterial catheter was implanted into the abdominal aorta via the tail artery.

On completion of each surgery, antibiotics were given I.P. (Fradiomycin 200 mg/kg, Mochida-Seiyaku, Tokyo, Japan). The animals were individually housed in transparent plastic cages and allowed standard laboratory rat chow and water ad libitum, and weighed and handled every day, and the status of the animals was checked by experienced researchers. Arterial catheters were filled with heparin sodium solution (250 i.u. /ml) and were flushed every day.

Measurements

Central amygdala neuronal activity recording from each microwire were obtained using the differential amplifier that connects to a multichannel neuronal recording system (plexon Inc., Dallas, TX) and store the disk for offline spike discrimination. Extraceller single units were discriminated using time-voltage windows and a principal component-based spike-sorting alogorithm. Fire rate of central amygdala neuronal activity was estimated every 1 sec bin. The EEG, ECG, cervical EMG, RSNA, and LSNA signals were amplified by a different amplifiers (MK-2, Bioteck, Kyoto, Japan). AP was measured by connecting its catheter to a pressure transducer (DX-100, Nihon Kohden, Tokyo, Japan). Heart rate (HR) was determined with a cardiotachometer (AT-601G, Nihon Kohden, Tokyo, Japan) triggered by the ECG. Physiological data were recorded simultaneously on thermal head paper recorder (ORP1200, Yokogawa, Tokyo, Japan) and analog-to-digital conversions were

taken at 2 kHz sampling rates (Labview, National Instruments, Austin, Texas). EEG was Fourier analyzed in 1 s epochs using a data acquisition program for computer. The power spectrum was averaged in three frequency bands: Delta (0.5-4Hz), theta (6-9Hz). The root mean square value of EMG was calculated simultaneously. The mean values of the data were calculated simultaneously and continuously displayed on the computer monitor every 1 sec, and stored on a hard disk.

Experimental protocols

After the second surgery, rats were allowed a minimum of 15 hours to recover. Experiments were performed with the animals in their home cage (26×17×32 cm), and they were given free access to food and water. Each experiment was performed after an hour rest when all parameters had been connected to the measuring instruments. The rats were rested for 30 minutes from the start of the experiment. And then rats were randomly presented 3 different odors for 30s with a 10min interval. The presented odors are anisole (ANS) paired 5mA foot shock, eugenol (EGN), and odor-free (CNT). CNT is a plain filter paper (0.6 cm × 15 cm) for the control condition. Anisole and eugenol (30 μl) was pipetted onto a filter paper (0.6 cm × 15 cm). Rats were presented a filter paper with each odor hanging in the middle of their home cage. After finishing home cages procedure, animals were placed in foot shock chamber for 60 min, in which rats received twice foot shock paired with anisole. This procedure was repeated once a day for 4days in freely moving rats. All parameters were measured continuously and simultaneously, and behavioral observations were recorded through out the experimental period.

Olfactory fear conditioning

Fear conditioning were done in a shock cage (26×17×32 cm) with a grid floor composed of 16 stainless steel rods (5 mm in diameter), spaced 1 cm apart and wired to a shock generator (SGA-2010, O'Hara & Co., Ltd). For fear conditioning, rats were placed in a shock cage with a metal grid floor. Rats were presented a filter paper with anisole hanging in the middle of a shock cage to learn the odor of anisole. And then rats were given an electrical shock (1sec, 5mA) after 25 seconds from presented ANS. With this protocol, rats associated a foot shock with anisole.

Histology

At the end of the entire procedure, rats were anaesthetized and the location of electrodes was marked by passing a DC current of 40μA for as anode. The rats were killed using an intravenous overdose of pentobarbital sodium (> 200 mg kg^{-1}) and the brain was removed and fixed by immersion in 1 % potassium ferrocyanide in formalin for 7days. With time, ferrocyanide caused the conversion of the iron deposit to a Prussian blue spot. The brains were transferred to a 15% sucrose in .1-mol/L phosphate buffer solution, after 24 hours were stored in a 25% sucrose in .1-mol/L phosphate buffer solution in 48 hours. Brains were sliced into 50μm section with a freezing microtome. Every other section was collected on a slide and stained cresyl violet and recoding electrode placements were identified.

Statistical Analysis

Statistical evaluation was performed with analysis of variance (ANOVA) for repeated measures. When the F values were significant ($P<0.05$), individual comparison were made by Fisher's least significant difference test (Sachs, 1982). Correlations between two variables were analyzed by a least squares linear regression. Values were reported as means ± SE.

RESULT

Basal levels of measured parameters were shown Table.1. Repeated fear conditioning over 4 days caused no changes in basal levels of EEG theta power, EEG delta power, HR, and EMG. However in contrast CeANA increased significantly by 14.6%, LSNA by 23.3%, MAP by 17mmHg due to the repeated fear conditioning. The basal levels of RSNA decreased significantly by 15%.

Fig.3 shows the time course of changes in freezing rate before and after exposure. On the exposure of a filter paper and eugenol, the freezing rate increased immediately to 52% and 64 % respectively at 11sec. And then it decreased rapidly to the pre-exposure level within 2min. On the exposure of anisole, the freezing rate increased immediately to 76% at 8 sec, and then reached maximum to 88%. Increased level was maintained around 60% from 2min to 6min.

Fig.4 shows the time course of changes in CeANA, RSNA, LSNA, HR, and MAP from the basal levels, pre-exposure during 30 sec exposure of a filter paper either with odor (EGN) or without odor (CNT), and post-exposure. CeANA increased fragmentally but significantly in response to ANS and EGN exposure while it did not change significantly in response to CNT exposure. The other parameters measured in this study did not significantly the odor exposures. After repeated fear conditioning over 4 days, CeANA increased significantly during odor exposure by 9.9±1.7, 7.5±1.6, 5.3±1.7% from 6sec to 30sec in ANS, EGN, CNT, respectively. Then, CeANA decreased pre-exposure levels within 2min in EGN and CNT experiment. In ANS, CeANA remained significantly increased level until 2min and 55sec. There was a significantly but fragmentarily difference in CeANA between ANS vs EGN, and ANS vs CNT until 6min.two peaks observed before and after odor exposure in ANS, EGN, CNT experiment were corresponded to the events of opening and closing the door of the experimental chamber. RSNA increased significantly in response to ANS

exposure only from 11sec to 35sec in while that in EGN and CNT did not change significantly. There was significantly difference in RSNA between ANS and CNT from 11sec to 25sec. LSNA increased significantly from 6sec to 2min 5sec in response to ANS while that in EGN and CNT did not change significantly. Odor exposure increased MAP rapidly by 5.0±0.8, 3.8±1.0, 2.4±1.0 mmHg from 6sec to 30sec in ANS, EGN, CNT experiment respectively. The MAP in in ANS experiment remained higher level with 3min, while it in EGN and CNT decreased rapidly to the pre-exposure level in 1min. Odor exposure of A and E caused on gradually increased HR reaching peak level to 17.1±5.6 at 2min 13sec, and 16.0±4.6 beats/min at 2min 42sec in ANS and EGN experiment, respectively. The HR in CNT remained changed during though out the observation period. There was a significantly difference in HR between A vs C, E vs C, fragmentarily from 1min 11sec to 4min 20sec.

Fig.6 showed the relationship between changes in CeANA and RSNA (Fig.6A), changes in CeANA and LSNA (Fig.6B), CeANA and MAP (Fig.6C), and changes in CeANA and HR (Fig.6D) for 3 min from the onset of odor exposure. There was a significant ($P<0.05$) inverse linear relationship between CeANA and RSNA, CeA and LSNA, CeANA and MAP, and CeA and HR.

DISCUSSION

Major findings in this study were repeated olfactory fear conditioning result in patterned changes in CeANA, RSNA, LSNA, MAP, and HR following odor cue exposure. There were significant linear relationships between CeANA versus RSNA, LSNA, MAP, and HR. We therefor concluded that repeated olfactory fear conditioning potentiate robust neuronal network between CeANA – SNA – MAP axis.

Anatomical study clearly showed the CeANA neuronal projection to sympathetic premotor neuron RVLM. Amygdala plays a central role in learning fear conditioning. Thus it has been suggest that there should be a relationship between CeANA and SNA in fear-conditioned animals. However we have not aware of any studies where CeANA and SNA measured simultaneously and the freely moving rats. The present study provides direct and quantity evidence at the relationship between CeANA and SNA in fear conditioned animals.

Firstly, repeated olfactory fear conditioning resulted in greater and sustained increase in CeANA following the exposure of cue odor (ANS) compared with odor–free (CNT) and unpaired odor (EGN). Although fear conditioning by tone–shock pairing has been extensively studied, fear conditioning by odor – shock pairing reported fragmentarily. Dielenberg et al. reported that innate fear (cat odor) increases CeA activity measured by c-fos. The present data showed clearly olfactory fear conditioning results in the increase in CeANA triggered by odor cue. Learning fear conditioning is consisted of acquisition, consolidation, and recall process. Thus 4 days repeated olfactory fear conditioning established the odor cue patterned responses triggered by odor cue.

Secondly, change in CeANA triggered by the odor cue was well associated with RSNA, LSNA, MAP. These observations are consistent with anatomical study on the neuronal networks between CeA and sympathetic premotor neuron in RVLM. Consistently, Hori et al. showed that TMT innate odor increases in adrenal sympathetic nerve activity in urethane-anesthetized rats. The increase in RSNA, LSNA could well explain the increase in MAP. The fact that increase MAP in response to odor cue is well consisted with previous reports where MAP increase in response to the cat odor exposure(Dielenberg *et al*., 2001). However interestingly HR response showed negative linear relationship between CeANA and HR. Consistent with this result, there has been reported showing the significant linear relationship between CeANA ans HR in fear conditioned rabbits(Pascoe &

Kapp, 1985). This suggests that the increase CeANA might cause an increase in cardiac para-sympathetic nerve activity such that cardiac para-sympathetic nerve activity changes HR predominantly, causing the increase relationship between CeANA and HR. Taken together, these results showed that the transient increased in CeANA triggered by odor cue caused an increased RSNA, LSNA, and possibly cardiac pare sympathetic nerve activity, causing vasoconstriction of peripheral such that MAP increased transiently.

This study is consistent with previous report reported that impaired amygdala function diminished freezing response in fear conditioned rats. CeANA plays a critical role in inducing freezing behavior in fear-conditioned rats. In present study, we could compare the time course of changes in CeANA and percentage changes in freezing behavior. CeANA significantly increased from 0sec to 2 min 55 sec and then it kept increased until 6 min while it did not reach statistical difference. This is similar to the time course of changes in freezing behavior. It should be emphasis the peak percent of freezing behavior was observed at 50 sec in ANS while that of at 11sec both CNT and EGN experiment. The discrepancy of time between11 sec and 50 sec could be a neuronal processing time for distinction of the odor. Isosaka et al. and Sevelinges et al. showed that the magnitude of increase in percentage of freezing rate was greater in conditioned odor than non-conditioned odor (Sevelinges *et al*., 2004; Isosaka *et al*., 2015). CeANA in CNT and EGN returned pre–exposure level at 50sec. These data in CNT, EGN, and ANS suggest that the time course of changes in CeANA were directly related to that of freezing rate. The about view is well consistent with the previous report where function of amygdala impaired by pharmacologically inactivate by muscimol, anisomysin (protein synthesis inhibitor), ibotenic aci (agonists of NMDA-type receptors and metabotropic receptors,) and by electrical lesion. This study consistently reported that impaired amygdala function diminished freezing response in fear conditioned rats.

EEG theta power decrease and EEG delta power increased in response to odor exposure in CNT, EGN, and ANS experiment. There were no statistical differences in EEG theta power and EEG delta power between CNT, EGN, and ANS experiment. These data suggest that EEG theta and delta power could not represent neuronal activity modulation in fear conditioning.

The time course of change in RSNA, LSNA, MAP, and freezing rate well consisted with that of the change in CeANA. It is therefor concluded that the time course of the changes in CeA activity reflect directly and quantity to the changes in RSNA, LSNA, MAP, and freezing behavior.

REFERENCES

Behbehani MM. (1995). Functional characteristics of the midbrain periaqueductal gray. *Progress in neurobiology* **46,** 575-605.

Dielenberg RA, Carrive P & McGregor IS. (2001). The cardiovascular and behavioral response to cat odor in rats: unconditioned and conditioned effects. *Brain research* **897,** 228-237.

Goosens KA & Maren S. (2001). Contextual and auditory fear conditioning are mediated by the lateral, basal, and central amygdaloid nuclei in rats. *Learn Mem* **8,** 148-155.

Isosaka T, Matsuo T, Yamaguchi T, Funabiki K, Nakanishi S, Kobayakawa R & Kobayakawa K. (2015). Htr2a-Expressing Cells in the Central Amygdala Control the Hierarchy between Innate and Learned Fear. *Cell* **163,** 1153-1164.

McDonald AJ. (1998). Cortical pathways to the mammalian amygdala. *Progress in neurobiology* **55,** 257-332.

Nader K, Majidishad P, Amorapanth P & LeDoux JE. (2001). Damage to the lateral and central, but not other, amygdaloid nuclei prevents the acquisition of auditory fear conditioning. *Learn Mem* **8,** 156-163.

Pascoe JP & Kapp BS. (1985). Electrophysiological characteristics of amygdaloid central nucleus

neurons during Pavlovian fear conditioning in the rabbit. *Behavioural brain research* **16,** 117-133.

Price JL. (1973). An autoradiographic study of complementary laminar patterns of termination of afferent fibers to the olfactory cortex. *The Journal of comparative neurology* **150,** 87-108.

Rizvi TA, Ennis M, Behbehani MM & Shipley MT. (1991). Connections between the central nucleus of the amygdala and the midbrain periaqueductal gray: topography and reciprocity. *The Journal of comparative neurology* **303,** 121-131.

Sachs. (1982). *Applied Statistics*. Springer-Verlag, New York, NY, USA.

Saha S, Drinkhill MJ, Moore JP & Batten TF. (2005). Central nucleus of amygdala projections to rostral ventrolateral medulla neurones activated by decreased blood pressure. *The European journal of neuroscience* **21,** 1921-1930.

Salome N, Viltart O, Leman S & Sequeira H. (2001). Activation of ventrolateral medullary neurons projecting to spinal autonomic areas after chemical stimulation of the central nucleus of amygdala: a neuroanatomical study in the rat. *Brain research* **890,** 287-295.

Sevelinges Y, Gervais R, Messaoudi B, Granjon L & Mouly AM. (2004). Olfactory fear conditioning induces field potential potentiation in rat olfactory cortex and amygdala. *Learn Mem* **11,** 761-769.

Wilensky AE, Schafe GE, Kristensen MP & LeDoux JE. (2006). Rethinking the fear circuit: the central nucleus of the amygdala is required for the acquisition, consolidation, and expression of Pavlovian fear conditioning. *The Journal of neuroscience : the official journal of the Society for Neuroscience* **26,** 12387-12396.

Zimmerman JM, Rabinak CA, McLachlan IG & Maren S. (2007). The central nucleus of the amygdala is essential for acquiring and expressing conditional fear after overtraining. *Learn Mem* **14,** 634-644.

Table 1.basal level

	Day 1	*Day 4*
EEG theta power (a.u.)	5.2 ± 0.3	3.0 ± 0.2*
EEG delta power (a.u.)	10.0 ± 0.04	10.1 ± 0.04
CeANA (%)	100.1 ± 0.3	114.6 ± 2.9*
RSNA (%)	101.1 ± 2.2	86.1 ± 5.6*
LSNA (%)	103.0 ± 2.8	126.3 ± 8.2*
MAP (mmHg)	103.2 ± 0.7	120.2 ± 1.2*
HR (beats/min)	451.9 ± 2.8	447.2 ± 2.7
EMG (a.u.)	0.5 ± 0.02	0.6 ± 0.03

Values are means ± S.E.M. EEG,electroencephalogram; CeANA, central amygdala neuronal activity; RSNA, renal sympathetic nerve activity; LSNA, lumber sympathetic nerve activity; MAP,mean arterial pressure;HR, heart rate; EMG,cerebral electromyogram.*P<0.05 vs. Day1.

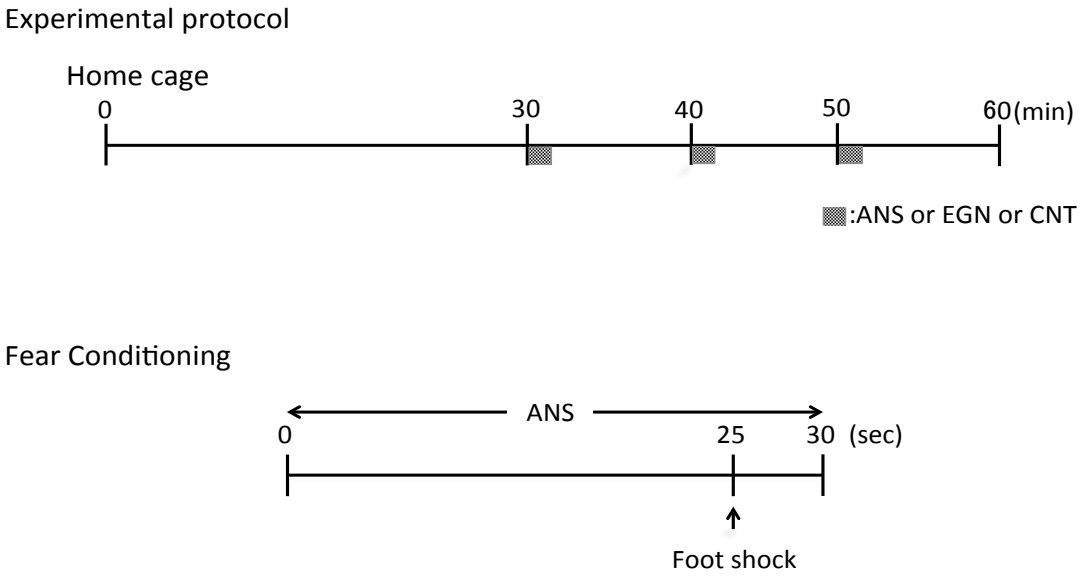

Figure 1. A: Schematic diagram of the experimental protocol for odor rest in home cage over 60 min in home cages. Anisole (ANS) paired with 5mA foot shock, eugenol (EGN), or odor-free (CNT) was randomly presented for 30s with a 10 min interval. Dot pattern squares represent odor exposure for 30 sec. CNT is a plain filter paper for the control condition. B: Schematic diagram of the fear conditioning. Fear conditioning was carried out in a shock cage. The ANS odor paired with a 5mA foot shock was given to animals two times with a 10 min interval per day over 3 days.

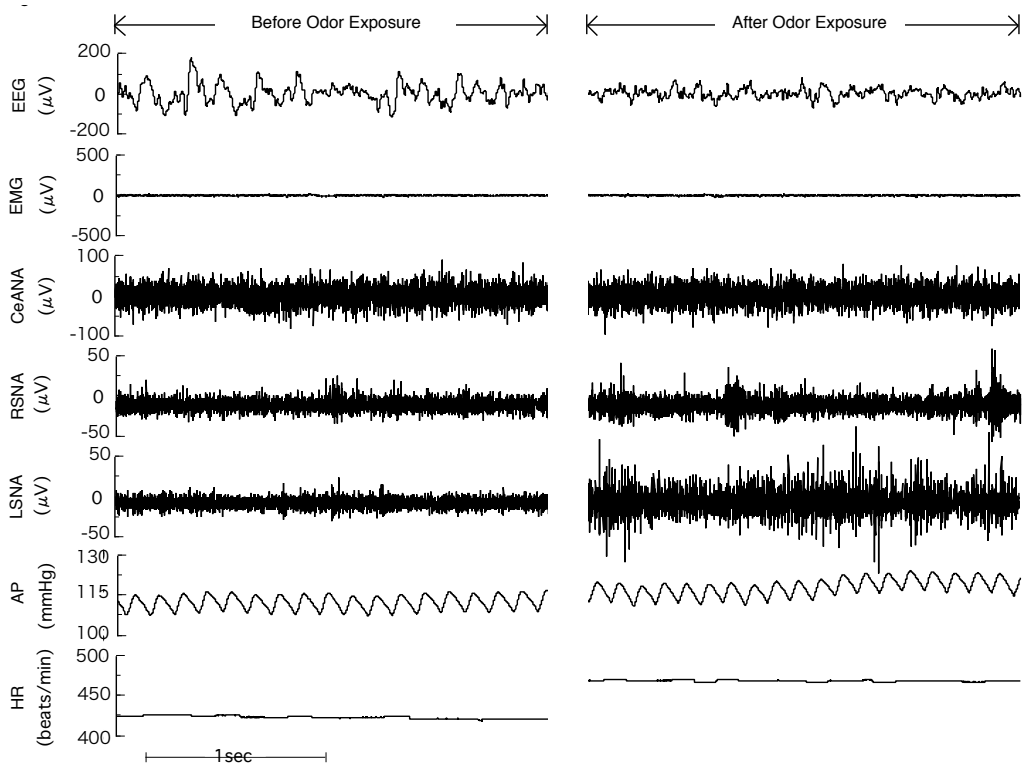

Figure 2. Typical recordings from an individual rat. Parameters are shown the electroencephalogram (EEG), cervical electromyogram (EMG), central amygdala neuronal activity (CeANA), renal sympathetic nerve activity (RSNA), lumbar sympathetic nerve activity (LSNA), arterial pressure (AP), and heart rate (HR). These were observed before and after odor exposure.

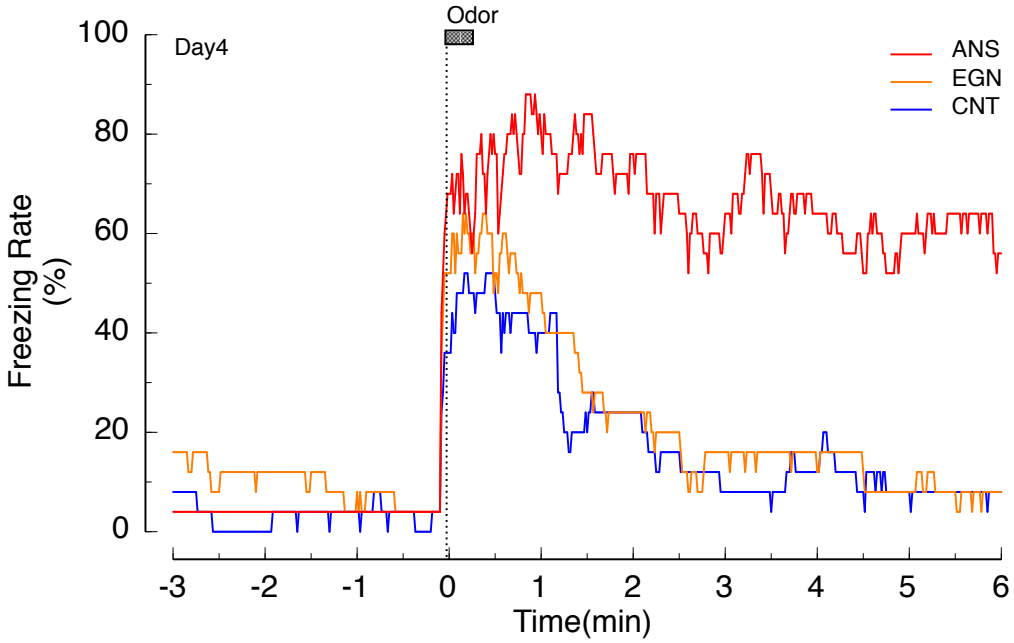

Figure 3. Changes in freezing rate before during 30sec and after odor exposure in control (CNT, blue line), eugnole (EGN, orange line), and anisole (ANS, red line) experiments. Lines show mean value obtained from 25 rats. Control is a plain filter paper.

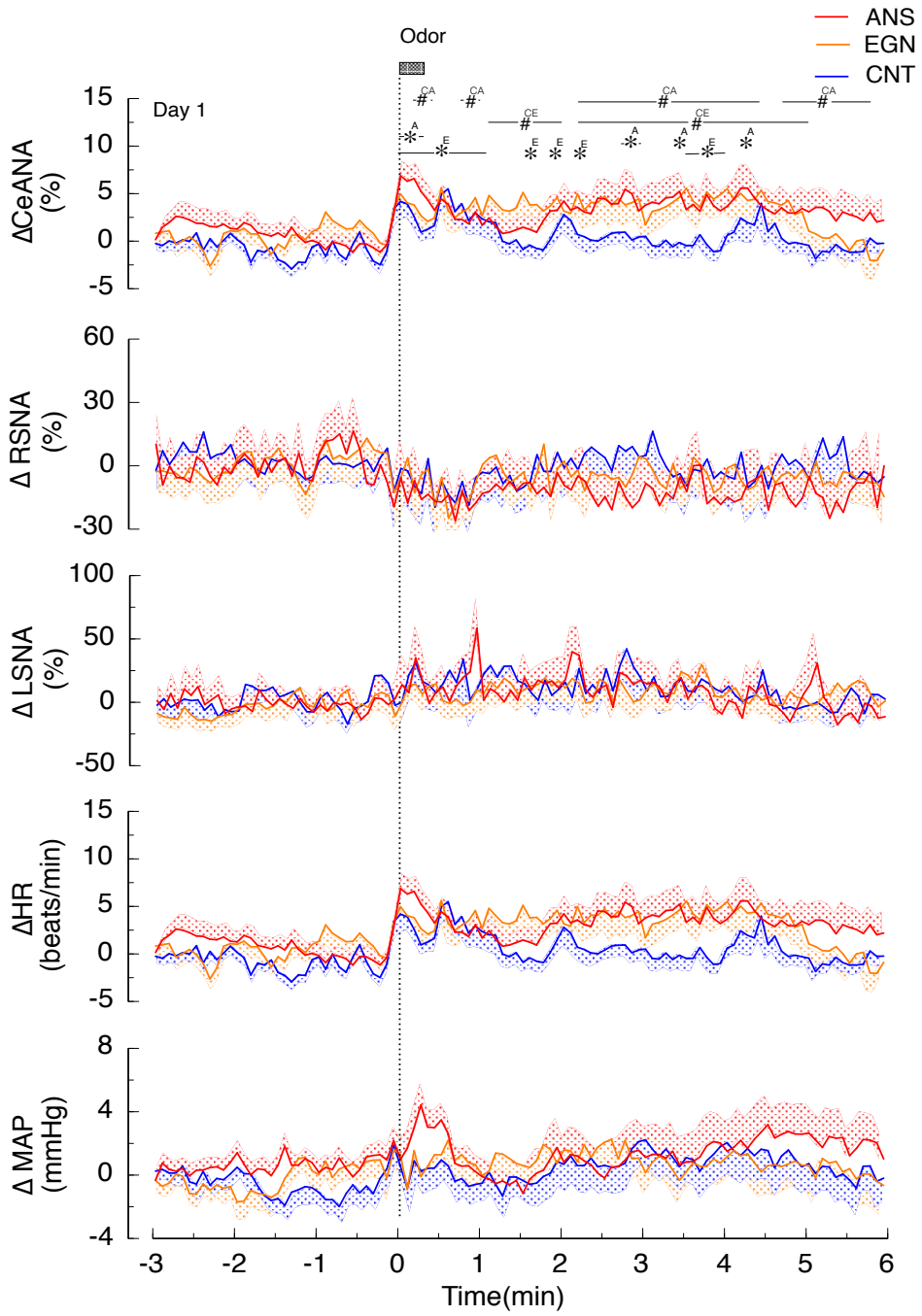

Figure 4. Changes in CeANA, RSNA, LSNA, HR, and MAP before during 30sec and after odor exposure in control (CNT, blue line), eugnole (EGN, orange line), and anisole (ANS, red line) experiments before fear conditioning (Day 1). Mean values obtained for every 5 sec bin relative to the mean level of the pre-exposure period in 25 rats as shown. Shaded area above and below mean lines represents ±SEM. Dot line represent to start odor exposure. Dot pattern square represent odor exposure for 30 sec. $*_{C,E,A}$ Statistically different (P<0.05) from pre-exposure level in CNT(C), EGN(E), ANS(A), respectively. $\#_{CE,CA}$Statistically different (P<0.05) between CNT versus EGN (CE), CNT versus ANS (CA), respectively at corresponding time.

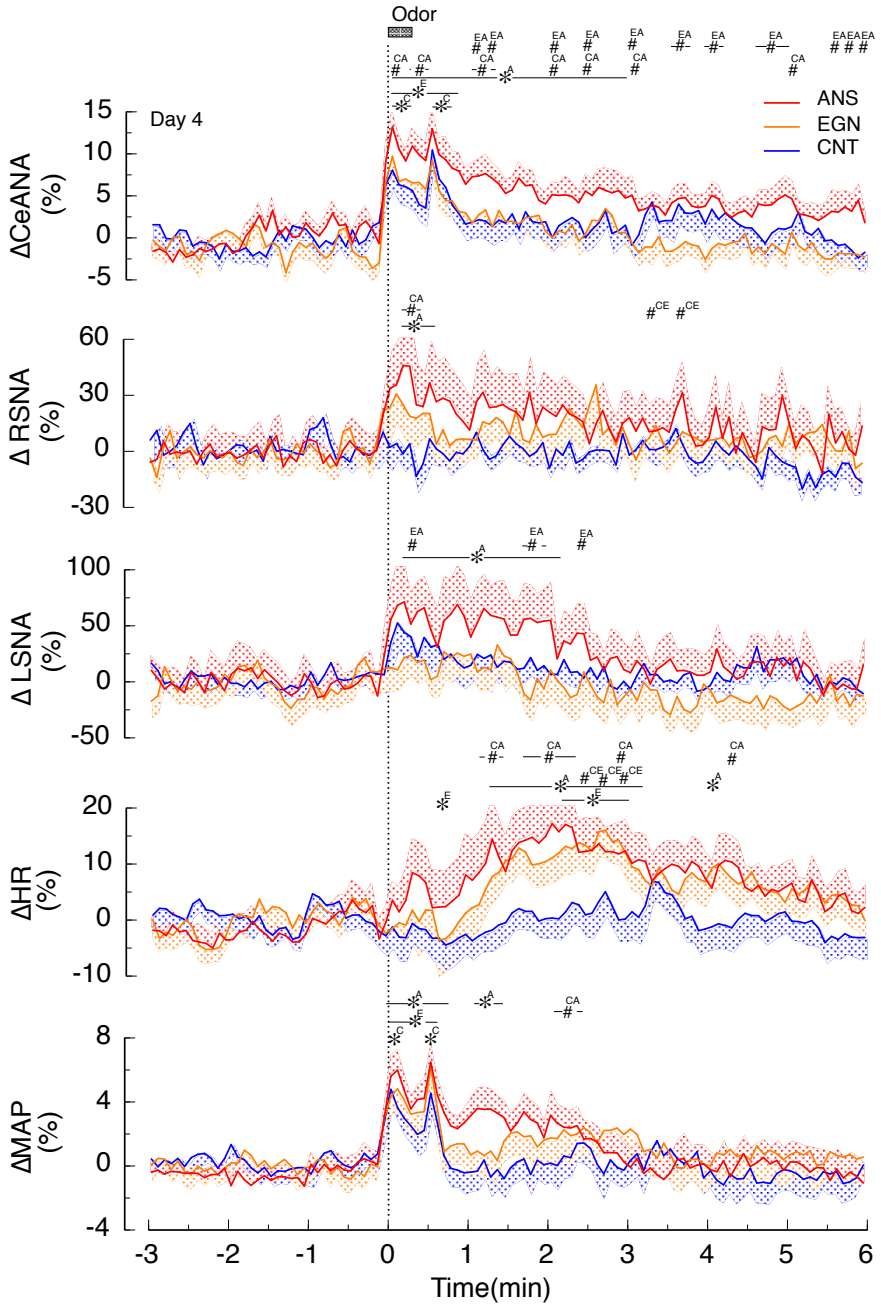

Figure 5. Changes in CeANA, RSNA, LSNA, HR, and MAP before during 30sec and after odor exposure in control (CNT, blue line), eugnole (EGN, orange line), and anisole (ANS, red line) experiments after fear conditioning (Day 4). Mean values obtained for every 5 sec bin relative to the mean level of the pre-exposure period in 25 rats as shown. Shaded area above and below mean lines represents ±SEM. Dot line represent to start odor exposure. Dot pattern square represent odor exposure for 30 sec.*^{C,E,A}Statistically different (P<0.05) from pre-exposure level in CNT(C), EGN(E), ANS(A), respectively. #^{CE,CA,EA}Statistically different (P<0.05) between CNT versus EGN (CE), CNT versus ANS (CA), EGN versus ANS (EA), respectively at corresponding time.

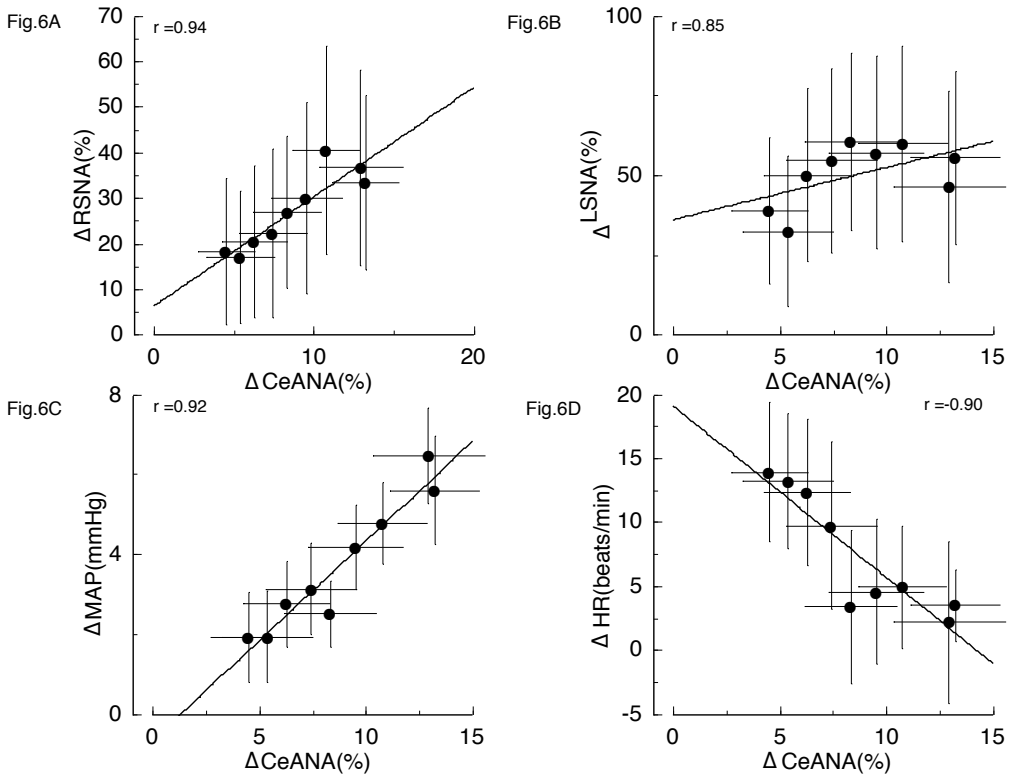

Figure 6. A: The relationship between central amygdala neuronal activity (CeANA) and renal sympathetic nerve activity (RSNA) during and after odor exposure. Mean values of CeANA and RSNA over each 1% bin of CeANA obtained from 36 values from 25 rats were plotted and a regression line Error bars represent S.E.M. in each bin. There was a significant (p<0.05) inverse liner relation relationship between CeANA and RSNA. B: The relationship between central amygdala neuronal activity (CeANA) and lumber sympathetic nerve activity (LSNA) during and after odor exposure. Mean values of CeANA and LSNA over each 1% bin of CeANA obtained from 36 values from 25 rats were plotted and a regression line Error bars represent S.E.M. in each bin. There was a significant (p<0.05) inverse liner relation relationship between CeANA and LSNA. C: The relationship between central amygdala neuronal activity (CeANA) and mean arterial pressure (MAP) during and after odor exposure. Mean values of CeANA and MAP over each 1% bin of CeANA obtained from 36 values from 25 rats were plotted and a regression line Error bars represent S.E.M. in each bin. There was a significant (p<0.05) inverse liner relation relationship between CeANA and MAP. D: The relationship between central amygdala neuronal activity (CeANA) and heart rate (HR) during and after odor exposure. Mean values of CeANA and HR over each 1% bin of CeANA obtained from 36 values from 25 rats were plotted and a regression line Error bars represent S.E.M. in each bin. There was a significant (p<0.05) inverse liner relation relationship between CeANA and HR.

Chapter 3

The Paraventricular Nucleus Impacts Sympathetic Nerve Activity, Heart Rate, and Arterial Pressure through the Very Low and Low Frequency Bands

ABSTRACT

The hypothalamic paraventricular nucleus (PVN) contains the autonomic premotor neurons of the sympathetic nervous system and is known to play an critical role in the regulation of sympathetic nerve activity (SNA) and in the regulation of heart rate (HR), and arterial pressure (AP). Although there have been extensive studies on the neuronal circuitry of the PVN and SNA and its neurotransmitters, how the PVN is involved in SNA, HR, and AP regulation, particularly with regard to the dynamic regulatory mechanisms including time axis, is still unclear. In this study, we investigated the possibility of which frequency bands are involved in the regulation of the PVN by measuring simultaneously and continuously the PVN, renal SNA (RSNA) and lumbar SNA (LSNA), HR, and AP during non-rapid eye movement (REM) and REM sleep in conscious rats. We used male Wistar rats to examine extracellular neuronal activity in PVN, RSNA, LSNA, HR, AP, electroencephalogram, and electromyography were chronically implanted with electrodes and catheter. The results demonstrated that the paraventricular nucleus nerve activity exhibited a power spectrum with two peaks: very low frequency (VLF, 0.06~0.2 Hz) and low frequency (LF, 0.2 Hz~1.0 Hz). On the other hand, renal and lumbar sympathetic nerve activity and arterial pressure showed four peaks in the respiration-related frequency band (RF, 1-3 Hz) and the cardiac-related frequency band (CF, 6-8.5 Hz) in addition to VLF and LF. Heart rate had three frequency bands: VLF, LF, and RF. In other words, PVN-SNA-HR and -AP have common frequency bands of VLF and LF. During the REM sleep phase, the VLF and LF power of the RSNA and LSNA decreased, but the power of the PVN, AP, and HR did not. These data suggest that VLF and LF frequency band oscillations in heart rate and arterial pressure may not always be linked to SNA but may be directly influenced by PVN

INTRODUCTION

The paraventricular nucleus plays a major role in regulating sympathetic nerve activity and arterial pressure (Swanson & Sawchenko, 1980). Small pre-autonomous neurons in the paraventricular nucleus project to the rostral medullary ventral lateral area and to the intermediate lateral nucleus where pre-sympathetic ganglion neurons are located (Pyner & Coote, 2000) and are thought to be directly or indirectly involved in the regulation of sympathetic activity (Badoer, 2001). Sympathetic activity has also been reported to be altered by glutamate and GABA intrinsic to the PVN (Akine *et al*., 2003; Li *et al*., 2006). Furthermore, administration of bicuculline to the PVN has been reported to increase arterial pressure and heart rate (Schlenker *et al*., 2001). Thus, although anatomical and pharmacological evidence indicates that the paraventricular nucleus is involved in the regulation of sympathetic nerve activity and arterial pressure, there is as yet no direct evidence of how paraventricular nucleus neural activity is involved in the regulation of sympathetic nerve activity and arterial pressure.

Sympathetic activity is characterized by rhythmic activity, and frequency components of sympathetic activity have been shown to be related to arterial pressure regulation. It has been reported that renal sympathetic activity in conscious rats consists of four frequency components of 0.5, 1.5, 6, and 12 Hz, corresponding to low frequencies of heart rate and arterial pressure, respiration, heart rate, and harmonics of heart rate (harmonics), respectively (Kunitake & Kannan, 2000). It is widely accepted that the frequency components of sympathetic activity depend on reflexive control of respiration and heart rate. On the other hand, the lower frequency components below the respiratory frequency continue to be debated (Kuusela *et al*., 2003).

The paraventricular nucleus has been implicated in the generation of the frequency component of sympathetic activity (Kenney *et al*., 2003). Administration of bicuculline to the paraventricular nucleus has been reported to increase the low-frequency component of renal, adrenal, and lumbar sympathetic nerve activity (Kenney *et al*., 2001). The rostral medullary ventral lateral area has also been reported to contain neurons with a common rhythm with a frequency component below 1 Hz

of sympathetic activity (Tseng *et al*., 2009). Based on these findings, it is possible that the paraventricular nucleus may also contain neurons with a common rhythm with sympathetic activity. However, to the best of our knowledge, there have been no reports on the frequency components of paraventricular nucleus neural activity, and it remains unclear how the frequency components of paraventricular nucleus neural activity are involved in the frequency components of sympathetic neural activity.

The purpose of this study was to investigate how the frequency components of paraventricular nucleus nerve activity are involved in sympathetic nerve activity and arterial pressure regulation. To achieve this objective, simultaneous measurements of paraventricular nucleus nerve activity, renal and lumbar sympathetic nerve activity, heart rate, and arterial pressure were performed in conscious rats. To date, most studies on the relationship between the paraventricular nucleus and sympathetic nerve activity have been performed under anesthesia. However, anesthesia has been reported to alter sympathetic nerve activity, arterial pressure, and heart rate (Matsukawa *et al*., 1993). It has also been reported that the response of sympathetic nerve activity to electrical stimulation of the paraventricular nucleus differs between anesthetized and conscious subjects (Kannan *et al*., 1989). Although data from conscious animals are needed to clarify the quantitative relationship between the paraventricular nucleus and sympathetic nerve activity, there are no examples of simultaneous measurements of paraventricular nucleus nerve activity, sympathetic nerve activity, and arterial pressure in conscious rats.

To clarify the effects of frequency components of paraventricular nucleus nerve activity on sympathetic nerve activity and arterial pressure, frequency components of paraventricular nucleus nerve activity, renal and lumbar sympathetic nerve activity, heart rate, and arterial pressure during sleep were also determined. Sleep consists of non-REM and REM sleep. During non-REM sleep, arterial pressure regulation is very stable, but when transitioning from non-REM sleep to REM sleep, arterial pressure regulation becomes unstable (Sei, 2012). Therefore, by comparing the frequency components of paraventricular nucleus nerve activity, renal and lumbar sympathetic

nerve activity, heart rate, and arterial pressure during non-REM and REM sleep, we thought we could clarify how the frequency components of paraventricular nucleus nerve activity contribute to stable arterial pressure regulation.

METHODS

Ethical approval

All procedures were conducted in accordance with the Guiding Principles in the Care and Use of Animals in the Fields of Physiological Sciences published by The Physiological Society of Japan (Physiological Society Japan, 2015) with the prior approval of the Animal Care Committee of Nara Women's University.

Animals

Male Wistar rats weighing 272.8 ± 18.4 g (mean ± standard deviation, n=25) were used all experiments, purchased from SLC (Hamamatsu, Shizuoka, Japan). Rats were housed individually and kept in a chamber (Espec, Osaka, Japan) with controlled temperature (24◦C) and humidity (60%) and a 12 h:12 h light–dark cycle (light on at 07.00 h). Rats were allowed standard laboratory rat chow and water ad libitum and were handled every day. All procedures were undertaken in accordance with the Guiding Principles in

the Care and Use of Animals in the Fields of Physiological Sciences published by the Physiological Society of Japan (Physiological Society of Japan, 2015) , and with the prior approval of the Animal Care committee of Nara Women's University.

Fabrication of the electrode for measurement of PVNNA

The electrode for the measurement of PVNNA was made of two epoxy-coated stainless steel wires (length 2.5cm, diameter 100μm) and connected to two conductors shielded cable (length 65cm,

diameter 1.8mm). A 0.5 cm length of the coat was removed from each of the conductor shielded cables and epoxy-coated stainless- steel wires so that each of the conductor shielded cable could be soldered to one of the stainless- steel wire; these served as the electrodes for PVNNA neuronal recording. The two epoxy-coated stainless- steel wires were pass through stainless needle (26G, length 7mm) for keeping a proper distance between the wires. The shielding of the cable was soldered to the multiple stranded wires (length 45mm, Biomed wire AS633) and served as the grounding electrode.

Surgical procedures

The animals were operated on in two stages. All procedures were performed aseptically in operating theater. The rats were intra- peritoneally premedicated with pentobarbital sodium (65 mg/kg), anaesthetized with isoflurane (1.5–2.0% with air at a rate of 1–1.5 l/min), and given antibiotics (gentamicin sulfate, 10 mg/kg S.C., Schering-Plough K.K., Whitehouse Station, NJ, USA).

During the first surgical procedure, implantation of the electrodes for measurement for RSNA and LSNA, and electrocardiogram (ECG), cervical electromyogram (EMG) electrodes was performed. Briefly, the electrodes for measurement for RSNA and LSNA were implanted as described in our previous reports (Miki *et al*., 2002) (Miki *et al*., 2004). To implant the RSNA electrode, the left kidney was exposed retroperitoneally through a left flank incision, and a branch of the renal nerve running on or beside the renal artery was carefully isolated. Bipolar stainless-steel wire electrodes were hooked onto the nerve, and both were embedded in two-component silicone rubber (Miki *et al*., 2002). To implant the LSNA electrode, a midline abdominal incision was made. After retraction of the intestines, the abdominal aorta and vena cava were gently pulled aside to expose a lumbar nerve. Approximately 3mm of the left lumbar sympathetic trunk was carefully isolated from the connective tissue. A bipolar stainless steel wire electrode (AS633; Cooner Wire, Chatsworth, CA, USA) was hooked onto the sympathetic trunk between L3 and L4, both were embedded in a two-

component silicone rubber (Miki *et al*., 2004). The bipolar EMG electrodes were implanted bilaterally in both trapezium muscles. The bipolar ECG electrode was implanted under the skin at the manubrium of the sternum and xiphoid process. The electrodes and the catheter were tunneled subcutaneously, exteriorized at the back of the neck and protected by plastic tubes.

A period of at least 4 days was allowed before second surgery, at which time the electrodes for measurement of PVNNA, and cervical electromyogram electrode, and arterial catheter were implanted. The head of the rat was then secured in a stereotaxic apparatus (David Kopf, Tujunga, CA), EEG electrodes were implanted over frontal cortex (AP: 1.5 mm, ML: -2.0 mm from the bregama), parietal cortex (AP: -3 mm, ML: -2.0 mm from the bregama), and over the cerebellum (1.5mm posterior to lambda). Three stainless steel miniature screws (1.0 mm diamerer), which served as electrodes, were screwed in the skull. Then, the implantation of the electrode for measurement of PVNNNA was carried out. An area approximately 1.5mm in diameter was thinned in parietal cortex (anteroposterior -1.8 mm, mediolateral -0.4 from bregma) bone using a dril. Drilling was performed until episual and pial vessels were visible. The thin cranial plate and the dura in a hole was carefully removed by distorted needle under the microscope (POM-50II, Konan Medical Inc. , Hyogo, Japan). The electrode then was lowered stereotaxically into the right hypothermic paraventricular nucleus through the cranial hole at the speed of 0.1 mm per 5min until action potentials with pyramidal cell firing characteristics were recorded. The signal of electrodes was amplified by a differential amplifier (Biotex, Kyoto, Japan) and displayed on an oscilloscope and made audible with an audio amplifier. After confirming the PVNNA, PVNNA and EEG electrodes were isolated and fixed on the skull with dental cement. And then, the arterial catheter was implanted into the abdominal aorta via the tail artery.

Finally, the electrodes and the catheter were exteriorized at the back of the neck and passed through the center of circular Ducron sheet, which was fixed into lace by suturing to the skin and protected by plastic tubes. The electrodes were exteriorized as described above.

Upon completion of each surgery, antibiotics were given intra- peritoneally (fradiomycin 200

μg/kg, Mochida-Seiyaku, Tokyo, Japan) and then jelly and a blanket were provided. To control postoperative pain, a non-steroidal anti-inflammatory drug (diclofenac sodium, 0.5–3.0 mg/kg; Novartis Japan, Tokyo, Japan) mixed with jelly was given orally when necessary. The animals were individually housed in transparent plastic cages and allowed standard laboratory rat chow and water ad libitum, and weighed and handled every day, and the stat us of the animals was checked by experienced researchers. Arterial catheters were filled with heparin sodium solution (250 i.u. /ml) and were flushed every day.

Measurements

PVNNA, RSNA, and LSNA were obtained using the differential amplifier that connects to a multichannel neuronal recording system (plexon Inc. , Dallas, TX) and store the disk for offline spike discrimination. Extraceller single units were discriminated using time-voltage windows and a principal component-based spike-sorting alogorithm. Fire rate of PVNNA, RSNA, LSNA was estimated every 1 sec bin.

EEG, EMG, ECG, RSNA and LSNA signals were amplified by a differential amplifier (MK-2, Biotech, Kyoto; the gain and bandwidth, respectively, were as follows: ×10,000 and 0.16–50 Hz (EEG); ×100 and 100–2000 Hz (EMG); ×1000 and 0.16–150 Hz (ECG); ×10,000 and 150–2000 Hz (RSNA and LSNA)). The arterial pressure (AP) was measured by connecting the arterial catheters to pressure transducers (DX-100, Nihon Kohden, Tokyo, Japan). The HR was determined with a cardiotachometer (AT-601G, Nihon Kohden) triggered by the ECG. The amplified RSNA was integrated using a voltage integrator with a time constant of 50 ms (AD-600G, Nihon Kohden). The signals for EEG, EMG, ECG, RSNA, integrated RSNA, LSNA, integrated LSNA, AP and HR were displayed continuously on an oscilloscope and recorded simultaneously on thermal head recording paper (Figure 1a; ORP1200, Yokogawa, Tokyo, Japan). The EEG, EMG, AP, HR, integrated RSNA and integrated LSNA signals were sampled for analog-to-digital conversion at 2 kHz intervals. The digitized EEG signal underwent Fourier analysis in 1 s epochs using a

computerized data acquisition program (LabVIEW, National Instruments, Austin, TX, USA). The power spectrum was averaged simultaneously in two frequency bands: delta (0.5–4 Hz) and theta (6–9 Hz). The digitized EMG signal was simultaneously converted to the mean square root value. With the aid of a data acquisition program (LabVIEW), data for the power spectrums of EEG and the root mean square value of EMG, AP, HR, integrated RSNA and integrated LSNA were averaged simultaneously and continuously every 1 s, displayed on the computer monitor and stored on a hard disk.

Experimental protocols

After the second surgery, rats were allowed a minimum of 15 hours to recover. Experiments were performed with the animals in their home cage, and they were given free access to food and water. Each experiment was performed after an hour rest when all parameters had been connected to the measuring instruments.

Behavioral states were scored by standard criteria on the basis of EEG and EMG as well as behavioral observations noted at the time of date collection. The animal's behavior was classified as rapid eye movement sleep (REM), non-eye movement sleep (NREM), and awake state. REM was characterized by body relaxation, irregular breathing, and muscle twitches in different parts of the body. The EEG was desynchronizes and displayed low voltage and high-frequency waves; the predominant EEG power density occurred within the date frequency band, with a high value of the theta/delta ratio with a dramatic suppression of EMG. Onset of REM was defined at the point where both high value of the theta/delta ratio and complete suppression of EMG occurred. During NREM, the animal lay immobile with eyes closed; the EEG was synchronized and displayed high-voltage and low-frequency waves, high-power density values in the delta-frequency band, and the EMG was low.

Histology

At the end of the entire procedure, rats were anaesthetized and the location of electrodes was marked by passing a DC current of 40μA for as anode. The rats were killed using an intravenous overdose of pentobarbital sodium (> 200 mg kg^{-1}) and the brain was removed and fixed by immersion in 1 % potassium ferrocyanide in formalin for 7days. With time, ferrocyanide caused the conversion of the iron deposit to a Prussian blue spot. The brains were transferred to a 15% sucrose in .1-mol/L phosphate buffer solution, after 24 hours were stored in a 25% sucrose in .1-mol/L phosphate buffer solution in 48 hours. Brain were sliced into 50 μm section with a freezing microtome. Every other section was collected on a slide and stained cresyl violet and recoding electrode placements were identified.

Frequency analysis

Frequency analysis was performed using a program written in Labview, with measurement data converted from 2 kHz data to 200 Hz. NeuroExplorer was used for frequency analysis to obtain power spectral density of PVNNA, RSNA, LSNA, HR, and AP. Data from non-REM or REM sleep lasting more than 60 seconds were used for analysis. Non-REM sleep was recorded 1-3 episodes/animal and REM sleep 1-2 episodes /animal. Peak analysis was performed using Origin pro for frequency band determination. Gaussian fitting was performed on the peaks that appeared in each waveform of the power spectral density during non-REM sleep to determine the center frequency of each peak. The number of peaks present in each 0.1 Hz power spectral density of paraventricular nucleus nerve activity, renal and lumbar sympathetic nerve activity, heart rate, and arterial pressure was then calculated, and further Gaussian fitting was performed on the calculated number of peaks. The average center frequency and average peak power were determined for each of the frequency bands determined for PVNNA, RSNA, LSNA, HR, and AP.

Statistical analyses

Statistical analysis was performed with SPSS (IBM, Chicago, IL) for analysis of variance

(ANOVA) and multiple comparisons for repeated measures. When the F-values were significant ($P < 0.05$), individual comparisons were made using the Dunnett's multiple comparison test. Values are reported as means ± SD. $P < 0.05$ was considered to indicate a significant difference. Correlations between PVNNA and RSNA, LSNA, HR, AP, and EMG were quantified using a least-squares linear regression analysis (Pearson's r) using SPSS

RESULTS

The PVN has common frequency components in the VLF and LF bands with RSNA, LSNA, HR, and AP.

Measurements of paraventricular nucleus nerve activity were made with extracellular multi-unit recordings, and measurement locations were confirmed by cytochemical staining at the end of the experiment (Figure 1). The original waveform of paraventricular nucleus nerve activity showed sustained spike firing, which is shown in Figure 2. Although occasional large amplitude firing was observed, the firing was almost constant in amplitude, and no clusters of neural firing were observed. Integration of the PVNNA showed slow but not pronounced waves, indicating a periodicity. Raster plots of PVNNA also showed persistent but periodic firing. RSNA and LSNA, unlike PVNNA, had intermittent bursts of spike firing. When integrated, RSNA and LSNA were found to be periodic in their firing. RSNA and LSNA were similar but not perfectly coincident.

To clarify the frequency characteristics of PVNNA, RSNA, and LSNA, frequency analysis was performed. First, the power spectral density of the integrated waveforms of the paraventricular nucleus activity, renal and lumbar sympathetic activity, heart rate, and arterial pressure during non-REM sleep was determined (Figure 3). The power spectral density of PVNNA, RSNA, LSNA, HR, and all showed peaks below 1 Hz. Peaks also appeared at around 2 Hz for RSNA, LSNA, and HR, and around 7 Hz for RSNA, LSNA, and AP. Therefore, a peak analysis was performed to investigate each peak in detail. Gaussian fitting was performed on the peaks that appeared in each waveform

obtained from the power spectral density to determine the center frequency of each peak. The number of peaks present in each 0.1 Hz power spectrum density of the PVNNA, RSNA, LSNA, HR, and AP was then calculated, and Gaussian fitting was performed on the calculated number of peaks. The results of Gaussian fitting showed that the peaks below 1 Hz in the PVNNA consisted of two populations. RSNA, LSNA, HR, and AP also had two peak populations below 1 Hz. Based on these results and previous studies on frequency analysis of sympathetic nerve activity, four frequency bands were defined: the first was the very-low-frequency band (VLF) of 0.06-0.2 Hz, the second was the low-frequency band (LF) of 0.2-1 Hz, the third was the respiratory-related frequency band (HF), and the fourth is the cardiac-related frequency band (CF) of 6-8.5 Hz. The PVNNA, RSNA, LSNA, HR, and AP all had power spectral peaks in the VLF and LF. Renal and lumbar sympathetic nerve activity and arterial pressure also had peaks in RF and CF, but heart rate had a peak in RF but not in CF. These results indicate that during non-REM sleep, the PVNNA, RSNA, LSNA, HR, and AP had a common frequency band in the VLF and LF.

The impact of PVNNA on RSNA and LSNA was weakened during REM sleep

Paraventricular nucleus nerve activity increased during the transition from non-REM to REM sleep (Figures 4 and 5). Paraventricular nucleus nerve activity increased 8 seconds before the onset of REM sleep and remained high during REM sleep ($p<0.05$). RSNA decreased from 1 second after the onset of REM sleep and remained low during REM sleep ($p<0.05$). LSNA was significantly higher at times during REM sleep and tended to increase. Heart rate increased significantly from 3 seconds after the onset of REM sleep and remained low during REM sleep ($p<0.05$). AP significantly increased 22 seconds after the onset of REM sleep and remained high during REM sleep ($p<0.05$). During REM sleep, PVNNA and AP increased, and LSNA tended to increase. On the other hand, RSNA and HR.

Power spectral density analysis of PVNNA, RSNA, LSNA, HR, and AP was also performed during REM sleep (Figure 6). The mean center frequency and mean peak power of PVNNA, RSNA,

LSNA, HR, and AP during non-REM and REM sleep were calculated in the frequency bands where the peaks were observed during non-REM sleep. The mean power of the VLF of the paraventricular nucleus activity was significantly greater during REM sleep than during non-REM sleep, but the mean power of the LF was not different. The mean power of RSNA was not different between non-REM and REM sleep for VLF, LF, and CF but was significantly smaller for CF. The mean power of LSNA did not differ between non-REM and REM sleep in LF and CF but was significantly smaller in VLF and RF than in non-REM sleep. The mean peak power of HR was significantly greater in VLF and LF during REM sleep and significantly smaller in RF compared to non-REM sleep. The mean peak power of AP was significantly greater in VLF and significantly smaller in LF, RF, and CF during REM sleep compared to non-REM sleep.

DISCUSSION

In the present study, simultaneous measurement of paraventricular nucleus nerve activity and renal and lumbar sympathetic nerve activity in conscious rats was successfully performed. The results showed that during non-REM sleep, arterial pressure regulation was stable and that paraventricular nucleus nerve activity, renal and lumbar sympathetic nerve activity, heart rate, and arterial pressure had common frequency components in the VLF band (0.06-0.2 Hz) and LF band (0.2-1 Hz). On the other hand, during REM sleep, arterial pressure regulation became unstable, and the involvement of the VLF band and LF band in renal and lumbar sympathetic nerve activity by the paraventricular nucleus nerve activity was weakened, while the involvement of the VLF band and LF band involvement was found to be weakened. The results of this study indicate that the slow frequency components of the VLF and LF bands, which are common to paraventricular nucleus nerve activity, renal and lumbar sympathetic nerve activity, heart rate, and arterial pressure, may contribute to arterial pressure stability.

Paraventricular nucleus nerve activity and renal and lumbar sympathetic nerve activity were found

to have a common frequency component in the VLF band and LF band during non-REM sleep. In the present study, the paraventricular nucleus neural activity showed peaks in the VLF band and LF bandduring non-REM sleep. To the best of our knowledge, there have been no reports on the frequency components of the paraventricular nucleus neural activity during sleep in conscious rats. However, single-unit extracellular recordings in the paraventricular nucleus of conscious rats have reported that some neurons in the paraventricular nucleus show phasic activity and others show non-phasic activity (Watanabe *et al*., 2004), and in the multi-unit extracellular recordings of the paraventricular nucleus in the present study, we found that the paraventricular nucleus activity was not related to specific frequencies. It is quite possible that the paraventricular nucleus neuronal activity peaked at a specific frequency component in the paraventricular nucleus multi-unit extracellular recordings of the present study.

On the other hand, renal and lumbar sympathetic nerve activity was observed to peak in the VLF (0.06-0.2 Hz), LF (0.2-1 Hz), RF (1-3 Hz), and CF (6-8.5 Hz) bands during non-REM sleep. It has been reported that conscious rats show peaks in the low-frequency band below 1 Hz, respiration-related frequencies, and heart-related frequencies (Kunitake & Kannan, 2000), which is consistent with the results of this study. The peaks in the RF and CF bands of sympathetic activity are well known as respiration-related and heart-related frequencies, respectively (Barman, 2016). On the other hand, for the low-frequency component of sympathetic activity below 1 Hz, there are reports that the baroreceptors are the main origin (Julien *et al*., 2003) and that the central rather than the baroreceptors are involved (Preiss & Polosa, 1974), and the debate continues (Barman & Kenney, 2007).

Paraventricular nucleus nerve activity and renal and lumbar sympathetic nerve activity showed common peaks in the VLF band and LF band, i.e., below 1 Hz. This suggests that the VLF and LF bands of the paraventricular nucleus nerve activity are involved in generating the VLF and LF bands of the renal and lumbar sympathetic nerve activity. The paraventricular nucleus is also thought to be involved in the regulation of sympathetic nerve activity via the rostral medullary ventral

tegmental area (Pyner & Coote, 2000), and it has been reported that the rostral medullary ventral tegmental area contains nerves that peak at 0.2-0.8 Hz (Tseng *et al*., 2009). This report supports the present study's finding that paraventricular nucleus nerve activity and renal and lumbar sympathetic nerve activity have a common frequency component below 1 Hz. These results suggest that the VLF and LF bands of paraventricular nucleus nerve activity are involved in generating the VLF and LF bands of renal and lumbar sympathetic nerve activity.

Arterial pressure and heart rate were also found to have frequency components in the VLF bandand LF bandcommon to paraventricular nucleus nerve activity and renal and lumbar sympathetic nerve activity. During non-REM sleep, arterial pressure and heart rate peaked in the VLF (0.06-0.2 Hz), LF (0.2-1 Hz), and RF (1-3 Hz) bands. Arterial pressure also peaked in the CF band (6-8.5 Hz). The RF band (1-3 Hz) and CF band (6-8.5 Hz) of arterial pressure and RF band of heart rate are well known as respiratory-related and cardiac-related frequencies as well as sympathetic nerve activity (Parati *et al*., 1995). Although the peaks of arterial pressure and heart rate below respiratory-related frequencies, i.e., below 1 Hz, remain controversial (Stauss, 2007), previous studies have shown that sympathetic nerve activity is involved in the peaks below 1 Hz of arterial pressure and heart rate. Brown et al. Brown et al. reported that sympathetic activity and arterial pressure coherence peaked at 0.4 Hz both under anesthesia and in consciousness (Brown *et al*., 1994). At the same time, they also reported that coherence between sympathetic activity and heart rate was found below 0.2 Hz in conscious rats. The results of this study, in which arterial pressure and heart rate had frequency components below the respiration-related frequency in common with sympathetic activity, also support the idea that sympathetic activity is the source of the frequency components below 1 Hz of arterial pressure and heart rate. These results suggest that the VLF band and LF band of sympathetic nerve activity are involved in the generation of the VLF band and LF band of arterial pressure and heart rate, respectively.

Since the paraventricular nucleus has frequency components in the VLF and LF bands in common with renal and lumbar sympathetic nerve activity, heart rate, and arterial pressure, and

since sympathetic nerve activity is involved in generating the VLF and LF bands of arterial pressure and heart rate paraventricular nucleus nerve activity may be involved in the generation of the VLF and LF bands of arterial pressure and heart rate via sympathetic nerve activity. This idea is supported by previous studies of electrical stimulation of the paraventricular nucleus of conscious rats, in which Stauss et al. reported that electrical stimulation of the paraventricular nucleus of conscious rats at 0.1-0.5 Hz caused oscillations in arterial pressure via sympathetic nerve activity (Stauss *et al*., 1997). They also reported that stimulation of the paraventricular nucleus of conscious rats at 0.1-0.5 Hz caused fluctuations in heart rate during scopolamine-induced parasympathetic blockade (i.e., via the sympathetic pathway) (Stauss *et al*., 1997). These results suggest that paraventricular nucleus nerve activity is involved in the regulation of arterial pressure and heart rate in the VLF and LF bands via sympathetic nerve activity.

During the transition from non-REM to REM sleep, arterial pressure rises rapidly and fluctuates widely. How does this unstable arterial pressure regulation during REM sleep relate to the common frequency components observed during non-REM sleep?

First, the relationship in the VLF band and LF band common to sympathetic activity from paraventricular nucleus nerve activity may weaken during REM sleep. In the present study, the VLF power of paraventricular nucleus nerve activity increased during REM sleep compared to non-REM sleep, while the VLF power of renal sympathetic nerve activity remained unchanged and the VLF power of lumbar sympathetic nerve activity decreased. In contrast, LF band power was unchanged for all paraventricular nucleus nerve activity and renal and lumbar sympathetic nerve activity. Although the increase in paraventricular nucleus nerve activity during REM sleep may be related to regional differences in sympathetic nerve activity, the fact that regional differences in sympathetic nerve activity during REM sleep occur even after deafferentation suggests that the regulatory center for sympathetic nerve activity during REM sleep is in the brainstem (Silvani & Dampney, 2013). Based on the above, during REM sleep, the relationship between the VLF band and the LF band, which is common to both paraventricular nucleus nerve activity and sympathetic

nerve activity, is weakened, and regional differences in sympathetic nerve activity may be generated by the brainstem.

The involvement of arterial pressure in the VLF and LF bands by sympathetic activity is also weakened during REM sleep. In the present study, the VLF power of renal sympathetic activity was unchanged during REM sleep compared to non-REM sleep, while the VLF power of arterial pressure and heart rate increased. LF power of renal and lumbar sympathetic activity was also unchanged, while LF power of arterial pressure decreased and LF power of heart rate increased. To our knowledge, there have been no previous reports on the relationship between sympathetic activity during REM sleep and the frequency components of heart rate and arterial pressure. However, it has been reported that sympathetic denervation increased the power of the VLF band of arterial pressure and decreased LF power (Daffonchio *et al*., 1995), which is similar to the present results obtained during REM sleep. This suggests that the peak power in the VLF band and LF band of arterial pressure during REM sleep is less involved in sympathetic nerve activity. In summary, during REM sleep, the involvement of the VLF and LF bands in the regulation of sympathetic activity of the paraventricular nucleus nerve activity is weakened, and the involvement of the VLF and LF bands in arterial pressure regulation of sympathetic activity is weakened, which leads to REM This may result in unstable blood pressure regulation that is specific to REM sleep.

In conclusion, paraventricular nucleus nerve activity, renal and lumbar sympathetic nerve activity, heart rate, and arterial pressure share a common frequency component in the VLF and LF bands, and this slow frequency component may contribute to arterial pressure stability and play an important role in maintaining cardiovascular homeostasis. The results indicate that this slow frequency component may contribute to arterial pressure stability and play an important role in maintaining cardiovascular homeostasis.

Perspective

What is the significance of the VLF band and LF band frequency components of paraventricular nucleus nerve activity, renal and lumbar sympathetic nerve activity, heart rate, and arterial pressure? Previous studies have reported that SAD'ed rats show an increase in the power of the VLF band of arterial pressure and a decrease in the power of the LF band of heart rate and arterial pressure, while the power of the LF band of renal sympathetic activity is unchanged (Julien *et al*., 2003),(Cerutti *et al*., 1994). This result is similar to the results during REM sleep in the present study, and our group has previously reported that baroreceptor reflexes are suppressed during REM sleep compared to non-REM sleep. (Nagura *et al*., 2004)These findings suggest that the increase in the VLF component of arterial pressure and the decrease in the LF component of arterial pressure and heart rate may reflect impaired baroreceptor input. In summary, the frequency components in the VLF band and LF band are common to paraventricular nucleus nerve activity, and renal and lumbar sympathetic nerve activity, heart rate, and arterial pressure may reflect impaired central autonomic regulation.

REFERENCES

Akine A, Montanaro M & Allen AM (2003). Hypothalamic paraventricular nucleus inhibition decreases renal sympathetic nerve activity in hypertensive and normotensive rats. *Auton Neurosci* **108,** 17-21.

Badoer E (2001). Hypothalamic paraventricular nucleus and cardiovascular regulation. *Clin Exp Pharmacol Physiol* **28,** 95-99.

Barman SM (2016). What can we learn about neural control of the cardiovascular system by studying rhythms in sympathetic nerve activity? *International Journal of Psychophysiology* **103,** 69-78.

Barman SM & Kenney MJ (2007). Methods of analysis and physiological relevance of rhythms in sympathetic nerve discharge. *Clin Exp Pharmacol Physiol* **34,** 350-355.

Brown DR, Brown LV, Patwardhan A & Randall DC (1994). Sympathetic activity and blood pressure are tightly coupled at 0.4 Hz in conscious rats. *Am J Physiol* **267,** R1378-1384.

Cerutti C, Barres C & Paultre C (1994). Baroreflex modulation of blood pressure and heart rate variabilities in rats: assessment by spectral analysis. *Am J Physiol* **266,** H1993-2000.

Daffonchio A, Franzelli C, Radaelli A, Castiglioni P, Di Rienzo M, Mancia G & Ferrari AU (1995). Sympathectomy and cardiovascular spectral components in conscious normotensive rats. *Hypertension* **25,** 1287-1293.

Julien C, Chapuis B, Cheng Y & Barres C (2003). Dynamic interactions between arterial pressure and sympathetic nerve activity: role of arterial baroreceptors. *Am J Physiol Regul Integr Comp Physiol* **285,** R834-841.

Kannan H, Hayashida Y & Yamashita H (1989). Increase in sympathetic outflow by paraventricular nucleus stimulation in awake rats. *Am J Physiol* **256,** R1325-1330.

Kenney MJ, Weiss ML, Mendes T, Wang Y & Fels RJ (2003). Role of paraventricular nucleus in regulation of sympathetic nerve frequency components. *Am J Physiol Heart Circ Physiol* **284,** H1710-1720.

Kenney MJ, Weiss ML, Patel KP, Wang Y & Fels RJ (2001). Paraventricular nucleus bicuculline alters frequency components of sympathetic nerve discharge bursts. *Am J Physiol Heart Circ Physiol* **281,** H1233-1241.

Kunitake T & Kannan H (2000). Discharge pattern of renal sympathetic nerve activity in the conscious rat: spectral analysis of integrated activity. *J Neurophysiol* **84,** 2859-2867.

Kuusela TA, Kaila TJ & Kahonen M (2003). Fine structure of the low-frequency spectra of heart rate and blood pressure. *BMC Physiol* **3,** 11.

Li YF, Jackson KL, Stern JE, Rabeler B & Patel KP (2006). Interaction between glutamate and GABA systems in the integration of sympathetic outflow by the paraventricular nucleus of the hypothalamus. *Am J Physiol Heart Circ Physiol* **291,** H2847-2856.

Matsukawa K, Ninomiya I & Nishiura N (1993). Effects of anesthesia on cardiac and renal

sympathetic nerve activities and plasma catecholamines. *Am J Physiol* **265,** R792-797.

Miki K, Kosho A & Hayashida Y (2002). Method for continuous measurements of renal sympathetic nerve activity and cardiovascular function during exercise in rats. *Exp Physiol* **87,** 33-39.

Miki K, Oda M, Kamijyo N, Kawahara K & Yoshimoto M (2004). Lumbar sympathetic nerve activity and hindquarter blood flow during REM sleep in rats. *J Physiol* **557,** 261-271.

Nagura S, Sakagami T, Kakiichi A, Yoshimoto M & Miki K (2004). Acute shifts in baroreflex control of renal sympathetic nerve activity induced by REM sleep and grooming in rats. *J Physiol* **558,** 975-983.

Parati G, Saul JP, Di Rienzo M & Mancia G (1995). Spectral analysis of blood pressure and heart rate variability in evaluating cardiovascular regulation. A critical appraisal. *Hypertension* **25,** 1276-1286.

Preiss G & Polosa C (1974). Patterns of sympathetic neuron activity associated with Mayer waves. *Am J Physiol* **226,** 724-730.

Pyner S & Coote JH (2000). Identification of branching paraventricular neurons of the hypothalamus that project to the rostroventrolateral medulla and spinal cord. *Neuroscience* **100,** 549-556.

Schlenker E, Barnes L, Hansen S & Martin D (2001). Cardiorespiratory and metabolic responses to injection of bicuculline into the hypothalamic paraventricular nucleus (PVN) of conscious rats.

Brain Res **895,** 33-40.

Sei H (2012). Blood pressure surges in REM sleep: A mini review. *Pathophysiology* **19,** 233-241.

Silvani A & Dampney RA (2013). Central control of cardiovascular function during sleep. *Am J Physiol Heart Circ Physiol* **305,** H1683-1692.

Stauss HM (2007). Identification of blood pressure control mechanisms by power spectral analysis. *Clin Exp Pharmacol Physiol* **34,** 362-368.

Stauss HM, Persson PB, Johnson AK & Kregel KC (1997). Frequency-response characteristics of autonomic nervous system function in conscious rats. *Am J Physiol* **273,** H786-795.

Swanson LW & Sawchenko PE (1980). Paraventricular nucleus: a site for the integration of neuroendocrine and autonomic mechanisms. *Neuroendocrinology* **31,** 410-417.

Tseng WT, Chen RF, Tsai ML & Yen CT (2009). Correlation of discharges of rostral ventrolateral medullary neurons with the low-frequency sympathetic rhythm in rats. *Neurosci Lett* **454,** 22-27.

Watanabe S, Kunitake T, Kato K, Chu CP, Nakao H, Qiu DL & Kannan H (2004). Single-unit activity of paraventricular nucleus neurons in response to intero- and exteroceptive stressors in conscious, freely moving rats. *Brain Res* **995,** 97-108.

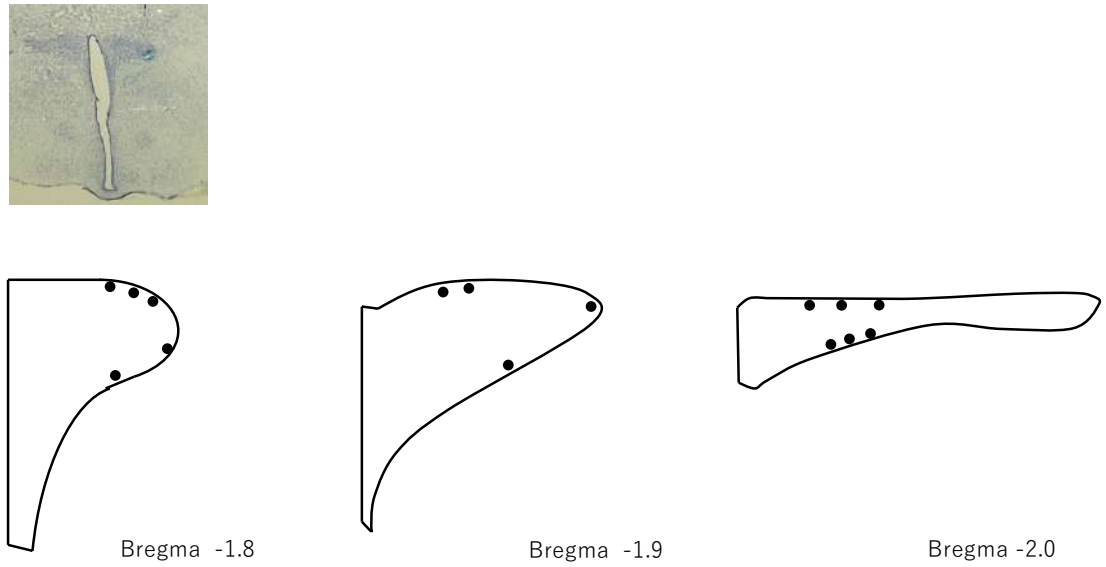

Figure 1. Site of the tip of the electrode where PVNNA was recorded

Coronal sections of PVN are shown. In cresyl violet staining of a coronal rat brain section, the blue spot indicated by the arrow marks the tip of the electrode in an individual rat. The areas marked in blue are the actual PVNNA measurement locations. The bottom row is a schematic diagram of all measurement positions of the PVNNA. The black circles represent the measurement positions. From left to right, the distances from bregma are -1.8 mm, -1.9 mm, and -2.0 mm, respectively.

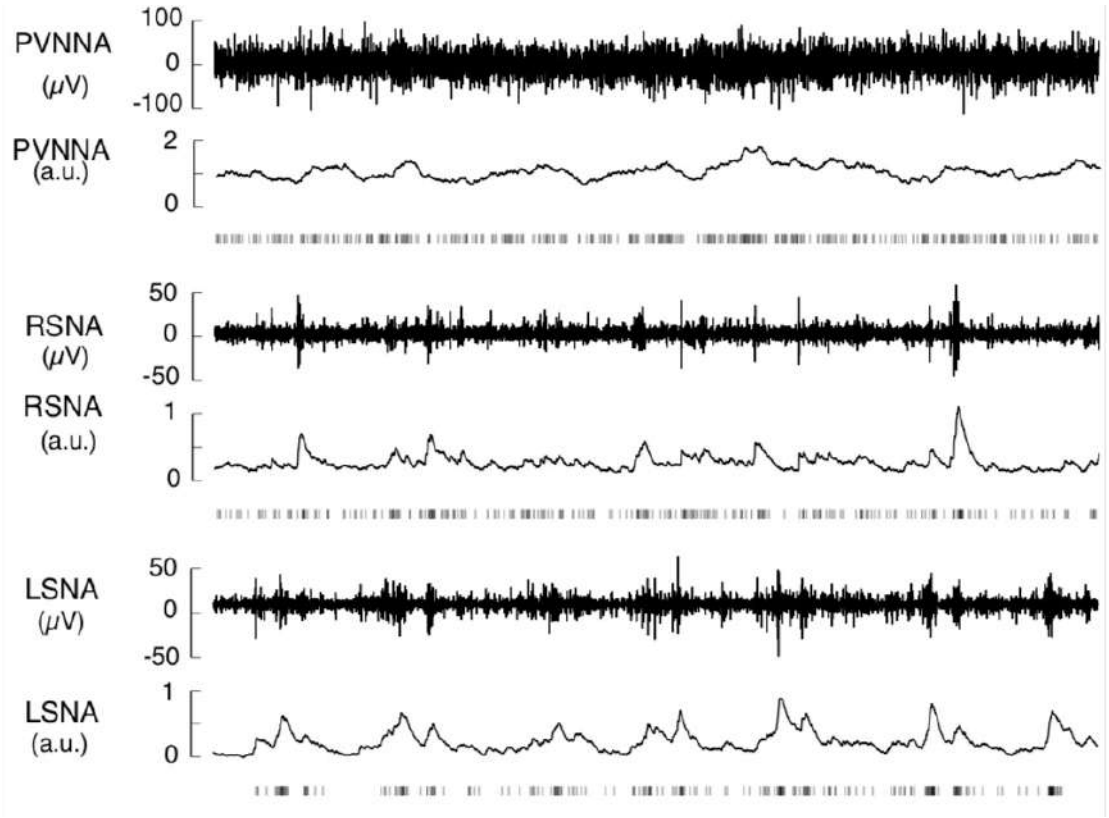

Figure 2. Typical recording of simultaneous continuous measurement of PVNNA, RSNA, and LSNA during non-REM sleep in an individual rat.

From top to bottom: original waveforms, integrated waveforms, and raster plots of PVNNA, RSNA, and LSNA, respectively.

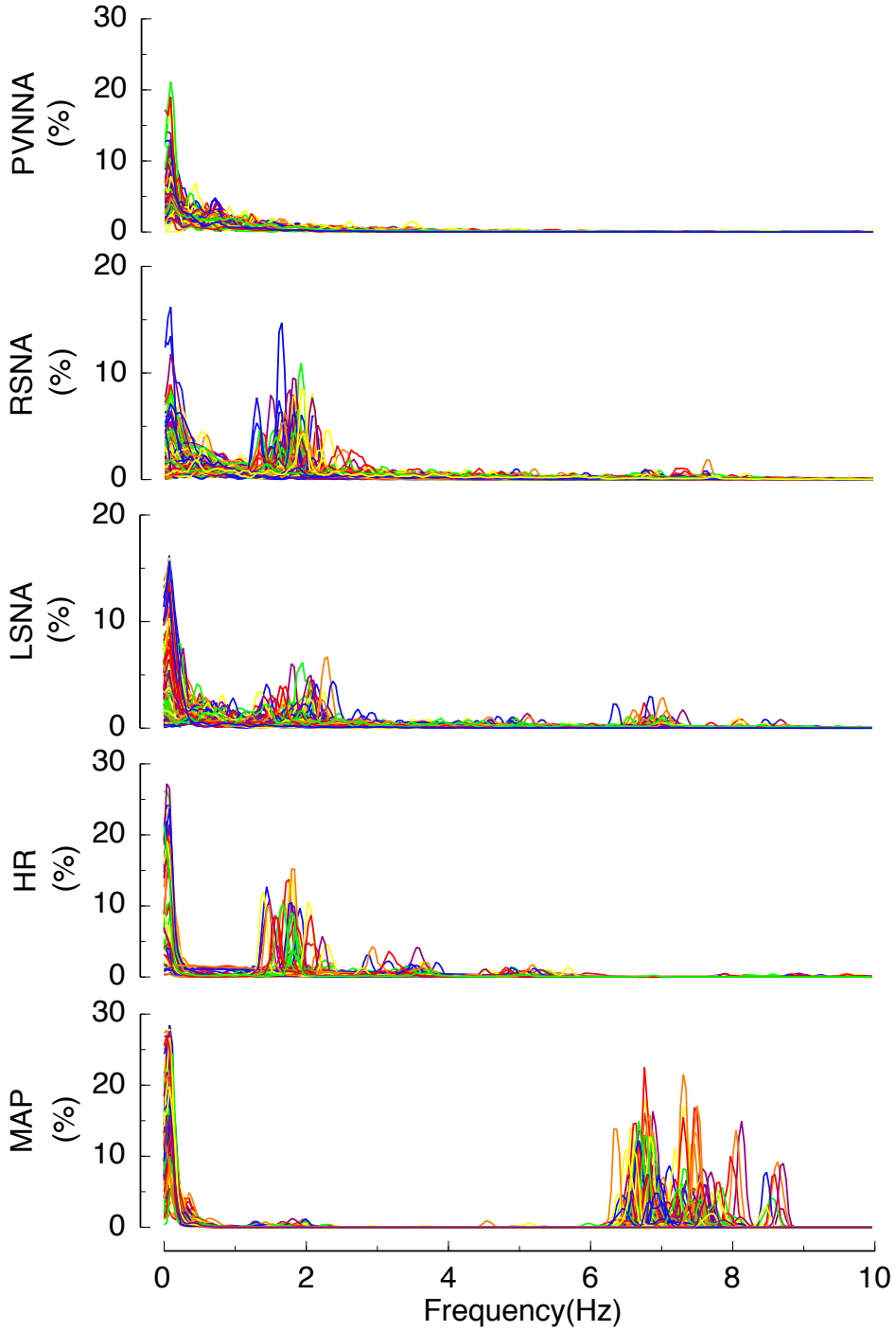

Figure 3. Power spectral density observed during NREM sleep.

Power spectral density of PVNNA (n=105 data, N=13 rats; top view), RSNA (n=112 data, N=14 rats; second view), LSNA (n=69 data, N=10rats; third view), HR (n=50 data, N=8 rats; forth view) and MAP (n=149 data, N=11 rats; bottom view) during NREM sleep. Each line represents an individual trace.

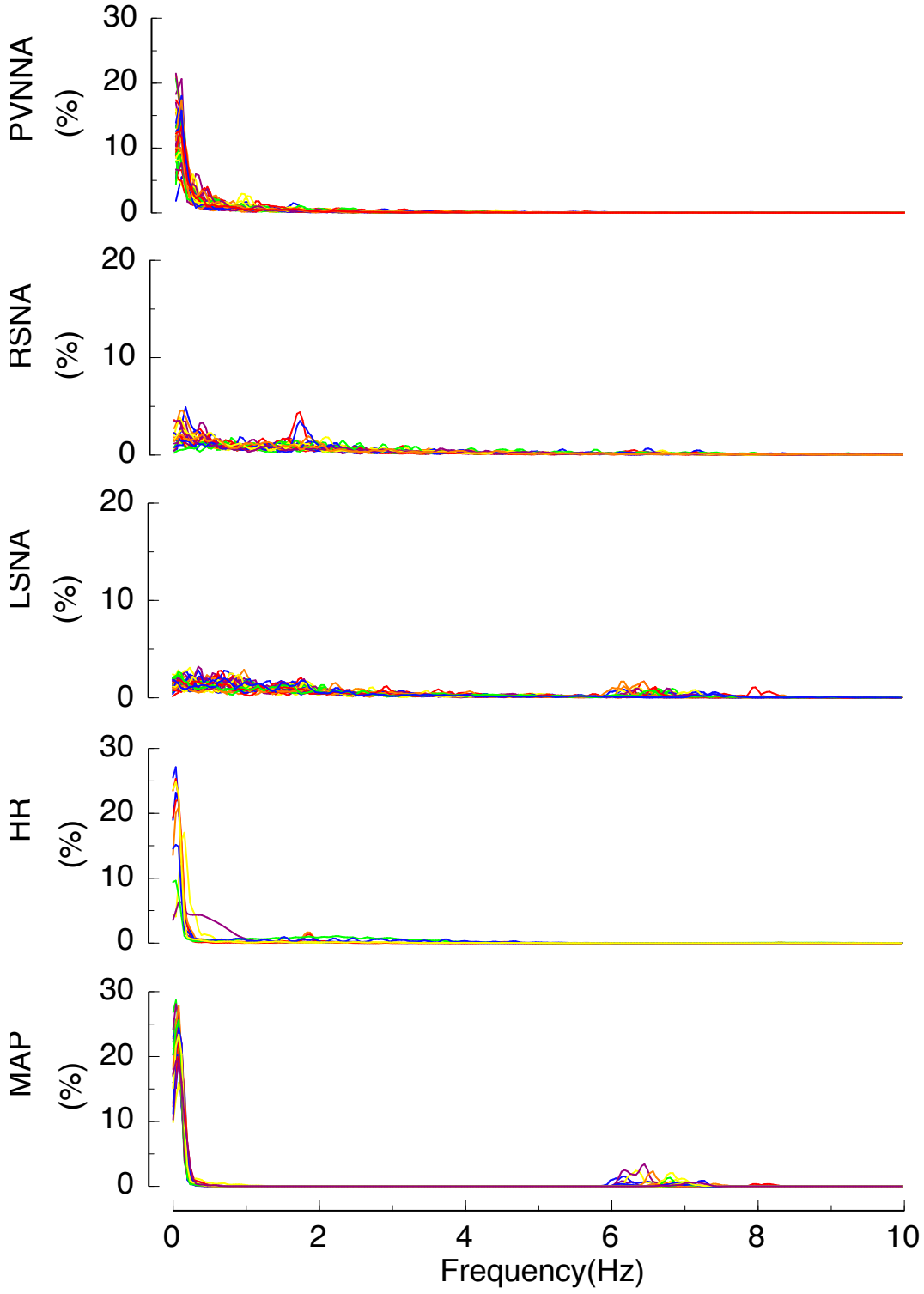

Figure 4. Power spectral density during REM sleep.

Power spectral density of PVNNA (n=43 data, N=13 rats; top), RSNA (n=18 data, N=6; second), LSNA (n=30 data, N=11; third), HR (n=10 data, N=6 rats; forth) and MAP (n=23 data, N=15 rats; bottom) during REM sleep. Each line represents an individual trace.

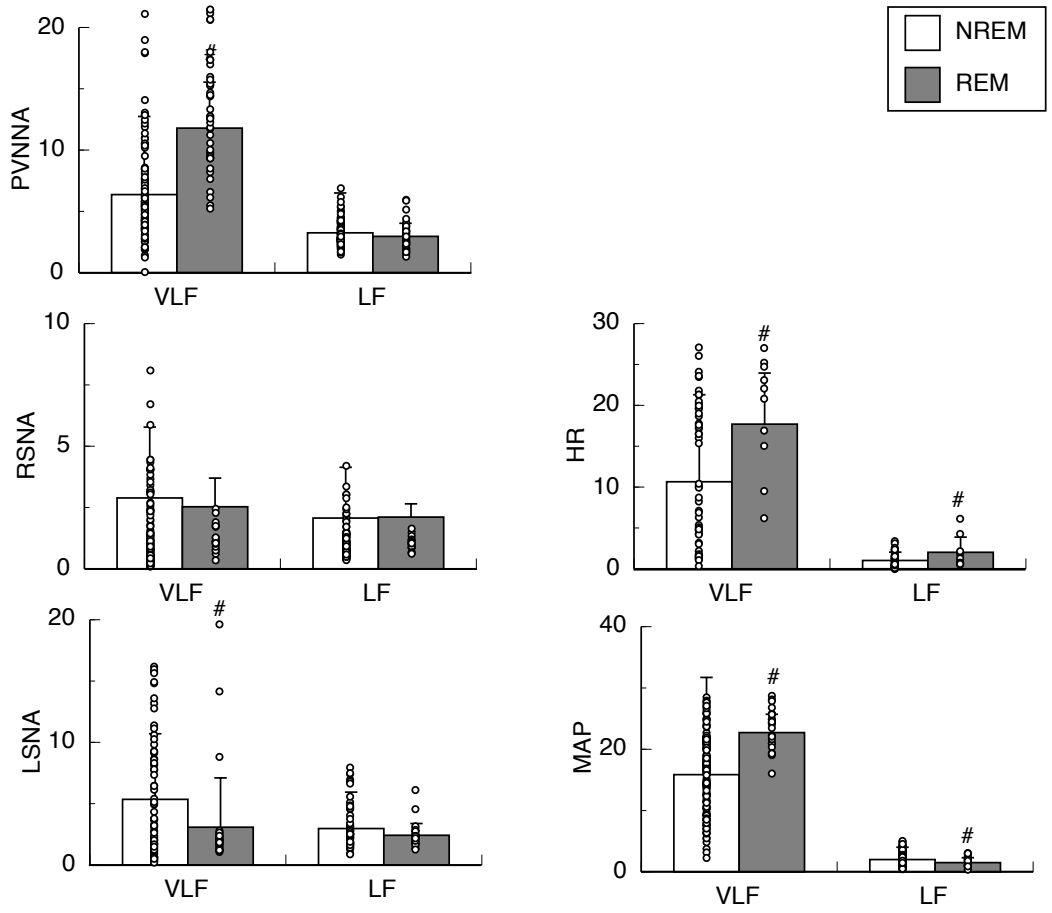

Figure 5. Changes in VLF and LF bands across NREM and REM sleep states.

The mean peak power of VLF band and LF band in PVNNA, RSNA, LSNA, HR, MAP during NREM sleep and REM sleep. Each column and error bar represents the mean ± SD. *P < 0.05 NREM vs REM. Open bar represents NREM sleep. Filled bar represents REM sleep.

Chapter 4

Roles of Hippocampal CA1 and Hypothalamic Paraventricular Nucleus Neuronal Activity in Regulating Sympathetic Nerve Activity and Cardiovascular Function in Fear Conditioning

ABSTRACT

Fear conditioning changes sympathetic nerve activity (SNA) and cardiovascular function. The hippocampus CA1 region (CA1) is an important brain region for learning fear conditioning and the hypothalamic paraventricular nucleus (PVN) plays an important role in the regulation of SNA and cardiovascular function. However, it is unclear how CA1 neuronal activity (CA1NA) and PVN neuronal activity (PVNNA) are involved in the regulation of SNA and cardiovascular function after fear conditioning. The present study aimed to investigate the roles of CA1NA and PVNNA in regulating SNA and cardiovascular function in contextual- and auditory-cued fear conditioning. Male Wistar rats were chronically instrumented with multiple electrodes to measure CA1NA, PVNNA, renal SNA (RSNA), lumbar SNA (LSNA), and electroencephalogram, electromyogram, and electrocardiogram, as well as a catheter to measure arterial pressure. In the fear conditioning, rats were presented with a tone (conditioned stimulus; CS) followed by a brief electrical shock in a shock cage. Rats were presented CS in their home cage and the shock cage before and after fear conditioning. Result of fear conditioning, rats have been shown the freezing behavior to CS. The RSNA, LSNA, and cardiovascular responses were found to be divided during and after CS. Heart rate (HR) was also found to be altered when CS presentation was performed in a shock cage. It was suggested that CA1NA may influence changes in HR in the shock cage and PVNNA may not play a major role in the regulation of SNA and cardiovascular function in response to fear conditioning.

INTRODUCTION

Animal survival depends on the ability to respond appropriately to stressors, which can be categorized into two different groups: interoceptive (also-called physical) stressors and exteroceptive (also-called psychological) stressors (Dampney 2015). Physical stressors stimulate pathways that respond to homeostatic stressors, and psychological stressors stimulate pathways of emotional responses to actual or learned threats in the external environment (Dayas et al. 2001). Psychological stress is known to activate sympathetic nerve activity (SNA) and increase arterial pressure (AP)(Kanbar et al. 2007). Fear conditioning has been established as a model of psychological stress. Fear conditioning is an experimental paradigm in which animals learn the relationship between an aversive stimulus (unconditioned stimulus), such as an electric shock, and an emotionally neutral (harmless) stimulus (conditioned stimulus). As a result, animals predict the aversive stimulus with the presentation of sound only and show freezing behavior (Baldi, Lorenzini and Bucherelli 2004). This behavior can also be triggered by re-exposure to the environment (contextual conditions) in which the fear conditioning took place (Carrive 2000). Although SNA and circulatory dynamics are known to change at this time, there are no reports directly measuring the response of SNA to fear-conditioned sounds. Fear conditioning alters SNA and cardiovascular function in response to conditioned stimuli and contextual conditions. However, the central pathways and mechanisms associated with fear conditioning remain unclear.

We focused on the hippocampus CA1 region (CA1), which is a critical brain region for learning fear conditioning, and the hypothalamic paraventricular nucleus (PVN), which plays a central role in the regulation of SNA and cardiovascular function. CA1 is responsible for transferring information from the hippocampus to the hippocampus and beyond (Witter et al. 2000). The hippocampal CA1 region is known to be important for the acquisition and recall of fear-conditioned contextual conditions (Daumas et al. 2005, Hunsaker and Kesner 2008, Lee and Kesner 2004). PVN has direct projections to the rostral ventrolateral medulla and intermediate lateral column (Pyner and Coote 2000) and plays a significant role in the regulation of SNA and cardiovascular function

(Badoer 2001). The PVN also serves as the last common pathway mediating activation of the hypothalamic-pituitary-adrenal axis, a hallmark of the stress response (Jiang, Rajamanickam and Justice 2019). Taken together, the PVN is thought to play a major role in the regulation of autonomic and endocrine responses during stress (Swanson and Sawchenko 1980). Indeed, it has been reported that fos expression in the PVN increases during psychological stress (Furlong et al. 2014). There are no reports of simultaneous recordings of hippocampal CA1 neuronal activity (CA1NA) or PVN neuronal activity (PVNNA) and SNA and cardiovascular function during fear conditioning, and it is greatly significant to clarify how CA1NA and PVNNA are involved in the regulation of SNA and cardiovascular function during fear conditioning.

The purpose of the present study was to investigate the role of CA1NA and PVNNA in the regulation of SNA and cardiovascular function during contextual- and auditory-cued classical fear conditioning. To achieve this goal, CA1NA or PVNNA and renal SNA (RSNA), lumbar SNA (LSNA), heart rate (HR), and AP were measured simultaneously and compared the responses of CA1NA, PVNNA, RSNA, LSNA, HR, and AP to the conditioned stimuli before and after the fear conditioning. We also presented fear-conditioned tone in a home cage and a shock cage (contextual condition) and examined whether the presence or absence of contextual conditions altered the role of CA1NA and PVNNA in the regulation of SNA, HR, and AP.

METHODS

Animals

Male Wistar rats weighing 272.8 ± 18.4 g (mean ± standard deviation, n=25) were used all experiments, purchased from SLC (Hamamatsu, Shizuoka, Japan). Rats were housed individually and kept in a chamber (Espec, Osaka, Japan) with controlled temperature (24◦C) and humidity (60%) and a 12 h:12 h light–dark cycle (light on at 07.00 h). Rats were allowed standard laboratory rat chow and water ad libitum and were handled every day. All procedures were undertaken in

accordance with the Guiding Principles in the Care and Use of Animals in the Fields of Physiological Sciences published by the Physiological Society of Japan (Physiological Society of Japan, 2015) , and with the prior approval of the Animal Care committee of Nara Women's University.

Surgical procedures

The animals were operated on in two stages. All procedures were performed aseptically in operating theater. The rats were intra- peritoneally premedicated with pentobarbital sodium (65 mg/kg), anaesthetized with isoflurane (1.5–2.0% with air at a rate of 1–1.5 l/min), and given antibiotics (gentamicin sulfate, 10 mg/kg S.C., Schering-Plough K.K., Whitehouse Station, NJ, USA).

During the first surgical procedure, implantation of the electrodes for measurement for renal sympathetic nerve activity (RSNA) and lumber sympathetic nerve activity (LSNA), and electrocardiogram (ECG), cervical electromyogram (EMG) electrodes was performed. Briefly, the electrodes for measurement for RSNA and LSNA were implanted as described in our previous reports (Miki, Kosho and Hayashida 2002) (Miki et al. 2004). To implant the RSNA electrode, the left kidney was exposed retroperitoneally through a left flank incision, and a branch of the renal nerve running on or beside the renal artery was carefully isolated. Bipolar stainless-steel wire electrodes were hooked onto the nerve, and both were embedded in two-component silicone rubber (Miki, Kosho and Hayashida 2002). To implant the LSNA electrode, a midline abdominal incision was made. After retraction of the intestines, the abdominal aorta and vena cava were gently pulled aside to expose a lumbar nerve. Approximately 3mm of the left lumbar sympathetic trunk was carefully isolated from the connective tissue. A bipolar stainless steel wire electrode (AS633; Cooner Wire, Chatsworth, CA, USA) was hooked onto the sympathetic trunk between L3 and L4, both were embedded in a two-component silicone rubber (Miki et al. 2004). The bipolar EMG electrodes were implanted bilaterally in both trapezium muscles. The bipolar ECG electrode was

implanted under the skin at the manubrium of the sternum and xiphoid process. The electrodes and the catheter were tunneled subcutaneously, exteriorized at the back of the neck and protected by plastic tubes.

A period of at least 4 days was allowed before second surgery, at which time the electrodes for measurement of hippocampal CA1 neuronal activity (CA1NA) or hypothalamic paraventricular nucleus neuronal activity (PVNNA), and electroencephalogram (EEG) electrodes, and the catheter to measure arterial pressure (AP) were implanted. Rats was placed in a stereotaxic head holder. EEG electrodes were implanted over the frontal cortex (anteroposterior +2mm, mediolateral -2mm from bregma), the parietal cortex (anteroposterior -3mm, mediolateral -2mm from bregma), and over the cerebellum (1.5mm posterior to lambda). Three stainless steels were arranged by coiling around screws (1.0mm diameter), which served as electrodes. Then, electrodes for measurement of CA1NA or PVNNA were implanted. the implantation of electrode for measurement of CA1NA was carried out in the following procedure. A screw was implanted over the frontal cortex (approximately mediolateral -2.0mm from bregma) which has a role of ground). A hole in cranial bone approximately 3 mm in diameter over the parietal cortex (anteroposterior -3.8mm, mediolateral -2.2mm from bregma) was made carefully using a drill. The cranial bone fragments and the dura in a hole was carefully removed by distorted needle under the microscope (POM-50II, Konan medical, Inc. , Hyogo). Then, the combined probe were lowered stereotaxically into the right hippocampal CA1 area through the hole at the speed of 0.1mm per 5 min until action potentials with pyramidal cell firing characteristics were recorded. The signal of electrodes was amplified by a differential amplifier (Biotex, Kyoto) and displayed on an oscilloscope and made audible with an audio amplifier. The electrodes for measurement of PVNNA were implanted as described in Chapter 3. After confirming the CA1NA or PVNNA and EEG electrode were isolate and fixed on the skull with dental cement. And then an arterial catheter was implanted into the abdominal aorta via the tail artery. Finally, the electrodes and the catheter were exteriorized at the back of the neck and passed through the center of circular Ducron sheet, which was fixed into lace by suturing to the

skin and protected by plastic tubes. The electrodes were exteriorized as described above.

Upon completion of each surgery, the rats were sprayed with antibiotics on the surgical wounds (FRANCETIN•T•POWDER, Mochida-Seiyaku, Tokyo, Japan) and then jelly was provided. To control postoperative pain, a non-steroidal anti-inflammatory drug (diclofenac sodium, 0.5–3.0 mg/kg; Novartis Japan, Tokyo, Japan) mixed with jelly was given orally when necessary. The animals were individually housed in transparent plastic cages and allowed standard laboratory rat chow and water ad libitum, and weighed and handled every day, and the status of the animals was checked by experienced researchers. Arterial catheters were filled with heparin sodium solution (1000 i.u. /ml) and were flushed every day.

Measurements

CA1NA, PVNNA, RSNA, and LSNA were obtained using the differential amplifier that connects to a multichannel neuronal recording system (plexon Inc. , Dallas, TX) and store the disk for offline spike discrimination. Extraceller single units were discriminated using time-voltage windows and a principal component-based spike-sorting alogorithm. Fire rate of CA1NA PVNNA, RSNA, LSNA was estimated every 1 sec bin.

EEG, EMG, ECG, PVNNA, RSNA and LSNA signals were amplified by a differential amplifier (MK-2, Biotech, Kyoto; the gain and bandwidth, respectively, were as follows: ×10,000 and 0.16–50 Hz (EEG); ×100 and 100–2000 Hz (EMG); ×1000 and 0.16–150 Hz (ECG); ×10,000 and 150–2000 Hz (RSNA and LSNA)). The arterial pressure (AP) was measured by connecting the arterial catheters to pressure transducers (DX-100, Nihon Kohden, Tokyo, Japan). The HR was determined with a cardiotachometer (AT-601G, Nihon Kohden) triggered by the ECG. The amplified RSNA and LSNA were integrated using a voltage integrator with a time constant of 50 ms (AD-600G, Nihon Kohden). The signals for EEG, EMG, ECG, CA1, integrated CA1, PVNNA, integrated PVNNA, RSNA, integrated RSNA, LSNA, integrated LSNA, AP and HR were displayed continuously on an oscilloscope and recorded simultaneously on thermal head recording paper

(Figure 1a; ORP1200, Yokogawa, Tokyo, Japan). The EEG, EMG, AP, HR, integrated CA1NA, integrated PVNNA, integrated RSNA and integrated LSNA signals were sampled for analog-to-digital conversion at 10 kHz intervals. The digitized EEG signal, the digitized CA1NA field potential, and the digitized PVNNA field potential signal underwent Fourier analysis in 1 s epochs using a computerized data acquisition program (LabVIEW, National Instruments, Austin, TX, USA). The power spectrum was averaged simultaneously in two frequency bands: delta (0.5–4 Hz) and theta (6–9 Hz). The digitized EMG signal was simultaneously converted to the mean square root value. With the aid of a data acquisition program (LabVIEW), data for the power spectrums of EEG and the root mean square value of EMG, AP, HR, integrated CA1NA, integrated PVNNA, integrated RSNA and integrated LSNA were averaged simultaneously and continuously every 1 s, displayed on the computer monitor and stored on a hard disk. To quantification the response of integrated PVNNA, integrated RSNA, and integrated LSNA, percent changes of the response were calculated by taking the mean of these values during the NREM period as 100% on each day.

Experimental protocols

After the second surgery, rats were allowed at least 1 day to recover. Experiments were performed with the animals in their home cage, and they were given free access to water. Each experiment was performed after an hour rest when all parameters had been connected to the measuring instruments.

Rats were rested for 30 minutes from the start of the experiment, and then rats were presented a tone (conditioned stimulus; CS, 5sec) in their home cage when non-rapid eye movement sleep (NREM) or quite awake (QA). After finishing the memory recalling trials, rats were moved to a shock cage. Fear conditioning was done in a shock cage (26×17×32) with a grid floor composed of 16stainless steel rods (5 mm in diameter), spaced 1 cm apart and wired to a shock generator (SGA-2010). After 30 minutes control period, rats were presented a tone (CS, 5sec) in NREM sleep or QA. In 15 minutes, rats were presented a tone (CS, 15sec) and given an electrical shock (unconditioned stimulus; US, 0.5mA, 1sec) every 5sec (Fig.1A). Rats were given twice foot shock

paired with a tone at intervals of 15 minutes. After 15minutes of a tone paired foot shocks presentation, rats were presented only a tone (CS, 5sec) in NREM sleep or QA.

With this protocol, rats associated a foot shock with a tone (Fig.1B). This procedure was repeated once a day for 2days in freely moving rats. All parameters were measured continuously and simultaneously, and behavioral observations were recorded throughout the experimental period.

Histology

At the end of the entire procedure, rats were anesthetized and the location of the electrodes was marked by passing a DC current of 40μA for as anode. The rats were killed using an intravenous overdose of pentobarbital sodium (> 200 mg kg^{-1}) and the brain was removed and fixed by immersion in 1 % potassium ferrocyanide in formalin for 7days. With time, ferrocyanide caused the conversion of the iron deposit to a Prussian blue spot. The brains were transferred to a 15% sucrose in .1-mol/L phosphate buffer solution, after 24 hours were stored in a 25% sucrose in .1-mol/L phosphate buffer solution in 48 hours. Brains were sliced into 50 μm section with a freezing microtome. Every other section was collected on a slide and stained cresyl violet and recoding electrode placements were identified (Fig.2A, B).

Statistical Analysis

Statistical evaluation was performed with analysis of variance (ANOVA) for repeated measures with SPSS. When the F values were significant ($P<0.05$), individual comparison were made by Fisher's least significant difference test. Correlations between two variables were analyzed by a least squares linear regression. Values were reported as means ± SD.

RESULTS

Figure 3 shows the typical recording of simalteniously and coutinuously measurement in CA1NA

or PVNNA, EEG, EMG, RSNA, LSNA, HR, and MAP.

Figure 4 shows the basal level in CA1NA, PVNNA, RSNA, LSNA, HR, and MAP before (Day1) and after fear conditioning (Day3) in home cage (Home) and shock cage (Shock). On Day1, CA1NA was 196.3±12.3spikes/sec in Home and 208.4±16.7spikes/sec in Shock. On Day3, CA1NA was 190.7±11.0spikes/sec in Home and 244.2±21.4spikes/sec in Shock. Shock was significantly high level compared with Home. There was no significant difference CA1NA between Day1 vs Day3 in Home and Shock, respectively. On Day1, PVNNA was 101.6±1.7% in Home and 112.7±5.5% in Shock. Shock was significantly high level compared with Home. On Day3, PVNNA was 99.7±0.8% in Home and 112.4±3.0% in Shock. Shock was significantly high level compared with Home at the same on Day1. There was no significant difference PVNNA between Day1 vs Day3 in Home and Shock, respectively. On Day1, RSNA was 103.1±3.3% in Home and 118.3±9.9% in Shock. On Day3, RSNA was 97.5±3.7% in Home and 107.6±6.3% in Shock. There was no significant difference RSNA between Day1 vs Day3 and Home vs Shock, respectively. On Day1, LSNA was 106.5±4.5% in Home and 119.9±10.9% in Shock. On Day3, LSNA was 128.4±14.5% in Home and 119.9±8.7% in Shock. There was no significant difference LSNA between Day1 vs Day3 and Home vs Shock, respectively. On Day1, MAP was 109.6±1.5mmHg in Home and 111.0±1.3 in Shock. On Day3, MAP was 115.3±2.1mmHg in Home and 118.7±1.4mmHg in Shock. There was significant difference MAP between Home vs Shock on Day1 and Day3, respectively. On Day1, HR was 443.0±5.2beats/min in Home and 448.4±5.6 beats/min in Shock. On Day3, HR was 429.8±4.9 beats/min in Home and 440.3±6.4 beats/min in Shock. There was no significant difference HR between Day1 vs Day3 and Home vs Shock, respectively.

Figure 5 shows the time course of changes in freezing rate, CA1NA, PVNNA, RSNA, LSNA, HR, and MAP from the basal levels before fear conditioning (Day1) and after fear conditioning (Day3) in the home cage. Before fear conditioning (Day1), the freezing rate increased from 3sec and reached 10 % at 7sec. Increased level was maintained around 10% until 120sec. CA1NA increased immediately to 48.081±0.97 spikes/sec in response to the US presentation compared with

basal levels, and then decreased to -17.460±7.68 spikes/sec at 13sec and back in the basal level. CA1NA significantly ($p<0.05$) increased from 0sec to 4sec in response to the US presentation compared with basal levels. PVNNA significantly ($p<0.05$) increased to 28.01±3.96% at 2sec in response to the US presentation compared with basal levels, and then decreased in the basal level, but maintained the significant ($p<0.05$) increase until 23sec. RSNA increased transiently at 2sec and 7sec in response to the US presentation. LSNA did not change significantly in response to the US presentation. MAP significantly ($p<0.05$) increased from 1sec to 3sec in response to the US presentation compared with basal levels, and reached 5.234±0.93mmHg at 2sec. And then MAP decreased in the basal level. HR immediately decreased to -9.372±2.88 beats/min at 2sec in response to the US presentation but back in the basal level at 13sec. After fear conditioning (Day3), the freezing rate increased immediately to 79%, and then reached maximum to 84%. Increased level was maintained around 63% until 120sec. CA1NA increased immediately to 58.132±7.30 spikes/sec in response to the US presentation compared with basal levels, and then decreased to -1.635±1.28 spikes/sec at 11sec. CA1NA significantly ($p<0.05$) increased from 0sec to 5sec in response to the US presentation compared with basal levels. There was a significantly ($p<0.05$) difference CA1NA between Day1 vs Day3 at 7sec, 9sec, 13sec, 15sec, from 23sec to 24sec, 26sec, from 32sec to 33sec, from 35sec to 37sec, 52sec, 54sec, from 57sec to 59sec, from 61sec to 63sec, from 69sec to 70sec, 74sec, 77sec, 82sec, 98sec 102sec. PVNNA increased immediately to 28.641±4.64% in response to the US presentation compared with basal levels, and then gradually decreased, but maintained the significant ($p<0.05$) increase until 120sec. There was a significantly ($p<0.05$) but fragmentarily difference in PVNNA between Day1 vs Day3 at 43sec, from 46sec to 49sec, and from 55sec to 59sec. RSNA significantly ($p<0.05$) increased to 111.981±39.0 at 4sec in response to the US presentation compared with basal levels, and then decreased to 5.839±13.51% at 6sec. But RSNA increased again to 67.364±13.13% at 11sec, and then decreased in the basal level. There was a significantly ($p<0.05$) but fragmentarily difference RSNA between Day1 vs Day3 at from 1sec to 4sec, 7sec, and from 10sec to 13sec. LSNA increased significantly ($p<0.05$) to

99.841±30.675%, and then reached maximum to 127.828±37.83% at 5sec in response to the US presentation compared with basal levels, and then decreased but maintained the significant ($p<0.05$) increase until 120sec. There was a significantly ($p<0.05$) difference LSNA between Day1 vs Day3 at from 1sec to 89sec. MAP significantly ($p<0.05$) increased from 1sec to 9sec in response to the US presentation compared with basal levels, and reached 14.371±2.43mmHg at 2sec, but decrease in the basal level at 10sec. There was a significantly ($p<0.05$) difference MAP between Day1 vs Day3 at from 1sec to 9sec. HR decreased immediately and reached minimum to -17.132±5.44 beats/min at 9sec, and then gradually back in the basal level. HR significantly ($p<0.05$) increased from 7sec to 10sec in response to the US presentation compared with basal levels. There was a significantly ($p<0.05$) difference HR between Day1 vs Day3 at from 8sec to 10sec. EMG increased immediately to 6.758±2.36 a.u. in response to the US presentation compared with basal levels, and then gradually decreased.

Figure 6 shows the time course of changes in freezing rate, CA1NA, PVNNA, RSNA, LSNA, HR, and MAP from the basal levels before fear conditioning (Day1) and after fear conditioning (Day3) in the home cage. Before fear conditioning (Day1), the freezing rate increased immediately and reached 10 % at 4sec. And then rats didn't show the freezing behavior at sec 33sec. CA1NA increased immediately to 71.11±16.2spikes/sec in response to the US presentation compared with basal levels, and then decreased to -33.21±-8.4 spikes/sec at 12sec and back in the basal level. CA1NA significantly ($p<0.05$) increased from 0sec to 5sec in response to the US presentation compared with basal levels. PVNNA significantly ($p<0.05$) increased to 22.17±5.2% at 1sec in response to the US presentation compared with basal levels, and then decreased in the basal level, but maintained the significant ($p<0.05$) increase until 20sec. RSNA and LSNA increased transiently at 0sec in response to the US presentation. MAP significantly ($p<0.05$) increased from 1sec to 3sec in response to the US presentation compared with basal levels, and reached 4.38±1.1mmHg at 2sec. And then MAP decreased in the basal level. HR did not change significantly in response to the US presentation. After fear conditioning (Day3), the freezing rate increased immediately to 67%, and

then reached maximum to 93%. Increased level was maintained around 72% until 120sec. CA1NA increased immediately and reached to 87.8±14.6 spikes/sec at 4sec in response to the US presentation. And then CA1NA decreased gradually to 0.21±13.4 spikes/sec at 65sec but increased again to 59.65±18.7 at 79sec and back in basal level. CA1NA significantly ($p<0.05$) increased from 0sec to 41sec and from76sec to 80sec in response to the US presentation compared with basal levels. There was a significantly ($p<0.05$) difference CA1NA between Day1 vs Day3 at 4sec, from 10sec to 28sec, from 32sec to 39sec, from 45sec to 49sec, from 78sec to 81sec, and from 110sec to 116sec. PVNNA increased immediately to 23.69±3.9% in response to the US presentation compared with basal levels, and then gradually decreased, but maintained increased level around 5.6% until 120sec. There was no significantly ($p<0.05$) difference in PVNNA between Day1 vs Day3. RSNA significantly ($p<0.05$) increased to 206.04±33.3% at 4sec in response to the US presentation compared with basal levels, and then decreased to -13.65±20.7% at 5sec. But RSNA increased again to 71.98±23.0 at 8sec, and then gradually decreased, but maintained increased level around 28.2% until 120sec. There was a significantly ($p<0.05$) but fragmentarily difference RSNA between Day1 vs Day3 at from 1sec to 4sec, from 6sec to 12sec, from 23sec to 24sec, from 42sec to 43sec, from 92sec to 93sec, from 97sec to 98sec, and from 102sec to 104sec. LSNA significantly ($p<0.05$) increased to 215.92±27.0% at 0sec in response to the US presentation compared with basal levels, and then decreased at 2sec. But RSNA increased again and reached 182.55±32.0 at 21sec, and then gradually decreased, but maintained increased level around 41.0% until 120sec. There was a significantly ($p<0.05$) but fragmentarily difference RSNA between Day1 vs Day3 at from 0sec to 56sec, from 64sec to 81sec, from 84sec to 89sec, and from 93sec to 98sec. MAP significantly ($p<0.05$) increased from 1sec to 10sec in response to the US presentation compared with basal levels, and reached 19.84±3.7mmHg at 2sec, and then immediately decreased, but maintained increased level around 5.6mmHg until 120sec. There was a significantly ($p<0.05$) difference MAP between Day1 vs Day3 at from 1sec to 11sec, from 60sec to 62sec, from 70sec to 73sec, from 78sec to 80sec, and from 84sec to 86sec. HR increased immediately to 9.48±4.4beats/min at 2sec, and

then gradually increased and reached 14.42±7.2beats/min at 120sec. HR significantly ($p<0.05$) increased from 50sec to 76sec and from 97sec to 120sec in response to the US presentation compared with basal levels. There was a significantly ($p<0.05$) difference HR between Day1 vs Day3 at from 2sec to 4sec, from 44sec to 83sec, and from 95sec to 120sec.

DISCUSSION

The present study was designed to investigate the roles of CA1NA and PVNNA in regulating sympathetic nerve activity and cardiovascular function in contextual- and auditory-cued classical fear conditioning. Rats have been shown freezing behavior to tone presentation (conditioned stimuli) paired with a foot shock due to fear conditioning. The RSNA, LSNA, and the cardiovascular response were found to be divided during and after tone presentation. HR was also found to be altered when tone presentation was performed in a shock cage (contextual condition). CA1NA is not important for RSNA, LSNA, and cardiovascular response in the home cage, but may influence changes in HR in the shock cage. It was also suggested that PVNNA may not play a major role in the regulation of s sympathetic nerve activity and cardiovascular function in response to fear.

Renal and LSNA Sympathetic nerve activity and Cardiovascular Function During Tone Presentation

Fear conditioning resulted in increases in RSNA and LSNA and arterial pressure during conditioned stimuli alone, and HR did not change during conditioned stimuli alone but increased when contextual conditions were added to the conditioned stimuli.

Before fear conditioning, there were no differences in RSNA and LSNA, arterial pressure, and HR in response to tone presentation in both the home or shock cages. In response to tone presentation, RSNA and LSNA and arterial pressure increased transiently, but most rats did not show freezing behavior. Because the tone presentations were made during non-rapid eye movement

sleep or quiet awake, the transient responses in RSNA, LSNA, and arterial pressure likely occurred simply in response to the external stimulus of tone before fear conditioning.

After fear conditioning, RSNA and LSNA and arterial pressure increased significantly when tones were presented in the home cage and remained increased during tone presentation. HR did not differ from that before fear conditioning. The rats have been shown freezing behavior in response to the sound presentation, suggesting that the sound caused them to recall fear. To our knowledge, there have been no reports directly documenting changes in sympathetic nerve activity in response to fear conditioning, but it has been reported that ASNA is increased by TMT, which induces instinctive fear (Horii et al. 2010). This suggests that sympathetic nerve activity may be increased by fear. Joseph et al reported arterial pressure increased in response to tone presentation which is consistent with our results (LeDoux et al. 1988). These results suggest that RSNA and LSNA and arterial pressure increase in response to fear-conditioned tone presentation.

When the contextual condition of the shock cage was added to the fear-conditioned tone presentation, RSNA and LSNA and arterial pressure responses were unchanged from the tone presentation only, but HR increased. Rats showed freezing behavior to the tone presentation as in the home cage. When rats feel fear, their skeletal muscles contract in fight-or-flight response or freezing behavior. Muscle metabolism increases, resulting in increased cardiac output and redistribution of blood flow from visceral organs to actively contracting muscles. However, previous studies have shown that exposure to contextual conditions alone results in a decrease followed by an increase in HR (Carrive 2006). These findings suggest that HR may have increased during tone presentation because exposure to the contextual condition completed the state of readiness for the upcoming shock. In other words, HR was increased by the combination of the conditioned stimulus and the contextual condition.

Taken together, these results suggest that fear conditioning causes increases in RSNA, LSNA, and arterial pressure to increase with the conditioned stimulus alone, but that the addition of the contextual condition to the conditioned stimulus causes an increase in HR.

Renal and LSNA Sympathetic nerve activity and Cardiovascular Function Following Tone Presentation

Fear conditioning resulted in regional differences in RSNA and LSNA responses after the presentation of conditioned stimuli, and HR responses differed between conditioned stimuli alone and when contextual conditions were added.

After fear conditioning, rats continued freezing behavior after tone presentation in the home cage. At this time, RSNA and arterial pressure returned to their original levels, while LSNA sympathetic nerve activity remained increased. HR decreased and then gradually increased and returned to its original level. We have previously shown that there are regional differences between RSNA and LSNA (Miki and Yoshimoto 2010, Yoshimoto, Yoshida and Miki 2011). Ramchandra et al. reported different responses of RSNA and LSNA to l-NAME administration and volume expansion (Ramchandra, 2006). It has also been reported that the neurons responsible for renal, muscular, and visceral vascular sympathetic nerve activity in the RVLM are distinct populations (McAllen and May 1994). These findings suggest that sympathetic nerve activity is not uniformly regulated but is likely to be regulated here in response to the situation, and that fear is one such pattern. The decrease in HR immediately after tone presentation occurs after an increase in arterial pressure and maybe a baroreceptor reflex.

When the contextual condition of the shock cage was added to the tone presentation after fear conditioning, RSNA and arterial pressure returned to their original levels but remained higher than before fear conditioning. LSNA sympathetic nerve activity increased, as in the home cage, and HR increased. Rats continued freezing after tone presentation as in the home cage. It is possible that the contextual condition combined with the conditioned stimuli strongly stimulated the fear conditioning circuit and that RSNA and LSNA and HR remained higher after tone presentation than before fear conditioning in the shock cage. The arterial pressure remained higher in the shock cage than before the fear conditioning condition, possibly due to RSNA and HR.

These results suggest that fear conditioning induces regional differences in RSNA and LSNA following the presentation of conditioned stimuli and that HR differs between responses to conditioned stimuli only and when contextual conditions are added.

The results of this study showed that RSNA and LSNA and cardiovascular responses after fear conditioning could be divided into responses during and after tone presentation. RSNA and LSNA increased during tone presentation, and regional differences in response occurred after tone presentation. HR responses were also found to change between responses to conditioned stimuli only and when contextual conditions are added.

Role of Hippocampal CA1 Neuronal Activity in Regulating Renal and LSNA Sympathetic nerve activity and Cardiovascular function during Fear Conditioning

CA1NA was found to be involved in the increase in HR during tone presentation in the shock cage. In this study, CA1NA increased during tone presentation in both home and shock cages. CA1NA did not change significantly in the home cage compared to before fear conditioning, but there was a significant increase in the shock cage compared to pre-conditioning. A previous study showed that disruption of ventral CA3 regions impairs fear memory recall by tone alone, while disruption of dorsal CA1 and ventral CA1 does not (Hunsaker and Kesner 2008). It is known that information input to the hippocampus is sent out of the hippocampal CA1 region (Witter et al. 2000), suggesting that the increase in CA1NA during tone presentation in the home cage is simply due to information transfer. On the other hand, CA1NA increased significantly during tone presentation in the shock cage compared to before fear conditioning. The hippocampal CA1 area is involved in the acquisition and recall of contextual conditions (Lee and Kesner 2004). It is possible that CA1NA showed a significant increase in a shock cage due to the addition of the contextual condition. In addition, HR increased during tone presentation only in the shock cage, suggesting that increased CA1NA may be involved in the increase in HR. These results suggest that CA1NA is involved in the increase in HR during tone presentation in the shock cage, but in the home cage.

CA1NA may also be involved in the increase in HR after tone presentation in the shock cage. In the present study, CA1NA showed a significant increase after the end of tone presentation in a piecewise manner compared to that before fear conditioning, and the maintenance of the increase was more pronounced in the shock cage. Baseline hippocampal CA1 activity was also increased in the shock cage after fear conditioning. Previous studies have shown that disruption of hippocampal CA1 regions not only impairs contextual memory recall, but also contextual memory acquisition. Thus, the maintenance of increased CA1NA after tone presentation in the shock cage may be due to the recall and acquisition of contextual memory, suggesting that a circuit of fear conditioning is at work. Taken together, increased CA1NA may be involved in the changes in RSNA and LSNA, and HR after tone presentation.

In summary, our results suggest that CA1NA is involved in the increase in HR and changes in RSNA and LSNA when contextual conditions are added to the conditioned stimulus.

Role of PVNNA in Regulating Renal and LSNA Sympathetic nerve activity and Cardiovascular function during Fear Conditioning

PVNNA may not play a major role in modulating sympathetic nerve activity and cardiovascular function during tone presentation. In the present study, PVNNA increased during tone presentation in both home and shock cages but did not change significantly compared to before fear conditioning. Although there have been no previous reports directly documenting changes in paraventricular nucleus neural activity in response to fear conditioning or CS, it has been shown that fos expression in the PVN is increased by air-puff stress, a form of psychological stress (Furlong, 2018) and that fos expression in the PVN is increased by restraint stress (Mohammad, 2000). These suggest that external stimuli (stress) can increase PVNNA. When rats moved to the shock cage, the baseline of PVNNA increased but there was no significant difference between before and after fear conditioning. This also suggests that paraventricular activity was not increased in response to fear but rather in response to general external stimuli. These findings suggest that fear conditioning does

not alter PVNNA and is not important for changes in sympathetic nerve activity and cardiovascular function during tone presentation.

PVNNA was also found to be unimportant for the regulating of sympathetic nerve activity and cardiovascular function after the end of tone presentation. In the present study, PVNNA gradually decreased and returned to its original level in both home and shock cages after tone presentation. The PVNNA continued to increase significantly after the end of the tone in the home cage compared to before the tone presentation. The PVN has projections to the RVLM and the intermediate lateral column (Pyner and Coote 2000) and is thought to be important in regulating sympathetic nerve activity and cardiovascular function. It has also been shown that PVNNA is involved in regional differences in sympathetic nerve activity (Kenny, 2001). Based on these findings, PVNNA may influence regional differences in RSNA and LSNA after tone presentation. However, after the end of the tone presentation in the shock cage, PVNNA remained higher than before fear conditioning, but the difference was not significant. There are projections from the amygdala, which is important for fear learning, to RVLM (Saha et al. 2005, Salome et al. 2001). This suggests that the effects of PVNNA on RSNA and LSNA and cardiovascular function may be attenuated during fear. These results suggest that PVNNA may influence regional differences in RSNA and LSNA after tone presentation, but the degree of involvement is small.

These findings suggest that PVNNA does not play a major role in regulating RSNA and LSNA and cardiovascular function during fear conditioning.

REFERENCES

Badoer, E. 2001. "Hypothalamic Paraventricular Nucleus and Cardiovascular Regulation." *Clin Exp Pharmacol Physiol* 28(1-2):95-9. doi: 10.1046/j.1440-1681.2001.03413.x.

Baldi, E., C. A. Lorenzini and C. Bucherelli. 2004. "Footshock Intensity and Generalization in Contextual and Auditory-Cued Fear Conditioning in the Rat." *Neurobiol Learn Mem* 81(3):162-6. doi: 10.1016/j.nlm.2004.02.004.

Carrive, P. 2000. "Conditioned Fear to Environmental Context: Cardiovascular and Behavioral Components in the Rat." *Brain Res* 858(2):440-5. doi: 10.1016/s0006-8993(00)02029-1.

Carrive, P. 2006. "Dual Activation of Cardiac Sympathetic and Parasympathetic Components During Conditioned Fear to Context in the Rat." *Clin Exp Pharmacol Physiol* 33(12):1251-4. doi: 10.1111/j.1440-1681.2006.04519.x.

Dampney, R. A. 2015. "Central Mechanisms Regulating Coordinated Cardiovascular and Respiratory Function During Stress and Arousal." *Am J Physiol Regul Integr Comp Physiol* 309(5):R429-43. doi: 10.1152/ajpregu.00051.2015.

Daumas, S., H. Halley, B. Frances and J. M. Lassalle. 2005. "Encoding, Consolidation, and Retrieval of Contextual Memory: Differential Involvement of Dorsal Ca3 and Ca1 Hippocampal Subregions." *Learn Mem* 12(4):375-82. doi: 10.1101/lm.81905.

Dayas, C. V., K. M. Buller, J. W. Crane, Y. Xu and T. A. Day. 2001. "Stressor Categorization: Acute Physical and Psychological Stressors Elicit Distinctive Recruitment Patterns in the Amygdala and in Medullary Noradrenergic Cell Groups." *Eur J Neurosci* 14(7):1143-52.

doi: 10.1046/j.0953-816x.2001.01733.x.

Furlong, T. M., L. M. McDowall, J. Horiuchi, J. W. Polson and R. A. Dampney. 2014. "The Effect of Air Puff Stress on C-Fos Expression in Rat Hypothalamus and Brainstem: Central Circuitry Mediating Sympathoexcitation and Baroreflex Resetting." *Eur J Neurosci* 39(9):1429-38. doi: 10.1111/ejn.12521.

Horii, Y., Y. Nikaido, K. Nagai and T. Nakashima. 2010. "Exposure to Tmt Odor Affects Adrenal Sympathetic Nerve Activity and Behavioral Consequences in Rats." *Behav Brain Res* 214(2):317-22. doi: 10.1016/j.bbr.2010.05.047.

Hunsaker, M. R. and R. P. Kesner. 2008. "Dissociations across the Dorsal-Ventral Axis of Ca3 and Ca1 for Encoding and Retrieval of Contextual and Auditory-Cued Fear." *Neurobiol Learn Mem* 89(1):61-9. doi: 10.1016/j.nlm.2007.08.016.

Jiang, Z., S. Rajamanickam and N. J. Justice. 2019. "Crf Signaling between Neurons in the Paraventricular Nucleus of the Hypothalamus (Pvn) Coordinates Stress Responses." *Neurobiol Stress* 11:100192. doi: 10.1016/j.ynstr.2019.100192.

Kanbar, R., V. Orea, C. Barres and C. Julien. 2007. "Baroreflex Control of Renal Sympathetic Nerve Activity During Air-Jet Stress in Rats." *Am J Physiol Regul Integr Comp Physiol* 292(1):R362-7. doi: 10.1152/ajpregu.00413.2006.

LeDoux, J. E., J. Iwata, P. Cicchetti and D. J. Reis. 1988. "Different Projections of the Central Amygdaloid Nucleus Mediate Autonomic and Behavioral Correlates of Conditioned Fear." *J Neurosci* 8(7):2517-29.

Lee, I. and R. P. Kesner. 2004. "Differential Contributions of Dorsal Hippocampal Subregions to Memory Acquisition and Retrieval in Contextual Fear-Conditioning." *Hippocampus* 14(3):301-10. doi: 10.1002/hipo.10177.

McAllen, R. M. and C. N. May. 1994. "Differential Drives from Rostral Ventrolateral Medullary Neurons to Three Identified Sympathetic Outflows." *Am J Physiol* 267(4 Pt 2):R935-44. doi: 10.1152/ajpregu.1994.267.4.R935.

Miki, K., A. Kosho and Y. Hayashida. 2002. "Method for Continuous Measurements of Renal Sympathetic Nerve Activity and Cardiovascular Function During Exercise in Rats." *Exp Physiol* 87(1):33-9. doi: 10.1113/eph8702281.

Miki, K., M. Oda, N. Kamijyo, K. Kawahara and M. Yoshimoto. 2004. "Lumbar Sympathetic Nerve Activity and Hindquarter Blood Flow During Rem Sleep in Rats." *J Physiol* 557(Pt 1):261-71. doi: 10.1113/jphysiol.2003.055525.

Miki, K. and M. Yoshimoto. 2010. "Role of Differential Changes in Sympathetic Nerve Activity in the Preparatory Adjustments of Cardiovascular Functions During Freezing Behaviour in Rats." *Exp Physiol* 95(1):56-60. doi: 10.1113/expphysiol.2009.050187.

Pyner, S. and J. H. Coote. 2000. "Identification of Branching Paraventricular Neurons of the Hypothalamus That Project to the Rostroventrolateral Medulla and Spinal Cord." *Neuroscience* 100(3):549-56. doi: 10.1016/s0306-4522(00)00283-9.

Saha, S., M. J. Drinkhill, J. P. Moore and T. F. Batten. 2005. "Central Nucleus of Amygdala

Projections to Rostral Ventrolateral Medulla Neurones Activated by Decreased Blood Pressure." *Eur J Neurosci* 21(7):1921-30. doi: 10.1111/j.1460-9568.2005.04023.x.

Salome, N., O. Viltart, S. Leman and H. Sequeira. 2001. "Activation of Ventrolateral Medullary Neurons Projecting to Spinal Autonomic Areas after Chemical Stimulation of the Central Nucleus of Amygdala: A Neuroanatomical Study in the Rat." *Brain Res* 890(2):287-95. doi: 10.1016/s0006-8993(00)03178-4.

Swanson, L. W. and P. E. Sawchenko. 1980. "Paraventricular Nucleus: A Site for the Integration of Neuroendocrine and Autonomic Mechanisms." *Neuroendocrinology* 31(6):410-7. doi: 10.1159/000123111.

Witter, M. P., F. G. Wouterlood, P. A. Naber and T. Van Haeften. 2000. "Anatomical Organization of the Parahippocampal-Hippocampal Network." *Ann N Y Acad Sci* 911:1-24. doi: 10.1111/j.1749-6632.2000.tb06716.x.

Yoshimoto, M., I. Yoshida and K. Miki. 2011. "Functional Role of Diverse Changes in Sympathetic Nerve Activity in Regulating Arterial Pressure During Rem Sleep." *Sleep* 34(8):1093-101. doi: 10.5665/SLEEP.1168.

(A)

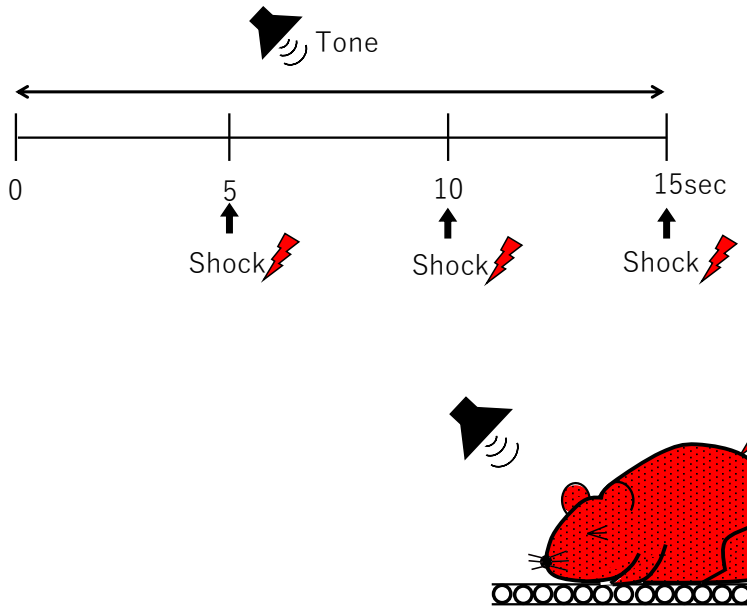

(B)

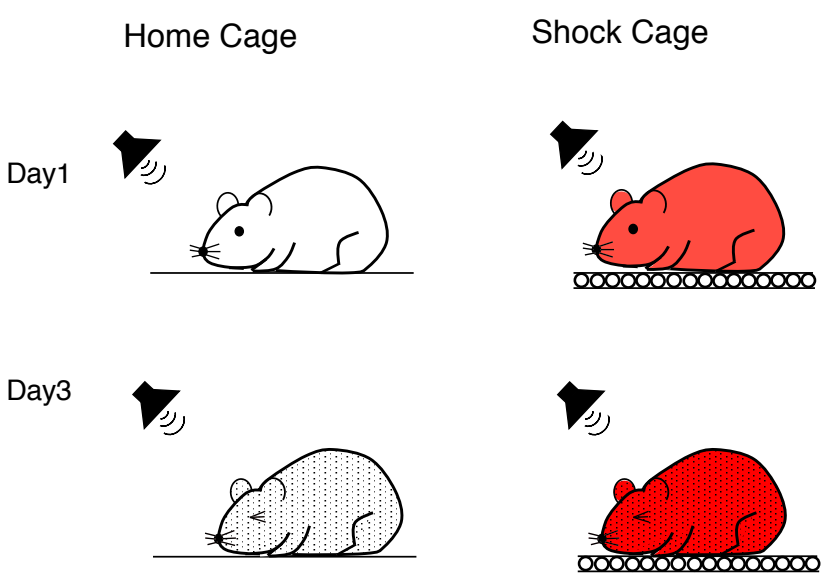

Figure 1. Schematic diagram of the experimental protocol.

A: Schematic diagram of the response of rats to tone presentation in the home cages or the shock cage. The dot pattern represents after fear conditioning.

B: Schematic diagram of the fear conditioning. Fear conditioning was carried out in a shock cage. rats were presented a tone (15sec) and given an electrical shock (0.5mA, 1sec) every 5sec. Rats were given twice foot shock paired with a tone at intervals of 15 minutes.

(A)

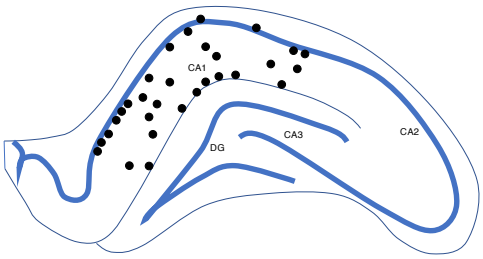

(B)

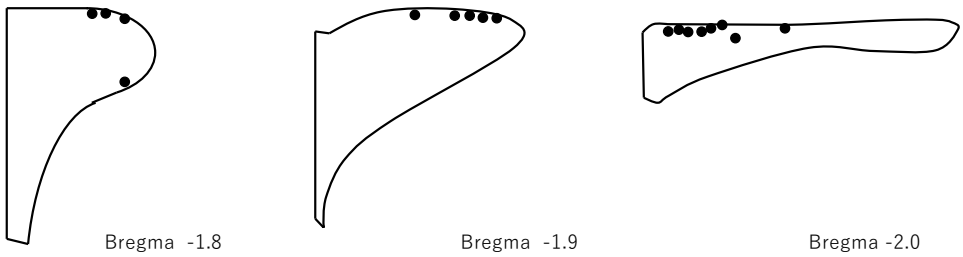

Figure 2. Site of the tip of the electrode where CA1NA and PVNNA was recorded

A: Coronal sections of the Hippocampal area are shown. The black circles represent the measurement positions. CA1; Hippocampal CA1 region, CA2 ; Hippocampal CA2 region, CA3; Hippocampal CA3 region, DG; Dentate gyrus.

B: Coronal sections of PVN are shown. The black circles represent the measurement positions. From left to right, the distances from bregma are -1.8 mm, -1.9 mm, and -2.0 mm, respectively.

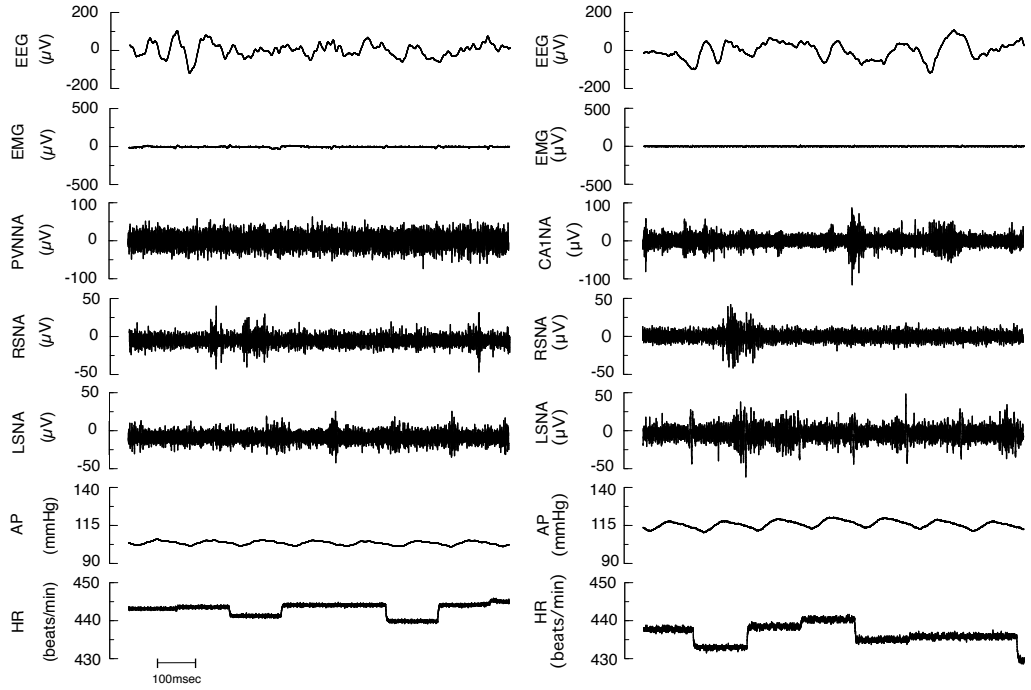

Figure.3 Typical recordings from an individual rat.

Parameters are shown as electroencephalogram (EEG), cervical electromyogram (EMG), Hippocampal CA1 neuronal activity (CA1NA), hypothalamus paraventricular nucleus neuronal activity (PVNNA), renal sympathetic nerve activity (RSNA), lumbar sympathetic nerve activity (LSNA), arterial pressure (AP), and heart rate (HR). These were observed before US exposure in the home cage.

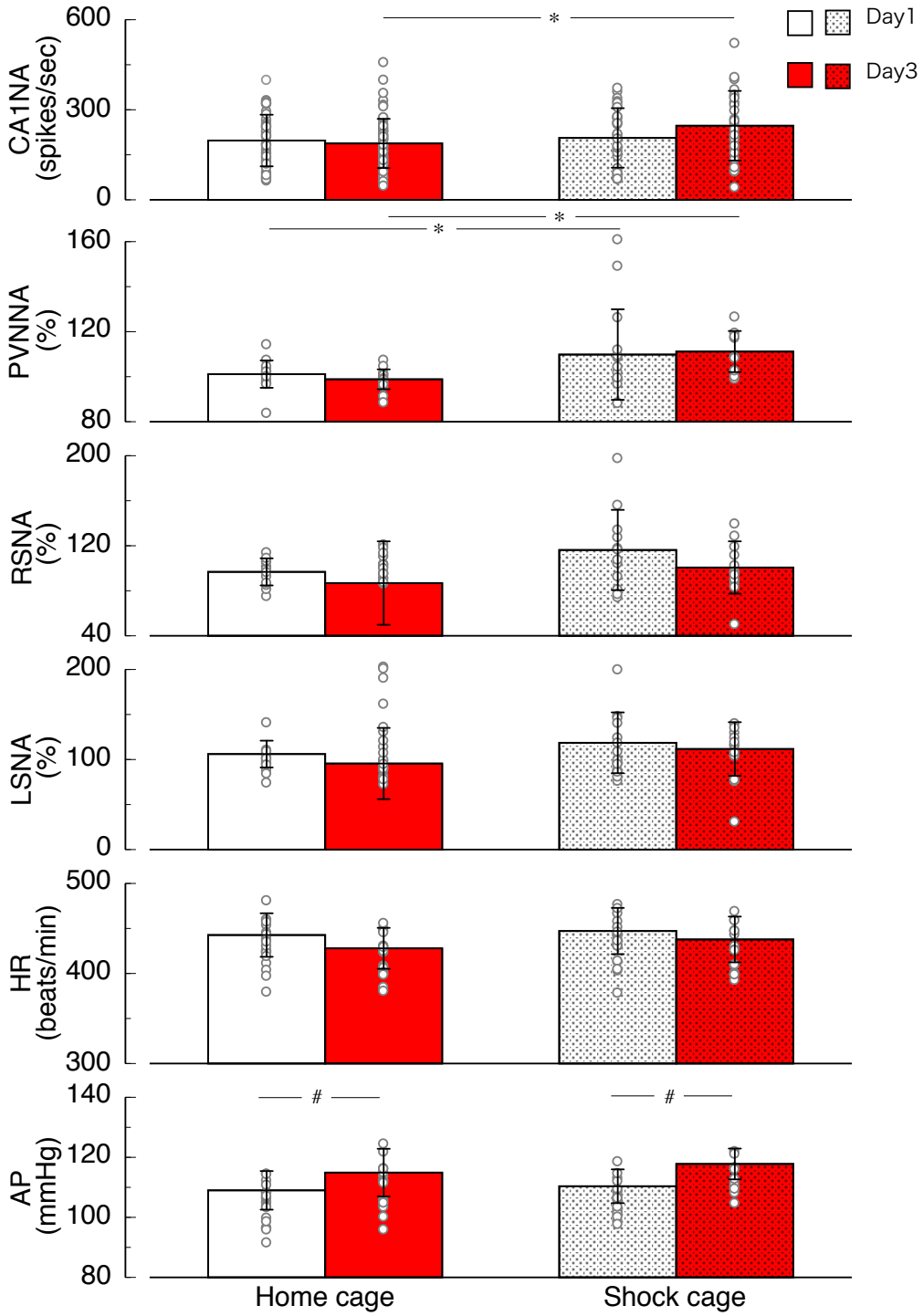

Fig.4 Baseline of CA1NA, PVNNA, RSNA, LSNA, HR, and MAP before the US presentation. Changes in the baseline of CA1NA, PVNNA, RSNA, LSNA, HR, and MAP before the US presentation on Day1 and Day3 experiments in the home cage and shock cage. White and gray bars represent the mean value in the home cage. Pink and red bars represent the mean value in the shock cage. Error bars and columns represent ± SD. *: Statistically different ($P<0.05$) between home cage vs shock cage. #: Statistically different ($P<0.05$) between Day1 vs Day3.

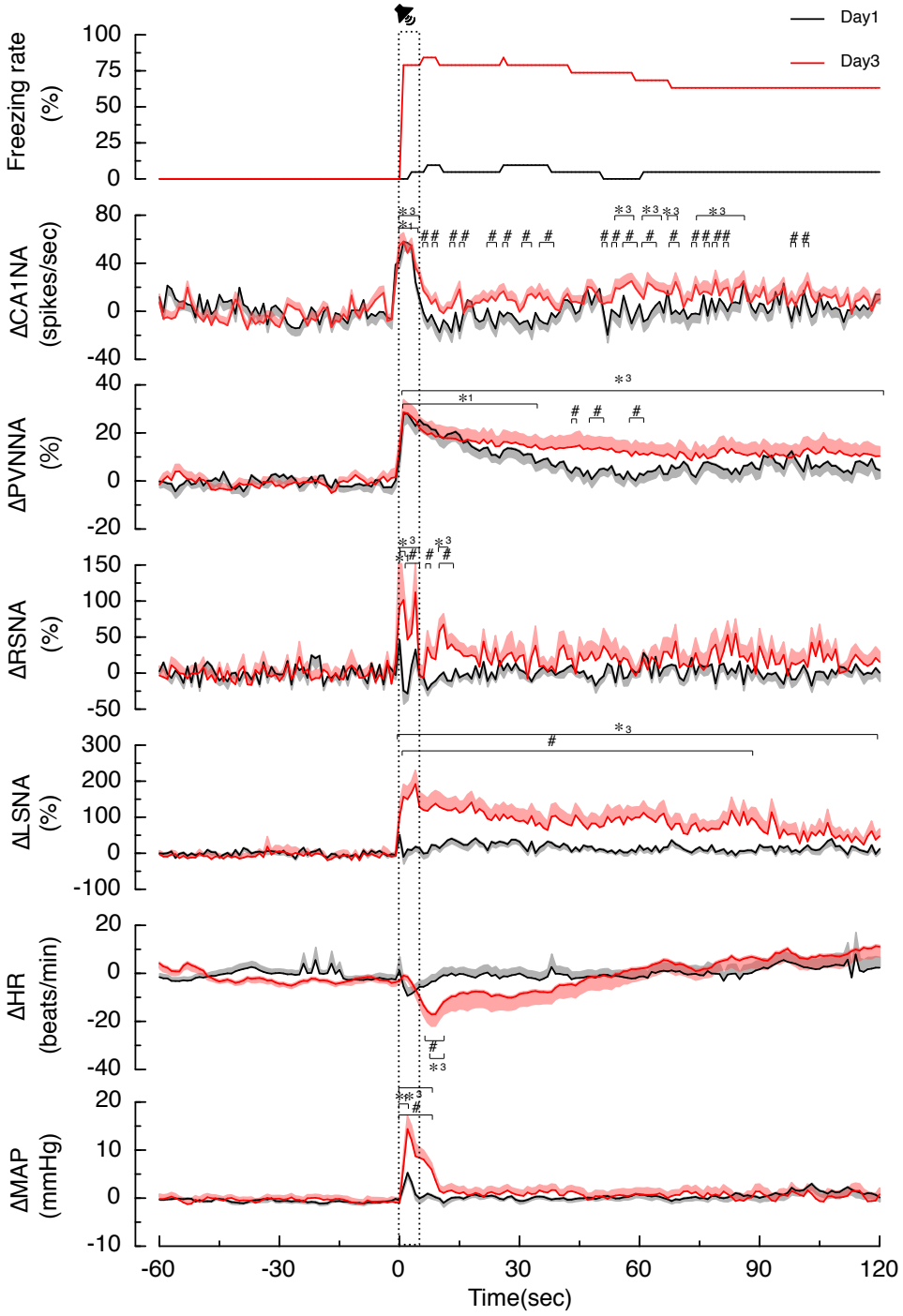

Fig.5 Time course of changes in response to the US presentation in the home cage.

Changes in Freezing rate, CA1NA, PVNNA, RSNA, LSNA, HR, and MAP before and after the US presentation on Day1(black line) and Day3 (red line) experiments in the home cage. Solid lines show mean values and solid areas above or below mean lines represent ±SD. The dot area represents to start of the US presentation. *1, *3: Statistically different (P<0.05) from the basal level on Day1 and Day3, respectively. #: Statistically different (P<0.05) between Day1 vs Day3 at the corresponding time.

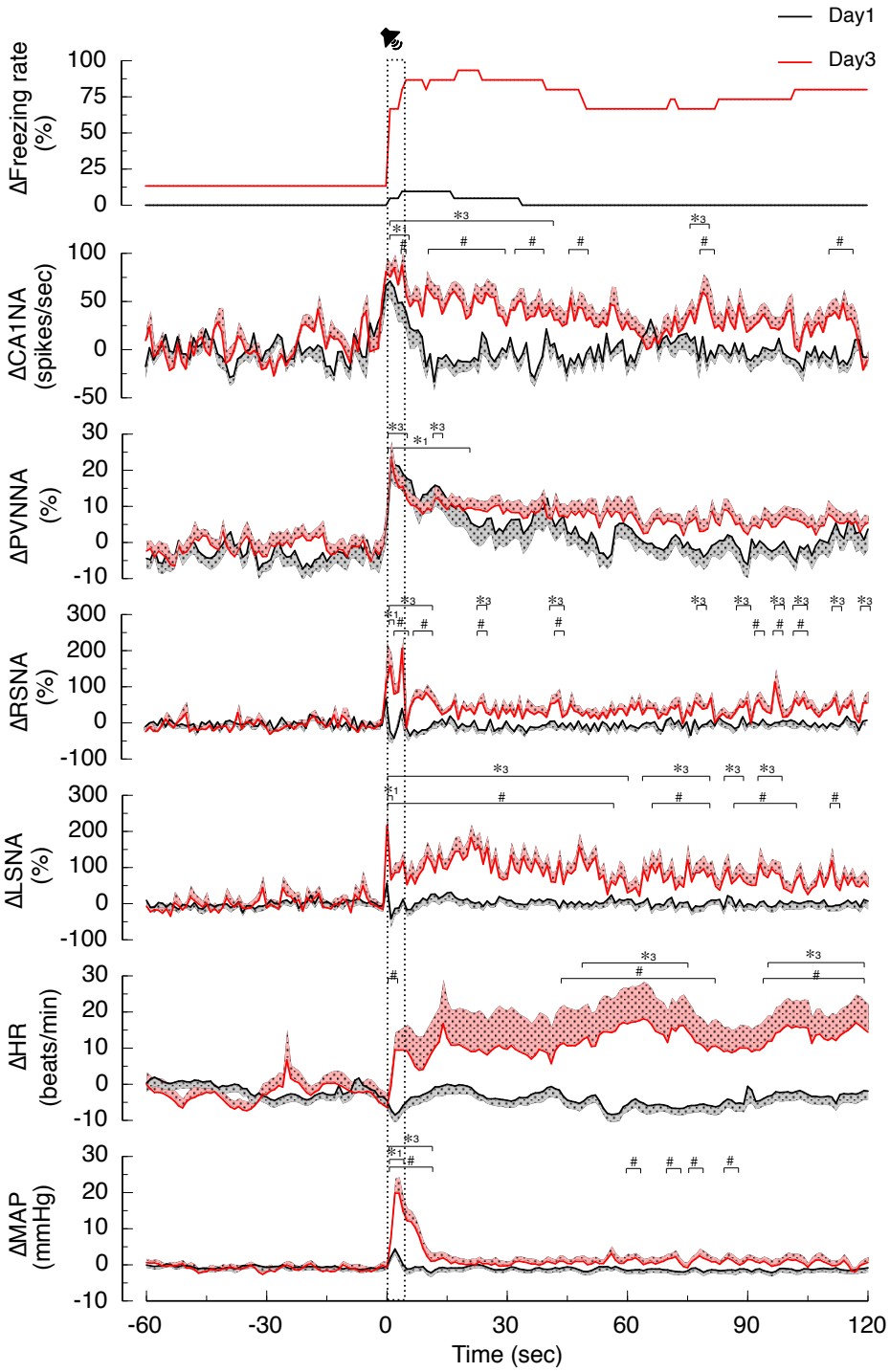

Fig.6 Time course of changes in response to the US presentation in the shock cage.

Changes in Freezing rate, CA1NA, PVNNA, RSNA, LSNA, HR, and MAP before and after the US presentation on Day1(black line) and Day3 (red line) experiments in the shock cage. Solid lines show mean values and solid areas above and below mean lines represent ±SD. The dot area represents to start of the US presentation. *1, *3: Statistically different (P<0.05) from the basal level on Day1 and Day3, respectively. #: Statistically different (P<0.05) between Day1 vs Day3 at the corresponding time.

List of Publication

Published paper

Shizuka Ikegame, Misa Yoshimoto, and Kenju Miki. Simultaneous Measurement of Central Amygdala Neuronal Activity and Sympathetic Nerve Activity during Daily Activity in Rats. Exp physiolo, volume107, issue9, 1071-1080. 2022.

Kenju Miki, Shizuka Ikegame, and Misa Yoshimoto. Regional Differences in Sympathetic Nerve Activity Are Generated by Multiple Arterial Baroreflex Loops Arranged in Parallel. Frontiers in physiology, volume13. 2022.

Naomi Kondo, Misa Yoshimoto, Shizuka Ikegame, and Kenju Miki. Differential shifts in baroreflex control of renal and lumbar sympathetic nerve activity induced by freezing behaviour in rats. Exp physiolo, volume106, issue10, 2060-2069. 2021.

Misa Yoshimoto, Yuko Onishi, Naoko Mineyama, Shizuka Ikegame, Mikiyasu Shirai, John W. Osborn, and Kenju Miki. Renal and Lumbar Sympathetic Nerve Activity During Development of Hypertension in Dahl Salt-Sensitive Rats. Hypertention, volume74, issue4, 888-895. 2019.

International conference presentations

Shizuka Ikegame, Misa Yoshimoto, and Kenju Miki. Simultaneous Measurement of Hypothalamic Paraventricular Nucleus Neuronal and Sympathetic Nerve Activity in Freely Moving Rats. Experimental Biology 2019, 744, Orlando.

Shizuka Ikegame, Misa Yoshimoto, and Kenju Miki. Measurement of paraventricular

nucleus neuronal and sympathetic nerve activities in conscious rats. FAOPS 2019, 2P-332, Kobe.

Misa Yoshimoto, Shizuka Ikegame, Yuki Shiwa, and Kenju Miki. Long-term recording of renal and lumbar sympathetic nerve activity in response to myocardial infarction in conscious rats. Europhysiology 2018, PCB003, London.

Kenju Miki, Yumiko Akiyama, Hiroka Ukita, Kana Nagao, Shizuka Kataoka, and Misa Yoshimoto. Intense fear induces low-frequency oscillation of cerebral blood flow, arterial pressure, and sympathetic nerve activity in conscious rats. Experimental Biology 2018, 737.12, San Diego.

Domestic conference presentations

Shizuka Ikegame, Misa Yoshimoto, Kenju Miki. How fear memory recall affects hypothalamic paraventricular nucleus neuronal activity and sympathetic nerve activity in conscious rats. 第 99 回日本生理学会大会, 1P07-10, Sendai, 2022.

Shizuka Ikegame, Misa Yoshimoto, Kenju Miki. Recall of fear memories activates hypothalamic paraventricular neuronal and sympathetic nerve activity in conscious rats. 第 97 回日本生理学会大会, 2P-144, Beppu, 2020.

池亀静香,吉本光佐,三木健寿.睡眠時の視床下部室傍核神経活動と交感神経活動の周波数分析. 第 58 回日本生気象学会大会, 相模原,2019.

池亀静香, 吉本光佐, 三木健寿. 意識下自由行動ラットにおける視床下部室傍核

神経活動と交感神経活動と同時測定.第 57 回日本生気象学会大会, 京都, 2018.

Acknowledgments

I would like to express my sincerest gratitude to Professor Misa Yoshimoto (Nara Women's University, Japan) for her constructive suggestions and continuous encouragement throughout this work.

I am grateful to Professor emeritus Kenju Miki (Nara Women's University, Japan) for his thoughtful guidance and continuous support during my doctoral study.

I would like to thanks Professors Keiko Morimoto (Kyoto Koka Women's University, Japan), Akira Takamata, Hiroko Kubo, and Manabu Shibasaki (Nara Women's University, Japan) for valuable advices and discussion throughout this work.

We gratefully acknowledge to past and present members of the research group of Professor Yoshimoto for all their help during my doctoral study.